MOLECULAR RECOGNITION BASED AGGLOMERATION OF QUANTUM DOT BIOCONJUGATES FOR MULTIPLEXED ANTIGEN DETECTION

By

Chinmay Prakash Soman

Dissertation

Submitted to the Faculty of the

Graduate School of Vanderbilt University

in partial fulfillment of the requirements

for the degree of

DOCTOR OF PHILOSOPHY

in

Interdisciplinary Materials Science

December, 2008

Nashville, Tennessee

Approved:

Professor Todd D. Giorgio

Professor Frederick R. Haselton

Professor James E. Crowe Jr.

Dr. James N. Higginbotham

ABSTRACT

Sensitive and quantitative detection of proteomic biomarker panels is expected to significantly improve early diagnosis and therapy monitoring for cancers and other diseases. We developed a novel *in-vitro* diagnostics approach to multiplexed biomarker detection based on molecular recognition mediated nanoparticle self-assembly. The nanoparticles self-assemble into agglomerates *via* a rapid, single step, fluid phase reaction. The individual nanoparticles and agglomerates can be discriminated based on their light scattering properties and by other analytical techniques.

Cadmium selenide quantum dots conjugated to polyclonal antibodies self-assemble to form quantum dot agglomerates in the presence of antigens, including angiopoietin-2, vascular endothelial growth factor A, and human immunoglobulin G. The reaction mixtures were characterized by one or more analytical techniques including dynamic light scattering, electrical sensing zone method (Coulter counter), and flow cytometry to characterize and quantify the self-assembled agglomerates. The size distribution of the quantum dot agglomerates was estimated to be between 500 nm and 4 microns. The individual components of the agglomerates are significantly smaller. Measured by dynamic light scattering, the quantum dot-antibody conjugates have a hydrodynamic diameter of 45 nm, while the antigens are 5 to 10 nm in diameter.

We demonstrated quantitative and sensitive detection using flow cytometry of the candidate cancer biomarkers vascular endothelial growth factor A and angiopoietin-2. Non-multiplexed detection of the antigens was demonstrated with 50 femtomolar sensitivity limit. Multiplexed detection, using two quantum dot populations with distinct

emission spectra of vascular endothelial growth factor A and angiopoietin-2 was demonstrated in the physiologically relevant picomolar concentration range.

The kinetics of the self-assembly process were examined by measurements of the angiopoietin-2 mediated self-assembly of quantum dots over time, revealing a sigmoidal process. Antigen concentration modulates the slopes and inflection times of the sigmoidal kinetics curves.

Further refinements to improve the sensitivity and specificity of this novel proteomic biomarker detection technique may improve the screening, diagnostics, and therapy response monitoring for cancers and other diseases. This approach to studying nanoparticle self-assembly may also provide a valuable tool for understanding the fundamental characteristics of nanoscale particle agglomeration.

To My Teachers

Thank you for the inspiration, motivation, and support.

ACKNOWLEDGEMENTS

I am deeply grateful to my advisor, Prof. Todd Giorgio, for his support, guidance, and advice during my graduate studies. His active and enthusiastic support for initiating new research projects, as well as for perusing non-research activities in support of the long term goals of these projects enabled me to achieve things that are unusual for the typical graduate school career. I am certain that in addition to the excellent scientific training, the non-science skills that I learnt from Dr. Giorgio will help me throughout my life.

I also wish to thank the members of my committee for providing valuable advice and direction for this research project, ensuring that this doctoral research was of the best possible quality. I have become a better researcher due to their constructive criticism. In particular, I would like to thank Dr. James Higginbotham for providing support and expert advice for small particle cytometry.

The many members of the Giorgio and Haselton groups unfailingly provided much needed scientific camaraderie and support, not to mention the regular moments of levity. Their presence made the past four years greatly enjoyable.

Finally, I could never express in words how grateful I am to my family. My parents supported my in all my endeavors, and inspired me to achieve all I could with words and by example. I am truly thankful to my wife, whose unwavering confidence in my ability was invaluable. Her love, (often manifested in the form of fantastic food!) provided me strength when I needed it the most.

TABLE OF CONTENTS

Page

LIST OF TABLES

LIST OF FIGURES

CHAPTER 1

INTRODUCTION

Rationale

The rapidly growing fields of genomics and proteomics are giving rise to a fundamentally molecular understanding of diseases. Genetic mutations translated to the proteome and the consequent abnormal protein function and altered intercellular signaling are at the root of many diseases. The discovery of the proteomic abnormalities underlying various pathologies is poised to lead to a revolution in medicine. The new proteome based understanding of diseases will provide new targets for therapy, as well as increase the use of protein detection technologies towards diagnosis, monitoring and management of many diseases in a highly effective and personalized manner. Antibody based detection technologies are prime candidates for this application, due to the proven and traditional use of the highly specific and well understood antibody-antigen interaction.

Cancers are a group of pathologies that constitutes one of the leading causes of mortality in the developed world. Moreover, the major factors leading to mortality in cancers are delayed detection, metastasis, and lack of data about the efficacy of therapy, hindering countermeasures to acquired drug resistance and relapse of the disease[1, 2]. Hence, discovery of cancer marker proteins is one of the leading goals of proteomics research. The diagnosis and treatment of other significant diseases, including heart disease and Alzheimer's disease, is also expected to benefit from proteomic approaches.

Many marker proteins that correlate with the presence and behavior of cancers have been identified [3-12], and more significant discoveries are expected. The predictive power of these marker proteins, as well as the significant increase in predictive power from examining a panel of molecules has also been recognized [13-16]. Hence, there is a strong motivation for detecting these proteins at very low concentration, enabling routine and frequent monitoring and successful management of the disease[14, 15, 17].

In research settings, proteomic profiling of cancers is carried out by analyzing proteins in sera and tissues from diseased subjects by mass spectrometry, ELISA assays, 2D-PAGE etc. However, a clinically suitable detection method for assessing a few specific molecules from the numerous present in a biological sample is, at present, a challenge. While they are suitable in research settings, the conventional protein detection methods are unsuitable for molecular profiling in clinical settings, falling short on one or more of the important parameters of speed, sensitivity, multiplexing capability, production of quantitative data, ease of implementation and cost.

The unique properties of nanoparticles and nanoparticle-biomolecule conjugates can provide novel ways of achieving these objectives. Our proposed approach – detection of micro-agglomerates formed by specific self assembly of nanostructures – offers a potent way to tackle this problem. Detection of pathogens by molecular recognition-based self-assembly was proposed as far back as 1956 in the form of the latex agglutination test[18], which is still used for detecting bacteria[19-21], and for determining blood types, but is unsuitable for sensitive detection of low concentration small molecules. Nanoparticle based variants of the agglutination test have been demonstrated for small molecules such as DNA fragments[22] and proteins[23]. In both

these demonstrations, the change in plasmon resonance due to self assembly of the metal nanostructures was spectroscopically monitored. Small molecules have also been detected using quantum dots using antibody mediated coincidence of multiple quantum dots with different emission wavelengths[24, 25].

Based on this evidence, I propose to develop a simple and robust method for quantitative multiplexed proteomic antigen detection using antibody-antigen molecular recognition mediated quantum dot self assembly.

Specific Aims

I propose to develop this proteomic diagnostic method over the course of three specific aims:

Aim 1 – Investigate quantitative correlation between antigen concentration and nanoparticle self-assembly.

I propose to develop and optimize the protocols for quantum dot-antibody conjugation for antigen detection, incubation of antigens with the biofunctionalized quantum dots, and characterization of the nanoparticle agglomerates with various analytical methods. I will characterize the biofunctionalized nanoparticles and nanoparticle agglomerates by dynamic light scattering, electrical sensing zone method, and flow cytometry. Based on the results of these characterizations, a method for investigating quantitative correlation between the antigen concentration and nanoparticle agglomerates will be selected. This correlation will be investigated for at least two

proteomic antigens, and the feasibility of using this technique for quantitative biomarker detection will be determined.

Aim II – Develop the protocol for multiplexed detection of two distinct proteomic biomarkers.

I propose to develop a protocol for quantitatively detecting two different antigens from a single multi-antigen solution. Two quantum dot populations with distinct fluorescence characteristics will be used for detecting one biomarker each. I will characterize the cross-reactivity between the biofunctionalized quantum dots and non-specific antigens at multiple concentrations, as well as the effect of using multiple quantum dot populations on the agglomerate characterization abilities of the analytical instrument and method. The reaction and analytical protocols will be modified to minimize the effect of these parameters on the antigen detection capabilities and the sensitivity limit will be optimized to enable multiplexed detection at physiologically relevant biomarker concentrations.

Aim III – Characterize the kinetics of molecular recognition mediated nanoparticle self-assembly.

The kinetics of nanoparticle agglomeration may provide important information about the agglomeration mechanism, as well as about optimizing the reaction and characterization protocol to enable rapid and sensitive detection. The kinetics of agglomeration mediated by specific and non-specific molecular recognition are expected to be significantly different, based on theoretical understanding of the process, as well as

literature evidence from similar techniques. I will quantify the kinetics of nanoparticle agglomeration for a range of physiologically relevant concentration values of a candidate cancer biomarker. The kinetics may suggest the feasibility of alternative system parameters that may be used for quantitatively detecting biomarkers, as well as the optimal protocols for minimizing the effect of non-specific intermolecular interactions on the sensitivity and specificity of biomarker detection.

Background

Intermolecular interactions - dipole-dipole, hydrogen bonding and electrostatic - are important physical phenomena. These interactions, which generate important effects such as the hydrophobic/hydrophilic forces, contribute to spontaneous and stable organization of simple molecules into interesting structures like the lipid monolayers, bilayers and vesicles that are of particular importance in biological systems. Biological evolution has further generated sophisticated molecules capable of taking advantage of such intermolecular forces and forming highly specific and functional multi-molecular structures, in effect leading to intermolecular recognition. One of the important recognition interactions is the antibody-antigen interaction that forms immunocomplexes. Along with being an extremely important biological process, the antibody-antigen interaction is useful as a core component of technologies used for diagnosing numerous pathologies by detecting and quantifying the corresponding antigens.

Molecular recognition, an important mechanism in biological systems, also provides a powerful tool for materials science, by directing the self assembly of nanoscale

molecules and particles into larger structures. Typically, these self assembled structures are significantly larger than their individual components, and hence can be detected easily by optical investigation, providing a simple and effective way to detect small molecules. In fact, agglomeration of micro particles into larger assemblies – specifically, latex agglutination - has been used since 1956 as a way of detecting pathogens. The unique optical properties of nanoparticles, such as fluorescence and plasmon resonance, offer the possibility of further increasing the sensitivity of aggregation based detection. We propose a technology involving molecular recognition mediated self assembly of fluorescent semiconductor nanoparticles (quantum dots). The resulting self assembled structures will be characterized, providing novel way to detect low concentrations of known antigens. This technique works completely in the fluid phase and has the potential for better sensitivity, quantification, multiplexing and ease of use than current detection methods.

Critical Requirements for a Clinically Applicable Proteomic Profiling Technique:

The goals of clinical proteomics are: a) early detection and diagnosis of diseases, b) determination of disease subtype and status to guide personalized therapy, and c) frequent monitoring of disease progress for checking effectiveness of the therapy. To fulfill these objectives, there are several attributes required of any proteomic profiling technology:

1) <u>High sensitivity and dynamic range:</u> While some disease states may involve uniquely expressed proteins, the difference between the proteome of diseased and normal states is often only in the different expression levels of the same proteins.

Furthermore, the amount of disease specific proteins in any diagnostic sample will likely be below the amount of abundant proteins by many orders of magnitude. This is especially true for early detection of diseases. In early stages of a disease, the amount of affected tissue is typically small, and consequently, the marker proteins are being presented in diminished quantities, especially in peripheral fluids. Hence, for successful detection, the profiling technology must be sensitive to extremely low concentration of proteins, while having a sufficient dynamic range of measurement.

2) Appropriate multiplexing capabilities: Many disease states will be best diagnosed and classified based on the expression levels of a panel of proteins, reflecting the complex multifaceted molecular basis of the diseases. Since successful early detection of diseases will likely involve routine screening for multiple diseases, multiplexing abilities will be required for detection of multiple panels of proteins – perhaps on the order of hundreds of proteins.

3) Minimally invasive, low sample volume: A routine and/or frequent diagnostic should be minimally invasive and require minimal total sample volume for successful detection. A serum based diagnostic requiring low blood volume will be ideal.

4) Rapid, easy to administer and cost effective: The most popular and effective diagnostics produce results quickly, do not require highly trained technical personnel, and cost very little per administration.

Molecular Profiling Methods

The most prominent of the numerous techniques for molecular profiling, from either clinical or research perspective, are discussed below, with respect to their

performance on the above mentioned attributes. Profiling methods that are currently used in clinical or research settings, as well as those that are currently being developed to take advantage of novel nanoscale phenomena are discussed.

Enzyme linked immunosorbent assay (ELISA) is possibly the most popular protein detection technique, employed widely in clinical settings as well as in molecular profiling research. The popularity of ELISA is partly because of its simplicity and cost effectiveness. Typically, the target antigen is captured by an antibody adsorbed on the polymer surface of the well plate. A second antibody, coupled to an enzyme is then added to the wells, followed by a chemiluminescent substrate for the enzyme. The presence and intensity of the luminescence is measured and provides a measure of the antigen. While ELISA is a simple and useful technique, it is also highly labor and time intensive, and typically requires on the order of 10^5 copies of the antigen for successful detection.

Polymerase chain reaction (PCR) is another widely used technique, although one that is usually applied to polynucleotide rather than protein detection. The target molecule is copied by cycling of the mixture of original sample, primers, excess nucleotides, and polymerase enzymes over a defined thermal program. PCR is remarkable for its sensitivity, with reports of successful detection of poly-nucleotides from sample containing only one copy/ml[26], although routine detection requires on the order of 10^1 -10^2 copies. One the other hand, any contaminant polynucleotide recognized by the same primers is also amplified, resulting in increased background.

Immuno-PCR , a hybrid of the above two techniques, utilizes PCR amplification of polynucleotide sequences associated with specific antibody-antigen complexes, resulting

in PCR-like sensitivity for protein detection[27, 28]. A nanoparticle based variant of this technique has also been developed recently[29].

All three of these techniques are generally considered unsuitable for high throughput assays and/or simultaneous detection multiple proteins as they are time intensive, and not inherently amenable to multiplexed detection.

Mass spectrometry (MS) is amenable to multi-protein detection, and is one of the techniques used for proteomic analysis of serum or tissue samples, mainly for discovery of disease biomarkers. MS generates information about the number of proteins in a sample, and the charge to molecular weight ratio of these proteins. Since these quantities are dependant mainly on the protein content of the sample, and are easy to compare across samples, MS is an excellent tool for recognizing protein expression patterns indicative of cancers[17, 30-32]. However, MS suffers from several drawbacks. Critically for early diagnosis applications, detection of low concentration proteins in the presence of abundant proteins by MS is difficult to achieve. MS and also requires expensive instrumentation and expertise, and is thus an unlikely choice for a clinical proteome profiling technique.

Gel electrophoresis (GE) is another technique that was widely used in early proteomics research, especially as two dimensional polyacrylamide gel electrophoresis (2D PAGE)[33, 34]. 2D PAGE has the highest resolving power of any protein separation technique – being able to separate up to 10^4 proteins[35]. The separated proteins can be analyzed with various analysis techniques including MS, antibody based detection similar to Western blot, and more. Despite its advantages, GE is not suitable for clinical proteomic profiling applications; especially since sensitivity of 2D PAGE is about 10^6

copies, and even then, the low concentration proteins are often go undetected in the presence of high concentration proteins. Furthermore, predominantly hydrophobic proteins, such as membrane proteins are often resolved poorly, and gel to gel replicability remains a problem. In addition, GE is also very labor and time intensive.

Antibody Microarrays, similar to DNA microarrays, and are also used for detecting numerous proteins simultaneously, often directly from biological fluids. In an antibody microarray, antibodies to 10^4 to 10^6 different proteins can be immobilized in an array of spots on a solid surface, with each spot containing a unique antibody. The captured antigens are detected by fluorescence measurements. Antibody microarrays, apart from being prone to several shortcomings of the antibody-antigen interaction based techniques, are also unsuitable for clinical profiling due to some inherent properties of the array based technique. Maximum sensitivity in an array technique would be achieved when each antigen interacts with all possible antibodies. Unfortunately, due to the diffusion limited interaction, and the large number of spots, this is not achievable in a practical amount of time[36].

Along with the technique specific limitations of the above multi-protein detection methods, they all have a common flaw that render them sub-optimal for diagnostic proteomic applications. These strategies are all suitable for detection of 10^3 or more proteins. For detecting a particular disease, or a set of diseases, it is unlikely that such large detection capabilities will be required.

The conventional single or multi protein detection methods mentioned above are a part of the biological and clinical toolkit. However, quite a few novel molecule detection methods are being developed to take advantage of the growing understanding

of nanoscale physical phenomena[37-39]. Some of the nano based methods that are promising for proteomic profiling applications are discussed below.

Nanocantilever Sensors involve lithographically manufactured arrays of cantilevers. Biomolecular interactions are detected by monitoring the mechanical properties of the detection device[40-44]. Antibodies can be bound to the cantilever surfaces, and upon antigen binding, the natural resonance frequency of the cantilever frequency of the cantilevers changes due to change in mass as well as change in elasticity of the composite structure[45, 46]. Currently, the sensitivity of these cantilever arrays - at the level of picograms/ml - is not the strongest advantage of the technique, but being based on lithographic technology, the cantilever arrays are promising due to their customizability, ease of production and cost of manufacturing.

Nanowire and Nanotube Sensors take advantage of the sensitivity of the conductive properties of the nanowires to the nearby environment. The conductivity of the nanostructures is monitored and a change in conductivity is indicative of a binding event[47-50]. Nanowire sensors usually require a combination of the bottom-up and top-down fabrication methods. While this technique is at the early stages of development, and many problems are yet to be solved, the fundamental principle makes it very attractive for the purpose of detecting multiple low concentration species rapidly[51].

Nanoparticle based methods that take advantage of unique electro-optical, chemical and structural properties of nanoparticle-biomolecule composites to detect the presence of the target analyte are also being actively researched[52-56]. Such systems take advantage of phenomena such as fluorescence resonance energy transfer (FRET)[57,

58], localized surface plasmon resonance (LSPR)[59-63], surface enhanced Raman scattering (SERS)[64-66]. While quantum dots are ideal candidates for FRET based sensors, metal nanoparticles are being investigated for LSPR and SERS based sensors. SERS especially is being investigated as an analysis technique for other protein binding or separation techniques such as ELISA and GE.

Nanoparticle Self Assembly based methods are a subset of the nanoparticle based methods that depend on formation of structures of various complexity and sizes from nanoparticle biomolecule conjugates in the presence of the target molecules. The colorimetric change in metal nanoparticle solution based on inter-nanoparticle distance has been long recognized[67]. The colorimetric monitoring of interactions between biomolecule-nanoparticle conjugates has also been carried out[68] and this phenomenon has been exploited for the detection of simple molecules like glucose[69], polynucleotides[70], and proteins[23]. Detection of target molecules based on coincidence of two different colored quantum dots has also been demonstrated[24, 25].

Core Components of the Proposed Technology

The fundamental phenomena related to the proposed technology are well understood. Quantum dots have been thoroughly investigated with regards to synthesis and fluorescence properties [71-77], surface modification for biological applications - including conjugation with proteins and antibodies [78-84] and multiplexed biological applications [85-88]. From this literature evidence, it is apparent that quantum dots are suitable for the proposed *ex-vivo* diagnostic technology[89].

Antibody-antigen interactions mediated self assembly is well established in the form of the agglutination test[18, 19] and nanoparticle self assembly based detection of proteins has also been demonstrated recently [23, 90, 91].

While the self assembled micro-structures can be detected via dynamic laser scattering (DLS) of the bulk solution, as well as by electro-resistive particle counting such as Coulter Counter, using a flow cytometer or similar instrument provides a much more powerful way of acquiring and analyzing the data. In a flow based setting, the small volumes of the sample can be analyzed – leading to improved sensitivity. Furthermore, flow cytometric analysis allows for simultaneous measurement of various properties of the particles such as forward scatter, side scatter, and the fluorescence intensity at multiple wavelengths, enabling sophisticated multiplexed detection. Flow cytometry is an established technology and the instrumentation is widely available in clinical settings. This can prove beneficial for clinical acceptance of the proposed technique.

Advantages of the Proposed Technology

Although of the proposed technology is currently in early stages of investigation, the basic capabilities, as predicted from the fundamental theoretical considerations and demonstrated by preliminary evidence, appear to be suitable for multiplexed proteomic profiling applications. These fundamental features are:

1) Multiplexing capabilities: Due to the tunable emission spectra of quantum dots, multiple colors can be detected simultaneously and from a single sample. If each antigen is detected by a single colored population of quantum dots, this enables simultaneous detection of multiple proteins. While the number different emission

wavelengths of the quantum dots currently commercially available is less than ten, this number can increase significantly by using quantum dots of different semiconducting materials [85, 92].

2) Sensitivity and Dynamic Range: The very high quantum efficiency and high fluorescence intensity of quantum dots is well known. Coupled with a sensitive detection technology such as photomultiplier tubes (PMT) or charge coupled diodes (CCD), an extremely low concentration of quantum dots can be detected. Since the proposed self assembly is a two component reaction, the dynamic range can be varied depending on the possible concentration range of the target antigen.

3) Minimally Invasive: The proposed diagnostic is *ex-vivo* and completely in the fluid phase, and hence can be carried out easily in serum, lymph or other suitable fluid samples.

4) Low sample volume: Due to the high sensitivity, and since the actual detection of agglomerates can be carried out in few microliters of the sample, a milliliter sample will likely be sufficient even for acquiring a statistically significant signal, as well as screening for multiple diseases, depending on the concentration of the target analyte.

5) Rapid results: The agglomeration reaction in a well dispersed solution proceeds very rapidly – in under an hour. The actual measurement is also fast, and results will likely be obtained in under a couple of hours

6) Cost effective: Quantum dots, one of the essential analytes needed for the diagnostic can be synthesized easily and cheaply. Antibodies are already a standard diagnostic product. Since very low quantities of these reagents will be needed, the diagnostic will be cost effective. Also, during development, the characterization is being

carried out on flow cytometers. However, standard FACS instrumentation is not a necessity. A simpler and cheaper dedicated instrument based on micro-fluidics and semiconductor optics can be envisioned for clinical application.

7) Easy to administer: In a dedicated instrument, the sample preparation and analysis from extracted fluid could be completely automated. Even in a cytometers based analysis, the initial sample preparation can be automated, and the analysis can be carried out using high throughput screening attachments, making the diagnostic administrable by a minimally trained operative.

Other Possible Applications

Since this technique is based on antibody antigen interaction, it can presumably be used to detect any analyte for which suitable molecular recognition molecules can be identified. Apart from being a general clinical diagnostics technique, applications in bio-defense and environmental monitoring are feasible for target analytes that can be suspended or dissolved in an aqueous buffer. This approach to studying nanoparticle self-assembly may also provide a valuable tool for understanding the fundamental characteristics of nanoscale particle agglomeration.

References

1. Jemal, A.; Tiwari, R. C.; Murray, T.; Ghafoor, A.; Samuels, A.; Ward, E.; Feuer, E. J. and Thun, M. J., Cancer Statistics, 2004. *CA: A Cancer Journal for Clinicians*, **2004**. *54*(1): 8-29.

2. Ries, L. A. G.; Eisner, M. P.; Kosary, C. L.; Hankey, B. F.; Miller, B. A.; Clegg, L.; Mariotto, A.; Fay, M. P.; Feuer, E. J. and Edwards, B. K., *SEER Cancer Statistics Review, 1975-2000*. 2003, National Cancer Institute: Bethesda, MD.

3. Classen, S.; Kopp, R.; Possinger, K.; Weidenhagen, R.; Eiermann, W. and Wilmanns, W., Clinical Relevance of Soluble c-erbB-2 for Patients with Metastatic Breast Cancer Predicting the Response to Second-Line Hormone or Chemotherapy. *Tumor Biology*, **2002**. *23*(2): 70-75.

4. Eccles, S. A., The Role of c-erbB-2/HER2/neu in Breast Cancer Progression and Metastasis. *Journal of Mammary Gland Biology and Neoplasia*, **2001**. *6*(4): 393-406.

5. Hung, T. L.; Chen, F. F.; Liu, J. M.; Lai, W. W.; Hsiao, A. L.; Huang, W. T.; Chen, H. H. W. and Su, W. C., Clinical Evaluation of HER-2/neu Protein in Malignant Pleural Effusion-Associated Lung Adenocarcinoma and as a Tumor Marker in Pleural Effusion Diagnosis 1. *Clinical Cancer Research*, **2003**. *9*(July 2003): 2605-2612.

6. Muller, V.; Witzel, I.; Pantel, K.; Krenkel, S.; Luck, H. J.; Neumann, R.; Keller, T.; Dittmer, J.; Janicke, F. and Thomssen, C., Prognostic and predictive impact of soluble epidermal growth factor receptor (sEGFR) protein in the serum of patients treated with chemotherapy for metastatic breast cancer. *Anticancer Res*, **2006**. *26*(2B): 1479-87.

7. Perik, P. J.; Van Der Graaf, W. T. A.; De Vries, E. G. E.; Boomsma, F.; Messerschmidt, J.; Van Veldhuisen, D. J.; Sleijfer, D. T. and Gietema, J. A., Circulating apoptotic proteins are increased in long-term disease-free breast cancer survivors. *Acta Oncologica*, **2006**. *45*(2): 175-183.

8. Zusman, I., Soluble tumor-associated antigens in cancer detection, prevention and therapy. *Med Sci Monit*, **2004**. *10*(12): 324.

9. Greatens, T. M.; Niehans, G. A.; Rubins, J. B.; Jessurun, J.; Kratzke, R. A.; Maddaus, M. A. and Niewoehner, D. E., Do Molecular Markers Predict Survival in Non-Small-Cell Lung Cancer? *American Journal of Respiratory and Critical Care Medicine*, **1998**. *157*(4): 1093-1097.

10. Kim, Y. C.; Park, K. O.; Kern, J. A.; Park, C. S.; Lim, S. C.; Jang, A. S. and Yang, J. B., The interactive effect of Ras, HER2, P53 and Bcl-2 expression in predicting the survival of non-small cell lung cancer patients. *Lung Cancer*, **1998**. *22*(3): 181-90.

11. Niklinski, J.; Niklinska, W.; Laudanski, J.; Chyczewska, E. and Chyczewski, L., Prognostic molecular markers in non-small cell lung cancer. *Lung Cancer*, **2001**. *34*(2): S53-8.

12. Onn, A.; Correa, A. M.; Gilcrease, M.; Isobe, T.; Massarelli, E.; Bucana, C. D.; O'Reilly, M. S.; Hong, W. K.; Fidler, I. J. and Putnam, J. B., Synchronous Overexpression of Epidermal Growth Factor Receptor and HER2-neu Protein Is a Predictor of Poor Outcome in Patients with Stage I Non-Small Cell Lung Cancer. *Clinical Cancer Research*, **2004**. *10*: 136-143.

13. Roboz, J., Mass Spectrometry in Diagnostic Oncoproteomics. *Cancer Investigation*, **2005**. *23*(5): 465-478.

14. Calvo, K. R.; Liotta, L. A. and Petricoin, E. F., Clinical Proteomics: From Biomarker Discovery and Cell Signaling Profiles to Individualized Personal Therapy. *Bioscience Reports*, **2005**. *25*(1): 107-125.

15. Meyerson, M. and Carbone, D., Genomic and Proteomic Profiling of Lung Cancers: Lung Cancer Classification in the Age of Targeted Therapy. *Journal of Clinical Oncology*, **2005**. *23*(14): 3219-3226.

16. Petricoin, E. F. and Liotta, L. A., Proteomic approaches in cancer risk and response assessment. *Trends Mol Med*, **2004**. *10*(2): 59-64.

17. Chanin, T. D.; Merrick, D. T.; Franklin, W. A. and Hirsch, F. R., Recent developments in biomarkers for the early detection of lung cancer: perspectives based on publications 2003 to present. *Curr Opin Pulm Med*, **2004**. *10*(4): 242-7.

18. Plotz, C. M. and Singer, J. M., The latex fixation test. I. Application to the serologic diagnosis of rheumatoid arthritis. *Am J Med*, **1956**. *21*(6): 888-92.

19. March, S. B. and Ratnam, S., Latex agglutination test for detection of Escherichia coli serotype O157. *Journal of Clinical Microbiology*, **1989**. *27*(7): 1675-1677.

20. van Griethuysen, A.; Pouw, M.; van Leeuwen, N.; Heck, M.; Willemse, P.; Buiting, A. and Kluytmans, J., Rapid Slide Latex Agglutination Test for Detection of Methicillin Resistance in Staphylococcus aureus. *Journal of Clinical Microbiology*, **1999**. *37*(9): 2789-2792.

21. Sulahian, A.; Tabouret, M.; Ribaud, P.; Sarfati, J.; Gluckman, E.; Latgé, J. P. and Derouin, F., Comparison of an enzyme immunoassay and latex agglutination test

for detection of galactomannan in the diagnosis of invasive aspergillosis. *European Journal of Clinical Microbiology & Infectious Diseases*, **1996**. *15*(2): 139-145.

22. Storhoff, J. J.; Elghanian, R.; Mucic, R. C.; Mirkin, C. A. and Letsinger, R. L., One-pot colorimetric differentiation of polynucleotides with single base imperfections using gold nanoparticle probes. *J. Am. Chem. Soc*, **1998**. *120*(9): 1959–1964.

23. Hirsch, L. R.; Jackson, J. B.; Lee, A.; Halas, N. J. and West, J. L., A Whole Blood Immunoassay Using Gold Nanoshells. *Analytical Chemistry*, **2003**. *75*: 2377-2381.

24. Ho, Y. P.; Kung, M. C.; Yang, S. and Wang, T. H., Multiplexed Hybridization Detection with Multicolor Colocalization of Quantum Dot Nanoprobes. *Nano Lett*, **2005**. *5*(9): 1693-1697.

25. Agrawal, A.; Tripp, R. A.; Anderson, L. J. and Nie, S., Real-Time Detection of Virus Particles and Viral Protein Expression with Two-Color Nanoparticle Probes. *Journal of Virology*, **2005**.

26. Palmer, S.; Wiegand, A. P.; Maldarelli, F.; Bazmi, H.; Mican, J. A. M.; Polis, M.; Dewar, R. L.; Planta, A.; Liu, S. and Metcalf, J. A., New Real-Time Reverse Transcriptase-Initiated PCR Assay with Single-Copy Sensitivity for Human Immunodeficiency Virus Type 1 RNA in Plasma. *Journal of Clinical Microbiology*, **2003**. *41*(10): 4531-4536.

27. Niemeyer, C. M.; Adler, M. and Wacker, R., Immuno-PCR: high sensitivity detection of proteins by nucleic acid amplification. *Trends Biotechnol*, **2005**. *23*(4): 208-216.

28. Sano, T.; Smith, C. L. and Cantor, C. R., Immuno-PCR: very sensitive antigen detection by means of specific antibody-DNA conjugates. *Science*, **1992**. *258*(5079): 120.

29. Nam, J. M.; Thaxton, C. S. and Mirkin, C. A., Nanoparticle-Based Bio-Bar Codes for the Ultrasensitive Detection of Proteins. *Science*, **2003**. *301*(5641): 1884.

30. Valle, R. P.; Chavany, C.; Zhukov, T. A. and Jendoubi, M., New approaches for biomarker discovery in lung cancer. *Expert Rev Mol Diagn*, **2003**. *3*(1): 55-67.

31. Shuan-ying, Y.; Xue-yuan, X.; Wang-gang, Z.; Xiu-zhen, S. U. N.; Li-juan, Z.; Wei, Z.; Bin, Z.; Guo-an, C. and Da-cheng, H. E., Application of serum surface-enhanced laser desorption/ionization proteomic patterns in distinguishing lung cancer patients from healthy people. *Chinese Medical Journal*, **2005**. *118*(12): 1036-1039.

32. Yang, S.; Xiao, X.; Zhang, W.; Zhang, L.; Zhou, B.; Chen, G. and He, D., Application of serum SELDI proteomic patterns in diagnosis of lung cancer. *BMC Cancer*, **2005**. *2005*(5): 83.

33. Hanash, S., Disease proteomics. *Nature*, **2003**. *422*: 226-232.

34. Hanash, S. M.; Madoz-Gurpide, J. and Misek, D. E., Identification of novel targets for cancer therapy using expression proteomics. *Leukemia*, **2002**. *16*: 478-485.

35. Nilsson, C. L. and Davidsson, P., New separation tools for comprehensive studies of protein expression by mass spectrometry. *Mass Spectrometry Reviews*, **2000**. *19*(6): 390-397.

36. Arrio-Dupont, M.; Foucault, G.; Vacher, M.; Devaux, P. F. and Cribier, S., Translational Diffusion of Globular Proteins in the Cytoplasm of Cultured Muscle Cells. *Biophysical Journal*, **2000**. *78*(2): 901-907.

37. Ferrari, M., Cancer nanotechnology: opportunities and challenges. *Nat Rev Cancer*, **2005**. *5*(3): 161-171.

38. Grodzinski, P.; Silver, M. and Molnar, L. K., Nanotechnology for cancer diagnostics: promises and challenges. *Expert Review of Molecular Diagnostics*, **2006**. *6*(3): 307-318.

39. Cuenca, A. G.; Jiang, H.; Hochwald, S. N.; Delano, M.; Cance, W. G. and Grobmyer, S. R., Emerging implications of nanotechnology on cancer diagnostics and therapeutics. *Cancer*, **2006**.

40. Majumdar, A., Bioassays based on molecular nanomechanics. *Disease Markers*, **2002**. *18*(4): 167-174.

41. Wu, G.; Datar, R. H.; Hansen, K. M.; Thundat, T.; Cote, R. J. and Majumdar, A., Bioassay of prostate-specific antigen (PSA) using microcantilevers. *Nature Biotechnology*, **2001**. *19*(9): 856-860.

42. Su, M.; Li, S. and Dravid, V. P., Microcantilever resonance-based DNA detection with nanoparticle probes. *Applied Physics Letters*, **2003**. *82*(20): 3562-3564.

43. Yue, M.; Lin, H.; Dedrick, D. E.; Satyanarayana, S.; Majumdar, A.; Bedekar, A. S.; Jenkins, J. W. and Sundaram, S., A 2-D Microcantilever Array for Multiplexed Biomolecular Analysis. *JOURNAL OF MICROELECTROMECHANICAL SYSTEMS*, **2004**. *13*(2).

44. Bashir, R., BioMEMS: state-of-the-art in detection, opportunities and prospects. *Adv Drug Deliv Rev*, **2004**. *56*(11): 1565-1586.

45. Bashir, R., Nano-mechanical Resonantor Sensors for Virus Detection. *American Physical Society, APS March Meeting, March 21-25, 2005, abstract# A4. 005*, **2005**.

46. Gupta, A. K.; Nair, P. R.; Akin, D.; Ladisch, M. R.; Broyles, S.; Alam, M. A. and Bashir, R., Anomalous resonance in a nanomechanical biosensor. *Proc Natl Acad Sci US A*, **2006**.

47. Patolsky, F.; Zheng, G. and Lieber, C. M., Nanowire-based biosensors. *Anal Chem*, **2006**. *78*(13): 4260-9.

48. Zheng, G.; Patolsky, F.; Cui, Y.; Wang, W. U. and Lieber, C. M., Multiplexed electrical detection of cancer markers with nanowire sensor arrays. *Nature Biotechnology*, **2005**. *23*: 1294-1301.

49. Wang, W. U.; Chen, C.; Lin, K.; Fang, Y. and Lieber, C. M., Label-free detection of small-molecule-protein interactions by using nanowire nanosensors. *Proceedings of the National Academy of Sciences*, **2005**. *102*(9): 3208-3212.

50. Kong, J.; Franklin, N. R.; Zhou, C.; Chapline, M. G.; Peng, S.; Cho, K. and Dai, H., Nanotube Molecular Wires as Chemical Sensors. *Science*, **2000**. *287*(5453): 622-625.

51. Heath, J. R.; Phelps, M. E. and Hood, L., NanoSystems biology. *Molecular Imaging and Biology*, **2003**. *5*(5): 312-325.

52. Brakmann, S., DNA-Based Barcodes, Nanoparticles, and Nanostructures for the Ultrasensitive Detection and Quantification of Proteins. *Angewandte Chemie International Edition*, **2004**. *43*(43): 5730-5734.

53. Niemeyer, C. M., Functional Hybrid Devices of Proteins and Inorganic Nanoparticles. *Angewandte Chemie International Edition*, **2003**. *42*(47): 5796-5800.

54. Katz, E. and Willner, I., Integrated Nanoparticle-Biomolecule Hybrid Systems: Synthesis, Properties, and Applications. *Angew. Chem., Int. Ed*, **2004**. *43*: 6042-6108.

55. Smith, A. M.; Dave, S.; Nie, S.; True, L. and Gao, X., Multicolor quantum dots for molecular diagnostics of cancer. *Expert Review of Molecular Diagnostics*, **2006**. *6*(2): 231-244.

56. Alivisatos, P., The use of nanocrystals in biological detection. *Nature Biotechnology*, **2004**. *22*(1): 47-52.

57. Clapp, A. R.; Medintz, I. L.; Uyeda, H. T.; Goldman, E. R. and Mattoussi, H., Quantum-dot-based multiplexed fluorescence resonance energy transfer. *Proceedings of SPIE*, **2005**. *5704*: 69.

58. Clapp, A. R.; Medintz, I. L. and Mattoussi, H., Quantum dot-based fluorescence resonance energy transfer multiplexing: applications for biosensing. *Proceedings of SPIE*, **2006**. *6096*: 609601.

59. Drachev, V. P.; Nashine, V. C.; Thoreson, M. D.; Ben-Amotz, D.; Davisson, V. J. and Shalaev, V. M., Adaptive Silver Films for Detection of Antibody-Antigen Binding. *Langmuir*, **2005**. *21*(18): 8368-8373.

60. Chem, A., Biosensing Based on Light Absorption of Nanoscaled Gold and Silver Particles. *Anal. Chem*, **2003**. *75*: 6894-6900.

61. Riboh, J. C.; Haes, A. J.; McFarland, A. D.; Yonzon, C. R. and Van Duyne, R. P., A Nanoscale Optical Biosensor: Real-Time Immunoassay in Physiological Buffer Enabled by Improved Nanoparticle Adhesion. *J. Phys. Chem. B*, **2003**. *107*(8): 1772-1780.

62. Chien, F. C.; Chen, S. J.; Hu, W. P.; Lin, G. Y. and Huang, K. T., Nanoparticle-enhanced ultrahigh-resolution surface plasmon resonance biosensors. *Proceedings of SPIE*, **2004**. *5327*: 140.

63. Haes, A. J.; Stuart, D. A.; Nie, S. and Van Duyne, R. P., Using Solution-Phase Nanoparticles, Surface-Confined Nanoparticle Arrays and Single Nanoparticles as Biological Sensing Platforms. *Journal of Fluorescence*, **2004**. *14*(4): 355-367.

64. Stuart, D. A.; Haes, A. J.; McFarland, A. D.; Nie, S. and Van Duyne, R. P., Refractive index sensitive, plasmon resonant scattering, and surface enhanced Raman scattering nanoparticles and arrays as biological sensing platforms. *Proc. SPIE, Int. Soc. Opt. Eng*, **2004**. *5327*: 60–73.

65. Talley, C. E.; Huser, T. R.; Hollars, C. W.; Jusinski, L.; Laurence, T. and Lane, S. M. *Nanoparticle Based Surface-Enhanced Raman Spectroscopy*. in *NATO Advanced Study Institute: Biophotonics*. 2005. Ottawa, Canada.

66. Cao, Y. W. C.; Jin, R. and Mirkin, C. A., Nanoparticles with Raman Spectroscopic Fingerprints for DNA and RNA Detection. *Science*, **2002**. *297*(5586): 1536.

67. Mulvaney, P., Surface plasmon spectroscopy of nanosized metal particles. *Langmuir*, **1996**. *12*(3): 788-800.

68. Sastry, M.; Lala, N.; Patil, V.; Chavan, S. P. and Chittiboyina, A. G., Optical Absorption Study of the Biotin-Avidin Interaction on Colloidal Silver and Gold Particles. *Langmuir*, **1998**. *14*(15): 4138–4142.

69. Aslan, K.; Lakowicz, J. R. and Geddes, C. D., Nanogold-plasmon-resonance-based glucose sensing. *Anal. Biochem*, **2004**. *330*(1): 145–155.

70. Elghanian, R., Selective Colorimetric Detection of Polynucleotides Based on the Distance-Dependent Optical Properties of Gold Nanoparticles. *Science*, **1997**. *277*(5329): 1078-1081.

71. Guzelian, A. A.; Banin, U.; Kadavanich, A. V.; Peng, X. and Alivisatos, A. P., Colloidal chemical synthesis and characterization of InAs nanocrystal quantum dots. *Applied Physics Letters*, **1996**. *69*(10): 1432.

72. Micic, O. I.; Sprague, J. R.; Curtis, C. J.; Jones, K. M.; Machol, J. L.; Nozik, A. J.; Giessen, H.; Fluegel, B.; Mohs, G. and Peyghambarian, N., Synthesis and Characterization of InP, GaP, and GaInP2 Quantum Dots. *The Journal of Physical Chemistry*, **1995**. *99*(19): 7754-7759.

73. Wang, H.; Li, X.; Uehara, M.; Yamaguchi, Y.; Nakamura, H.; Miyazaki, M.; Shimizu, H. and Maeda, H., Continuous synthesis of CdSe–ZnS composite nanoparticles in a microfluidic reactor. *Chem. Commun*, **2004**. *1*: 48–9.

74. Talapin, D. V.; Rogach, A. L.; Kornowski, A.; Haase, M. and Weller, H., Highly luminescent monodisperse CdSe and CdSe/ZnS nanocrystals synthesized in a hexadecylamine-trioctylphosphine oxide-trioctylphospine mixture. *Nano Lett*, **2001**. *1*(4): 207-211.

75. Hines, M. A. and Guyot-Sionnest, P., Synthesis and characterization of strongly luminescing ZnS-capped CdSe nanocrystals. *J. Phys. Chem*, **1996**. *100*(2): 468-471.

76. Ebenstein, Y.; Mokari, T. and Banin, U., Fluorescence quantum yield of CdSe/ZnS nanocrystals investigated by correlated atomic-force and single-particle fluorescence microscopy. *Applied Physics Letters*, **2002**. *80*(21): 4033.

77. Underwood, D. F.; Kippeny, T. and Rosenthal, S. J., Ultrafast Carrier Dynamics in CdSe Nanocrystals Determined by Femtosecond Fluorescence Upconversion Spectroscopy. *J. Phys. Chem*, **2001**: 436-443.

78. Medintz, I. L.; Uyeda, H. T.; Goldman, E. R. and Mattoussi, H., Quantum dot bioconjugates for imaging, labelling and sensing. *Nat. Mater*, **2005**. *4*(6): 435-446.

79. Chan, W. C., Quantum Dot Bioconjugates for Ultrasensitive Nonisotopic Detection. *Science*, **1998**. *281*(5385): 2016-2018.

80. Mattoussi, H.; Mauro, J. M.; Goldman, E. R.; Anderson, G. P.; Sundar, V. C.; Mikulec, F. V. and Bawendi, M. G., Self-assembly of CdSe-ZnS quantum dot

bioconjugates using an engineered recombinant protein. *J. Am. Chem. Soc*, **2000**. *122*(49): 12142-12150.

81. Gerion, D.; Pinaud, F.; Williams, S. C.; Parak, W. J.; Zanchet, D.; Weiss, S. and Alivisatos, A. P., Synthesis and properties of biocompatible water-soluble silica-coated CdSe/ZnS semiconductor quantum dots. *Journal of Physical Chemistry B*, **2001**. *105*: 37.

82. Bruchez Jr, M., Semiconductor Nanocrystals as Fluorescent Biological Labels. *Science*, **1998**. *281*(5385): 2013-2016.

83. Dubertret, B., In Vivo Imaging of Quantum Dots Encapsulated in Phospholipid Micelles. *Science*, **2002**. *298*(5599): 1759-1762.

84. Goldman, E. R.; Balighian, E. D.; Mattoussi, H.; Kuno, M. K.; Mauro, J. M.; Tran, P. T. and Anderson, G. P., Avidin: a natural bridge for quantum dot-antibody conjugates. *J. Am. Chem. Soc*, **2002**. *124*(22): 6378–6382.

85. Chan, W. C. W.; Maxwell, D. J.; Gao, X.; Bailey, R. E.; Han, M. and Nie, S., Luminescent quantum dots for multiplexed biological detection and imaging. *Current Opinion in Biotechnology*, **2002**. *13*(1): 40-46.

86. Xu, H., Multiplexed SNP genotyping using the QbeadTM system: a quantum dot-encoded microsphere-based assay. *Nucleic Acids Research*, **2003**. *31*(8): 43-43.

87. Goldman, E. R.; Clapp, A. R.; Anderson, G. P.; Uyeda, H. T.; Mauro, J. M.; Medintz, I. L. and Mattoussi, H., Multiplexed toxin analysis using four colors of quantum dot fluororeagents. *Anal. Chem*, **2004**. *76*(3): 684-688.

88. Gao, X.; Chan, W. C. W. and Nie, S., Quantum-dot nanocrystals for ultrasensitive biological labeling and multicolor optical encoding. *Journal of Biomedical Optics*, **2002**. *7*(4): 532-537.

89. Goldman, E. R.; Medintz, I. L. and Mattoussi, H., Luminescent quantum dots in immunoassays. *Analytical and Bioanalytical Chemistry*, **2006**. *384*(3): 560-563.

90. Liu, G.; Wang, J.; Kim, J.; Jan, M. R. and Collins, G. E., Electrochemical Coding for Multiplexed Immunoassays of Proteins. *Analytical chemistry(Washington, DC)*, **2004**. *76*(23): 7126-7130.

91. Thanh, N. T. K. and Rosenzweig, Z., Development of an aggregation-based immunoassay for anti-protein A using gold nanoparticles. *Anal. Chem*, **2002**. *74*(7): 1624-1628.

92. Wang, F.; Tan, W. B.; Zhang, Y.; Fan, X. and Wang, M., Luminescent nanomaterials for biological labelling. *Nanotechnology*, **2006**. *17*: R1-R13.

CHAPTER II

QUANTUM DOT SELF-ASSEMBLY FOR PROTEIN DETECTION WITH SUB-PICOMOLAR SENSITIVITY

Summary

A novel approach to sensitive and rapid antigen detection is described. In the presence of a specific antigen, quantum dot-antibody conjugates rapidly self-assemble into agglomerates that are typically more than one order of magnitude larger than their individual components. The size distribution of the agglomerated colloids depends on, among other things, the relative concentration of quantum dot conjugates and antigen molecules. Quantum dot agglomerates mediated by antigen recognition were characterized by measuring their light scattering and fluorescence characteristics in an unmodified flow cytometer. Protein antigens angiopoietin-2 and mouse IgG were detected to sub picomolar concentrations using this method. This simple technique enables the potential simultaneous detection of multiple antigenic biomarkers directly from physiological media and could be used for early detection and frequent screening of cancers and other diseases.

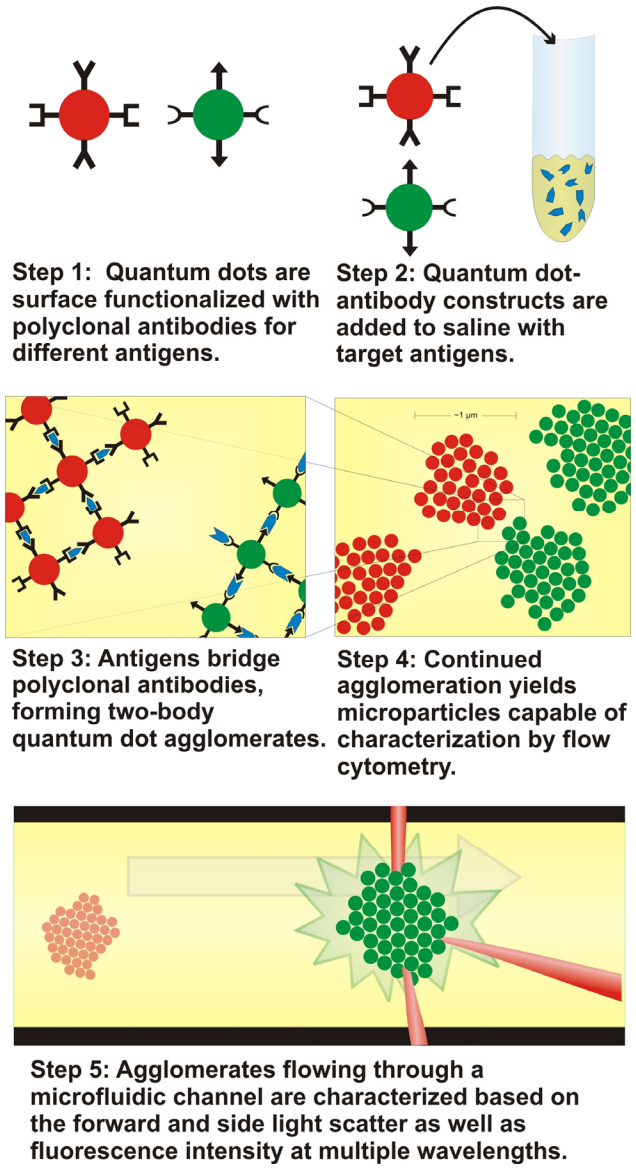

Figure 1. Schematic depiction of antigen detection by molecular interaction mediated self assembly. Multivalent interactions between molecular recognition elements such as antibody-antigen, complementary polynucleotide sequences, or aptamer-target could provide a simple technique for analyte detection. The capture molecules for different analytes can be conjugated with quantum dots with different fluorescence emission characteristics to enable multiplexed detection such as for biomarker panels. The analyte molecules mediate directed self-assembly of the quantum dot conjugates. The size distribution of these conjugates is proportional to the amount of analyte molecules present when other factors affecting self-assembly such as QD concentration and incubation period are constant. With techniques such as flow cytometry, a sophisticated and quantitative characterization of the colloidal solution is carried out, providing a simple, rapid and powerful technique for accurate quantification of analytes. Figure not to scale.

Introduction

The growing proteomic understanding of disease processes can be a powerful tool for diagnosing, prognosing and monitoring cancers and other medical conditions. An assay that detects multiple specific molecules from the complex mixture present in serum, and is rapid, sensitive and simple to administer, would be ideal for such an application. At present this is a practical, clinical challenge. Antibody-based recognition remains one of the most promising strategies for such applications but conventional approaches such as parallelized enzyme linked immunosorbent assay (ELISA), gel electrophoresis, and protein microarrays are suboptimal for point-of-care molecular profiling on the basis of cost, complexity, and speed.

Detection of pathogens by molecular recognition-based self-assembly of microspheres was proposed as far back as 1956 in the form of the semi-quantitative latex agglutination test[1], which is still used for detecting bacteria[2-4]. Nanoparticle-based agglutination tests utilizing surface plasmon resonance (SPR) shift have been recently demonstrated for the detection of DNA fragments[5] and proteins[6]. Biomolecules have also been detected using fluorescent semiconductor nanoparticles (quantum dots) by either spatial[7] or temporal[8] coincidence of multicolored quantum dot-antibody conjugates. Flow cytometric microsphere-based immunoassay (FMBA) has been proposed for the simultaneous detection of multiple proteins[9, 10]. FMBA assays are essentially antigen capture sandwich immunoassays on microspheres, and use microsphere size and/or fluorescence intensity as discriminating characteristics for multiplexing. Compared to these techniques, antigen mediated quantum dot

agglomeration combined with flow based detection on a microfluidic device, has the potential to offer better sensitivity, ease of use, speed, and cost of testing.

We demonstrate here this novel method for sensitive, simple, and rapid fluid phase detection of proteins based on simultaneous measurement of multiple properties of the colloidal mixture. Quantum dots (QDs) are conjugated with polyclonal antibodies (Ab) using a streptavidin-biotin interaction[11-13]. In the presence of the appropriate antigen molecules, these QD-Ab conjugates rapidly self-assemble into colloidal structures with sizes that are one to two orders of magnitude larger than the constituents (**Figure 1**). The size, structure and fluorescence characteristics of these self assembled structures are a function of the relative concentrations of the QD-Ab conjugates and the antigen molecules, among other factors. These attributes of the colloidal structures can be characterized by several techniques, including flow cytometry, dynamic light scattering, and electrical sensing zone or Coulter counter method. Flow cytometry is a powerful technique routinely used in biomedical laboratories for rapidly assessing multiple characteristics of a large population of cells and other microparticulates suspended in a hydrodynamically focused fluid stream[14]. The use of flow cytometers is common in clinical medicine, and the protein detection strategy described here could be adopted into clinical practice relatively easily. The basic principle of flow cytometric analysis can also be implemented on a microfluidic chip[15, 16], implying the ability to create a compact point-of-care diagnostic or field deployable analyte detection instrument. Conventional materials chemistry methods such as SPR shift assays measure the average spectral properties of the whole sample. By contrast, flow cytometry enables interrogation of virtually every individual particle in the sample and simultaneously

measures multiple characteristics such as forward light scatter, side light scatter, and fluorescence intensity at multiple wavelengths. This enables a sophisticated discrimination between individual events and detailed multiparametric mapping of the whole population. The detection of extremely rare events is thus possible, enabling detection of molecular analytes with high sensitivity and resolution. Furthermore, since flow cytometry is capable of detecting multiple flurophores, simultaneous QD based detection of multiple analytes could be achieved using different QD populations targeted for detection of different antigens.

The self assembled quantum dot structures generated in this study were detected based on their fluorescence intensity. The forward light scatter, side light scatter, and fluorescence emission at multiple wavelengths was recorded for each particle detected. The fraction of all events above a size threshold corresponding to 0.5 μm latex size standard spheres was proportional to the antigen concentration. One antigen used in these experiments was human angiopoietin-2 (ang-2), a 66kDa protein involved in neo-angiogenesis[17, 18]. Due to the importance of neo-angiogenesis in the proliferation of various cancers, ang-2 is a protein of interest as cancer marker and therapy target[19, 20] and has also been shown to correlate with the invasiveness and growth of various cancers[17, 21-23]. Detection of mouse IgG (mus) is also demonstrated using the same method.

The antigens in this study were detected to sub-picomolar concentration, comparable to the detection of the same molecules by conventional techniques such as ELISA or Western blot. Thus, the agglomeration based detection strategy is already comparable to conventional immunorecognition techniques in terms of sensitivity. The

flow based detection approach also enables characterization of multiple properties of individual self assembled structures, thus providing a tool for investigating self-assembly in a novel and powerful manner, which may lead to insights into this important nanoscale phenomenon.

Experimental

Materials

Streptavidin-coated quantum dots with 705 nm (#Q10161MP), 585 nm (#Q10111MP), and 525 nm (#Q10141MP) emission wavelengths were purchased from Invitrogen (Carlsbad, CA) and used as received for flow cytometry, bulk agglomeration fluorescence and dynamic light scattering experiments respectively. Biotin conjugated anti-angiopoietin-2 polyclonal antibody (anti-ang-2) (#BAF623) and recombinant human angiopoietin-2 (ang-2) (#623-AN-025) were purchased from R&D Systems (Minneapolis, MN), reconstituted in Tris-buffered saline (TBS) containing 0.1% bovine serum albumin (BSA). Mouse IgG (mus) (#23873), human IgG (hum) (#23872) and rabbit IgG (rab) (#23874) were purchased from Polysciences Inc (Warrington, PA), and reconstituted in 1x phosphate buffered saline (PBS). All reconstituted samples were aliquoted and stored at - 20°C. The aliquots were thawed and diluted to appropriate concentration using the PBS with 0.1% BSA (PBS-BSA) immediately prior to use. Biotin conjugated goat-anti-mouse IgG (GaM) (#553999) was purchased from BD Biosciences (San Jose, CA) and stored at 4°C. All other chemicals used were ACS reagent grade. 10mM borate buffer was used for Zetasizer and bulk fluorescence measurement

experiments. Buffers were prepared in deionized water, and filtered through a 0.2 μm filter prior to use.

Flow cytometric measurements were carried out on Beckton Dickinson (BD) FACSCalibur. BD FACSAria and BD LSR II flow cytometers were also used for optimizing detection parameters. Bulk fluorescence was measured in BioTek (Winooski, VT) Synergy HT multi-detection microplate reader. Dynamic light scatter (DLS) measurements were carried out on a Malvern Instruments (Malvern, UK) Zetasizer Nano ZS. Fluorescence measurements were carried out in a Nanodrop Technologies (Wilmington, DE) ND-3300 fluorospectrometer.

Quantum dot-antibody conjugation

The quantum dot-streptavidin conjugates (QD) and biotinylated anti-angiopoietin-2 polyclonal antibody (anti-ang-2) or biotinylated goat-anti-mouse polyclonal antibody (GaM) were mixed in PBS-BSA at QD:antibody molar ratio of 1:3 and 1nM QD concentration. The conjugation was monitored by particle size estimation in the reaction mixture by DLS. The conjugate was diluted to appropriate concentrations and used immediately after synthesis.

Antigen Induced Self Assembly

The QD-antibody (QD-Ab) conjugate solution and the antigen or control solution at the appropriate dilutions and volumes were added to PBS-BSA for a total volume of 1 mL. BSA, similar to ang-2 in terms of molecular weight, also acted as a negative control for ang-2. Rab and hum were used as negative control for mus. The reaction mixtures

were incubated at room temperature for 60 minutes and then analyzed by flow cytometry. Baseline event distribution of QD-Ab dispersed in PBS-BSA was also analyzed.

Results and Discussion

The candidate cancer biomarker protein, ang-2, was detected by flow cytometry to 0.5 pM concentration. Event classification between aggregates and individual particles was based on the observed bimodal population distribution. The forward scatter histogram (**Figure 3.b**), suggests that forward light scatter intensity of 10 a.u. is a suitable threshold value for this demarcation. The optimal side scatter threshold value of 10 a.u. was similarly identified. The fraction of events classified as aggregates were 10.1+/-2.2%, compared to the background control aggregate formation of 1.2+/-0.2%. The relationship between aggregate formation and concentration of ang-2 ([ang-2]) followed a log-linear correlation over the range of antigen concentrations from 0.5 pM to 100pM when detected with 10pM QD-AA2, and from 500 pM to 50000 pM when detected with 100pM QD-AA2 (**Figure 2**). The slopes of these relationship enabled resolution of [ang-2] between 0.5 pM and 50000 pM. Antigen concentration resolution in the 0.5 pM to 100 pM range is significantly higher based on the numerically greater slope of the log-linear curve fit to the data. The maximum detected [ang-2] was 50000 pM, limited primarily by the concentration of ang-2 stock available. Literature reports of [ang-2] detected in serum range from 23 to 44 pM[24], within the high resolution range of measurement with this QD agglomeration technique. Similarly, serum concentrations of

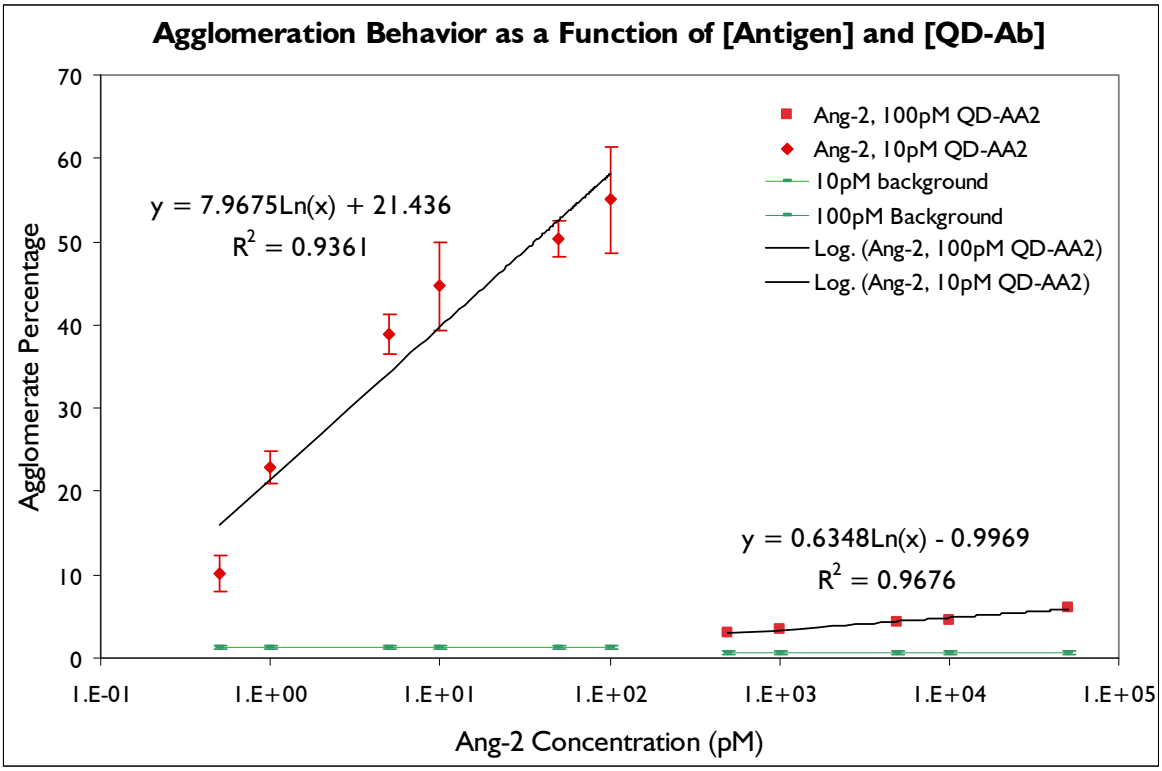

Figure 2. Agglomeration behavior as a function of reagent concentrations. Ang-2 was detected down to 0.5pM using the QD agglomeration technique. The percent of total events detected that were categorized as agglomerates (Y axis) is a log-linear function of the antigen concentration (X axis). Since the number of agglomerates in the two component reaction is limited by the availability of either or both of the components, the function is linear over a limited range. Hence, the agglomeration behavior of the lower concentration range of ang-2 (0.5pM-100pM) was linear when detected with 10pM QD-AA2, while the higher concentration range of ang-2 (500pM to 50000pM) exhibited a log-linear agglomeration behavior with 100pM QD-AA2. Data points are mean+/- standard deviation, n=3.

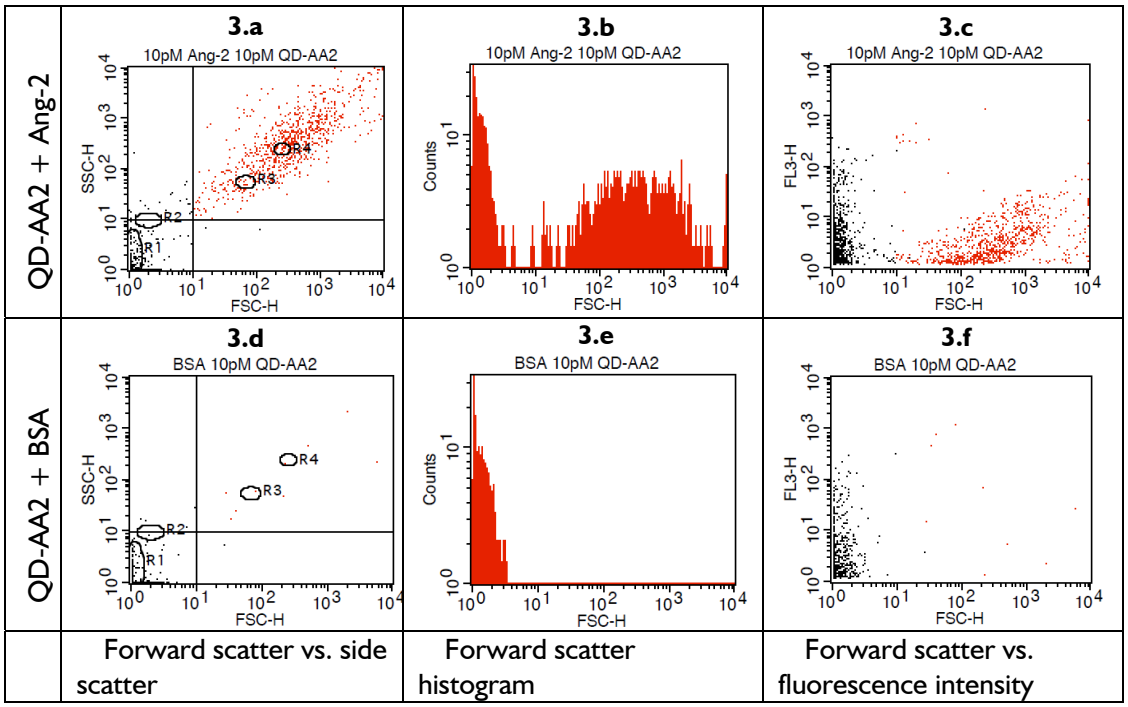

Figure 3. Flow cytometric data obtained by characterization of reaction mixtures. Flow cytometric detection of antigen is achieved by characterizing agglomerates as a fraction of total events. Each dot in panels a, d, c and f represents one particle or 'event' detected. Forward light scatter (FSC-H) and side light scatter (SSC-H) intensities are positively correlated with the size and complexity of the particles. In panels a and d, the ovals labeled R1 through R4 indicate standard latex beads of sizes 0.2, 0.5, 1.0, and 2.0 microns respectively, and provide an estimate of the diameter of the QD agglomerates detected. Panels b and e show the change in particle size distribution upon addition of the antigen. Panels c and f show the relation between fluorescence intensity (FL3) and size (FSC-H) for the agglomerates and the native QD-GaM respectively. The multivariate characterization of particles in the flow cytometer enables highly sophisticated analysis of the particles difficult to achieve by other methods including dynamic light scattering. This may increase the antigen detection sensitivity via better discrimination between specific and non specific self assembly. Detected values for the scatter and fluorescence intensities are digitized in1024 channels over the range of 1-10^4 a.u. Typical data obtained from one experiment from n=3.

other biomarkers are in the multi-picomolar range. Hence, exceeding the sensitivity of ELISA significantly is not an objective of the work presented, but is being pursued separately.

Mus, which was used as a model protein in the initial experiments to optimize the instrument detection parameters and experimental conditions was also detected by flow cytometry to 0.5 pM concentration. The fraction of events classified as aggregates was 1.0+/- 0.3%, compared to the negative control aggregate formation of 0.7+/-0.1%. Two different log-linear regimes were observed for aggregate formation, in a manner similar to that documented for ang-2. 10pM QD-GaM was used to detect mus from 0.5 pM to 500pM. 100pM QD-GaM was used to detect mus from 500 pM to 500,000 pM. The slope of these relationships effectivly enabled resolution of [mus] between 0.5pM and 500,000 pM. The use of different concentration of QD-GaM required for addressing this high range of concentrations is

The use of multiple reactions to detect a large range of analyte concentrations is comparable to other antibody based techniques, where separate reactions with optimized protocols and stoichiometry are often required to detect low concentration and high concentration of the same analyte. The incubation time for these experiments was optimized in preliminary studies. Initial experiments were carried out to characterize the kinetics of agglomeration by quantifying the fraction of all events indicating large agglomerates at several time points up to four hours. One hour incubation period was determined to be optimal based on rapid initial agglomeration leading to suitably high detection sensitivity in this time period. Since a differential signal is obtained with

identical reaction conditions for all samples, this detection protocol is suitable for quantitative detection of antigens.

These results indicate that the sensitivity of the QD agglomeration technique for ang-2 and mus is comparable to the limit using ELISA and Western blot [22, 23]. Mass spectroscopy, which is currently used for recognition of protein expression patterns, detects protein from clinical samples only semi-quantitatively [25], and is hence not directly comparable with the QD agglomeration technique. Furthermore, the sensitivity for target analytes in mass spectrometry is also highly variable with respect to molecular mass of the analyte, relative abundance compared to overall sample, and other factors. The clinical utility of any biomarker detection method depends on both sensitivity and selectivity, especially in complex mixtures such as serum. Positive results can be obtained when data are statistically different compared to the natural population variation in biomarker concentration, or by establishing personalized baseline values for significant biomarkers. The use of multiple biomarkers correlated with a single physiological state also increases predictive power of biomarkers significantly, compared to that of a single biomarker[26-29]. The suboptimal performance of prostate specific antigen (PSA) as a single marker for diagnosing and prognosing prostate cancer is a strong motivation for moving towards a multiple biomarker strategy for detecting disease.

The high sensitivity and selectivity of this technique is remarkable, especially considering the single step reaction mechanism, the short time required for the process, and ease of implementation compared to conventional techniques such as ELISA, Western Blot, 2D-GE, and mass spectrometry. These advantages suggest the possibility of further developing this method for sensitive, rapid, and economical point-of-care

proteomic diagnostics. The possibility of harnessing other types of intermolecular recognition reactions such as DNA-DNA, ligand-receptor, and aptamer-target suggests wider utility of this method, and is currently under investigation. Since the QD-Ab construct is modular, other types of nanoparticles may also be used in place of QDs and could enable alternate detection methods.

Polyvalent molecular recognition interactions between the reactants are required for the formation of self assembled structures in this manner. If only monoclonal antibodies were used, the QD-Ab-Antigen structures formed would be similar in size to the constituents, and thus harder to detect. To achieve polyvalent interactions, we have utilized quantum dots conjugated with polyclonal antibodies. However, monoclonal antibodies are also likely to be useful if the target antigen presents multiple copies of the epitope on its surface. While quantum dots with a single emission wavelength were used in these experiments to detect a single protein, preliminary evidence suggests that multiplexed protein detection using multiple quantum dot populations is also feasible. The studies reported here were conducted in samples of controlled and well-known composition. Biomarker detection capabilities in complex mixtures such as blood plasma are unknown. The performance of this approach for sensing biomarkers in clinical samples may be partially inferred from the control data and from the well known characteristics of immunorecognition methods such as ELISA which has a number of commonalities with the QD agglomeration method. Additional studies are required to characterize biomarker detection in serum using functionalized QDs and these are under way, but are not part of this work.

The percentage of self assembled agglomerates in a colloidal mixture can presumably be determined by flow cytometry using a variety of parametric combinations. We have utilized a combination of forward light scatter threshold and side light scatter threshold to demarcate agglomerates from smaller particles. The fraction of total events corresponding to the agglomerated sub-population serves as a metric correlated with antigen concentration. An example of the significant difference in the approximate size distribution of QD agglomerates mediated by ang-2 antigen in comparison with the BSA control appears as panels **3.b** and **3.e**, respectively. Forward light scatter intensity (FSC) is an approximate surrogate that is positively correlated with event diameter, suggesting that the addition of ang-2 mediates the formation of many aggregates significantly larger in diameter than can be triggered by the BSA control antigen. The correlation between forward light scatter and event size for this instrument is identified in panels **3.a** and **3.d** as the gated regions R1, R2, R3 and R4, which correspond to latex calibration sphere diameters of 0.2, 0.5, 1.0, and 2.0 μm, respectively. Events of these sizes are significantly larger than the diameter of antibody-functionalized QDs (**Figure 5**, approximately 0.045 μm, or 45 nm). Quadrant gating in the forward light scatter and side light scatter (SSC) space highlights events with diameters greater than approximately 0.5 μm (500 nm). The events in the upper right quadrant are highlighted in red and are defined to be QD agglomerates in this method. This gating also corresponds to the bimodal population distribution in the aggregated sample, as seen from the FSC histogram (panel **3.b**). The addition of 10pM ang-2 resulted in an agglomerate sub-population of 44% (panel **3.a**), significantly greater than the 1.2% mediated by addition of the control BSA antigen (panel **3.d**). The agglomerates

identified by forward light scatter intensity are also fluorescent in the FL3 wavelength range (650nm and longer), consistent with the fluorescence of QDs with an emission maxima of 705 nm (panels **3.c** and **3.f**). The fluorescence emission intensity of QD agglomerates is not a direct summation of the fluorescence emission intensities of each of the estimated 2500 QDs per agglomerate, suggesting that modulation of the excitation and/or fluorescence emission occurs in these agglomerates. Based on the expected structure of the agglomerates, the QD are likely to be separated by about 20nm. Hence, the cause of the quenching is unlikely to be based on fluorescence resonant energy transfer[30, 31]. However the formation of a network of QDs may reduce the intrinsic fluorescence quantum yield of each QD through modulation of the nanoscale surface characteristics. The large size and complex structure of the agglomerates may shield many of the QDs from the excitation light source, as well as trap emitted radiation, and hence part of the reason for the observed fluorescence quenching could be optical screening. While the exact mechanism of the fluorescence quenching is unclear, quenching upon agglomeration was confirmed separately by measuring the bulk fluorescence intensity (**Figure 4**) during the agglomeration reaction. The bulk fluorescence of reaction mixtures with different [mus] was observed over time in a plate reader. The fluorescence intensity of the mixture decreased with time for [mus]=666nM, the highest concentration of antigen used, while the reaction mixture with the negative control [hum]=666nM did not exhibit decreasing bulk fluorescence intensity.

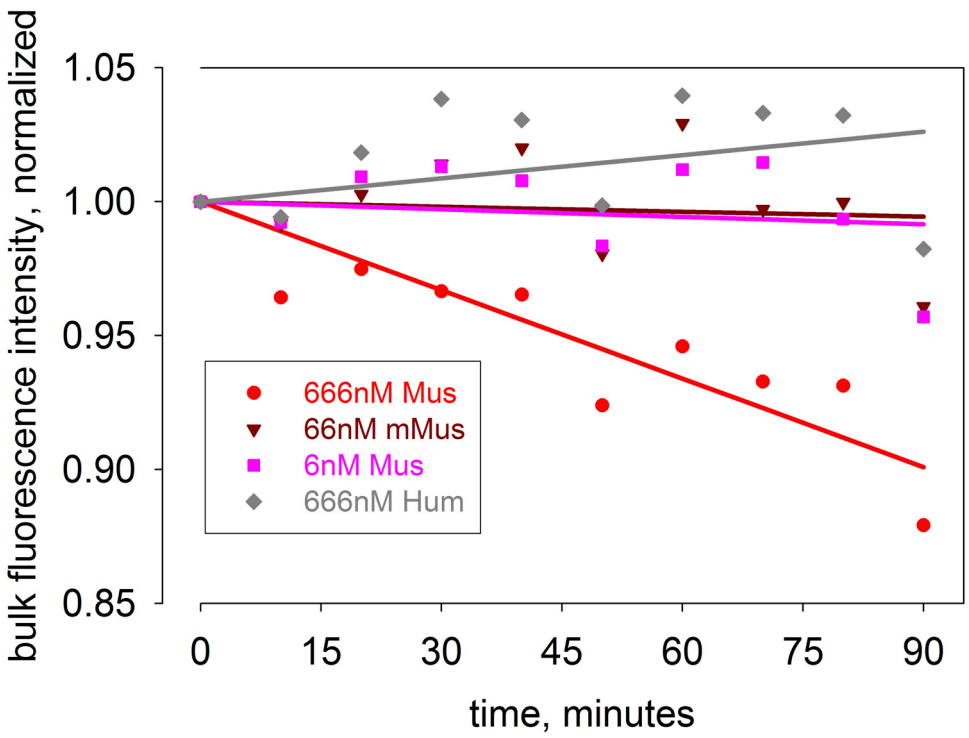

Figure 4. Modulation of bulk fluorescence of reaction mixture due to antigen induced self assembly of QD-Ab conjugates. The solution fluorescence intensity of 1nM QD-GaM solution decreases after addition mus, consistent with aggregation-modulated fluorescence quenching observed by flow cytometry. The largest decrease is seen in the sample containing the highest concentration of mus. Flow cytometric characterization of the same sample showed very high fraction of agglomerates. Optical screening of excitation and emission due to the large size and complex structures of the agglomerates, as well as modulation of nanoscale surface properties upon agglomeration are thought to be responsible for the observed fluorescence quenching. Data from one experiment, typical of the n=3.

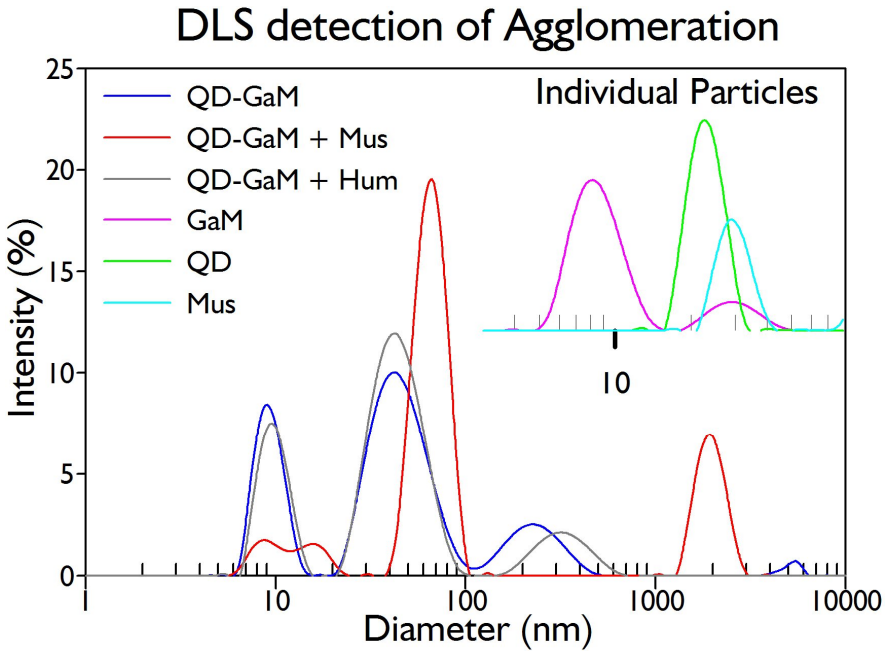

Figure 5. Dynamic light scattering characterization of antigen induced nanoparticle self-assembly. Nanoscale QDs surface functionalized with GaM antibody self-assemble into microscale agglomerates mediated by polyvalent antigen (red peak at 2,000 nm). Addition of nonspecific antigen (hum) fails to mediate large agglomerate formation (lack of grey peak > 700 nm).

The FL3-FSC representation (**3.c, 3.f**) provides an example of how the multiparametric data obtained from the flow cytometer enables sophisticated analysis of the sample, and may increase signal to noise ratio and sensitivity of detection. In this instance, two different populations of particles appear in the upper-right quadrant of the FSC-SSC space (**3.a**) but can not be distinguished from each other. However, in the forward scatter-fluorescence space (**3.c**), the non-specific agglomerates can be easily separated from the antigen mediated agglomerates. Most QD-AA2-ang2 agglomerates have high forward scatter and low fluorescence intensity (panel **3.c**). While the volume of these agglomerates is about 250-fold greater than the individual QD-AA2 agglomerates, the fluorescence intensity is only 3-fold greater. A very small fraction of particles (less than 0.1%) in this agglomerated sample show high FSC as well as high FL3 intensities. These anomalous events are likely due to electronic noise as well as non-specific agglomeration between QD-AA2 conjugates. While these two populations appear in the same region on the FSC-SSC plot (**3.a**), they can be easily distinguished from each other in the FL3-FSC representation (**3.c**). In samples where a higher concentration of the QD-Ab conjugate is used, the number of these anomalous events is even larger. Combined with the smaller overall fraction of the agglomerate population in these samples, the increased utility of the multiparametric characterization to increase signal to noise ratios and detection sensitivity is apparent.

The graphical representation of the flow cytometric data (**Figure 3**) also suggests that further improvement in the detection sensitivity may be achievable by fine tuning the threshold used here to demarcate agglomerates from non-agglomerates. Furthermore, while measuring the fraction of particles larger than a threshold is a simple way of

quantifying agglomeration, it does not take into account the full complexity of the self-assembly phenomenon. Detection sensitivity and resolution may also improved by creating sophisticated data processing algorithms that correlate antigen concentration with other measurable parameters such as agglomerate size distribution, population distribution in the light scatter vs. fluorescence intensity space, and kinetic measurement of the agglomeration. Using flow cytometry, these parameters can be easily measured for each of the particles. This may enable sophisticated and quantitative characterization of the agglomeration and hence sophisticated, automated, and simultaneous detection of multiple antigens.

Other parameters including antigen-antibody binding energies, fluid mixing energy and duration, and presence of non-specific reactants are also important to the characteristics of the agglomerates formed. In this work, time and relative concentration of QD and antigen was optimized based on measured aggregate formation, but the optimization of the reaction with respect to the other parameters is ongoing. The current data represents a system in equilibrium, but the final state may not provide optimum biomarker detection sensitivity. The kinetics of QD aggregate formation are presumably influenced in a multivariate way that is currently under investigation. Temporal differences in QD aggregate formation mediated by specific and nonspecific interactions are expected based on the range of immunorecognition kinetic parameters. The translation of a traditional kinetic ELISA approach to the present system is particularly elegant since each QD aggregate event is time-stamped during flow cytometric detection. In this way, additional discrimination between QD aggregation mediated by specific biomarker and nonspecific interactions may be achieved, improving

the sensitivity and selectivity of the proposed method. Parameters such as temperature, pH and ion concentration are also expected to have some effect on the agglomeration behavior. The characterization of the effects of these parameters is currently under way, however, the current reaction media was chosen to closely approximate the properties expected from a physiological sample such as serum.

In addition, the flow cytometric detection strategy influences the sensitivity of QD aggregate detection; optimization of triggering and amplification settings has been performed to obtain the results presented here, but additional improvements are likely with continued refinement. Preliminary investigation indicates that increased laser power, shorter excitation laser wavelengths, and better detection optics may provide significantly improved biomarker detection sensitivity. Improved understanding of QD aggregate detection by flow cytometry, a nonlinear optical process, may yield new approaches to improved biomarker detection performance through adjustment of instrument settings.

The AA2-ang2 and GaM-mus systems were both characterized by flow cytometry as well as DLS. Particle size and aggregation data measured by both modalities correlate well within each system. The data from flow cytometric characterization of the AA2-ang2 system and DLS characterization of GaM-mus system are shown in the interest of brevity. Preparation of the QD-Ab conjugates was monitored using a DLS particle sizer. Successful preparation of the QD-GaM conjugates was indicated by a shift in particle diameter from 25nm representing the unmodified QD to 45nm indicative of the formation of QD-GaM conjugates (**Figure 5**). This shift was not observed when QD were treated with the same volume of TBS-BSA. A similar change in particle size

distribution was observed upon conjugation of anti-ang-2 and QD. DLS measurements were also used to verify agglomeration in the presence of the antigen. The addition of Mus to the QD-GaM solution resulted in the formation of a new peak at 2000nm, indicating the formation of large agglomerates. The agglomerates are up to two orders of magnitude larger than the individual constituents, and as verified also by other methods including flow cytometry and electrical sensing zone method (data not shown). When the negative control antigen (hum) was added, this large peak was not observed in the DLS data, verifying the hypothesis that agglomeration occurs primarily by specific antibody-antigen recognition, rather than by other non-specific interactions.

Conclusions

In conclusion, we have demonstrated a novel antigen detection technique based on fundamental nanoscale phenomena. This technique has several advantages over conventional antigen detection strategies due to the use of solution phase biofunctionalized quantum dots and a microfluidics based detection strategy. Sensitive detection was carried out completely in the fluid phase, in a single step and with minimal incubation. In this work, we have separately detected two different proteins with high sensitivity and specificity. Simultaneous detection of multiple proteins from a complex mixture such as a serum is currently being investigated. The cross reactivity of antibodies as well as non-specific reactions both lead to agglomeration, and may limit sensitivity in these scenarios. These limits may be overcome through use of sample processing techniques from conventional immunorecognition methods as well as sophisticated methods for acquisition and processing of the data, including kinetic measurements,

which is not possible with other detection methods. Our technique requires minimal sample volume, is amenable to multiplexing, automation and implementation in a microfluidic chip, and is completely modular, making it an ideal candidate as a platform technology for frequent and low cost proteomic testing and monitoring of cancers, as well as an advanced point-of-care diagnostic based on a diverse array of intermolecular recognition based biomarker sensing.

References

1. Plotz, C. M. and Singer, J. M., The latex fixation test. I. Application to the serologic diagnosis of rheumatoid arthritis. *Am J Med*, **1956**. *21*(6): 888-92.

2. March, S. B. and Ratnam, S., Latex agglutination test for detection of Escherichia coli serotype O157. *Journal of Clinical Microbiology*, **1989**. *27*(7): 1675-1677.

3. van Griethuysen, A.; Pouw, M.; van Leeuwen, N.; Heck, M.; Willemse, P.; Buiting, A. and Kluytmans, J., Rapid Slide Latex Agglutination Test for Detection of Methicillin Resistance in Staphylococcus aureus. *Journal of Clinical Microbiology*, **1999**. *37*(9): 2789-2792.

4. Sulahian, A.; Tabouret, M.; Ribaud, P.; Sarfati, J.; Gluckman, E.; Latgé, J. P. and Derouin, F., Comparison of an enzyme immunoassay and latex agglutination test for detection of galactomannan in the diagnosis of invasive aspergillosis. *European Journal of Clinical Microbiology & Infectious Diseases*, **1996**. *15*(2): 139-145.

5. Storhoff, J. J.; Elghanian, R.; Mucic, R. C.; Mirkin, C. A. and Letsinger, R. L., One-pot colorimetric differentiation of polynucleotides with single base imperfections using gold nanoparticle probes. *J. Am. Chem. Soc*, **1998**. *120*(9): 1959–1964.

6. Hirsch, L. R.; Jackson, J. B.; Lee, A.; Halas, N. J. and West, J. L., A Whole Blood Immunoassay Using Gold Nanoshells. *Analytical Chemistry*, **2003**. *75*: 2377-2381.

7. Ho, Y. P.; Kung, M. C.; Yang, S. and Wang, T. H., Multiplexed Hybridization Detection with Multicolor Colocalization of Quantum Dot Nanoprobes. *Nano Lett*, **2005**. *5*(9): 1693-1697.

8. Agrawal, A.; Tripp, R. A.; Anderson, L. J. and Nie, S., Real-Time Detection of Virus Particles and Viral Protein Expression with Two-Color Nanoparticle Probes. *Journal of Virology*, **2005**.

9. Camilla, C.; Mely, L.; Magnan, A.; Casano, B.; Prato, S.; Debono, S.; Montero, F.; Defoort, J. P.; Martin, M. and Fert, V., Flow Cytometric Microsphere-Based Immunoassay: Analysis of Secreted Cytokines in Whole-Blood Samples from Asthmatics. *Clinical and Vaccine Immunology*, **2001**. *8*(4): 776-784.

10. Kellar, K. L. and Iannone, M. A., Multiplexed microsphere-based flow cytometric assays. *Exp Hematol*, **2002**. *30*(11): 1227-37.

11. Goldman, E. R.; Balighian, E. D.; Mattoussi, H.; Kuno, M. K.; Mauro, J. M.; Tran, P. T. and Anderson, G. P., Avidin: a natural bridge for quantum dot-antibody conjugates. *J. Am. Chem. Soc*, **2002**. *124*(22): 6378–6382.

12. Howarth, M.; Takao, K.; Hayashi, Y. and Ting, A. Y., Targeting quantum dots to surface proteins in living cells with biotin ligase. *Proceedings of the National Academy of Sciences*, **2005**. *102*(21): 7583-7588.

13. Gao, X.; Chan, W. C. W. and Nie, S., Quantum-dot nanocrystals for ultrasensitive biological labeling and multicolor optical encoding. *Journal of Biomedical Optics*, **2002**. *7*(4): 532-537.

14. Shapiro, H. M., *Practical flow cytometry*. 2003: Wiley-Liss New York.

15. Eyal, S. and Quake, S. R., Velocity-independent microfluidic flow cytometry. *Electrophoresis*, **2002**. *23*(16): 2653-2657.

16. Yao, B.; Luo, G.; Feng, X.; Wang, W.; Chen, L. and Wang, Y., A microfluidic device based on gravity and electric force driving for flow cytometry and fluorescence activated cell sorting. *Lab Chip*, **2004**. *4*: 603-607.

17. Lobov, I. B.; Brooks, P. C. and Lang, R. A., Angiopoietin-2 displays VEGF-dependent modulation of capillary structure and endothelial cell survival in vivo. *Proceedings of the National Academy of Sciences*, **2002**. *99*(17): 11205-11210.

18. Maisonpierre, P. C.; Suri, C.; Jones, P. F.; Bartunkova, S.; Wiegand, S. J.; Radziejewski, C.; Compton, D.; McClain, J.; Aldrich, T. H. and Papadopoulos, N., Angiopoietin-2, a natural antagonist for Tie2 that disrupts in vivo angiogenesis. *Science*, **1997**. *277*(5322): 55-60.

19. Carmeliet, P. and Jain, R. K., Angiogenesis in cancer and other diseases. *Nature*, **2000**. *407*(6801): 249-257.

20. Polanski, M. and Anderson, N. L., A List of Candidate Cancer Biomarkers for Targeted Proteomics. *Biomarker Insights*, **2006**. *2*.

21. Tanaka, S.; Mori, M.; Sakamoto, Y.; Makuuchi, M.; Sugimachi, K. and Wands, J. R., Biologic significance of angiopoietin-2 expression in human hepatocellular carcinoma. *Journal of Clinical Investigation*, **1999**. *103*(3): 341-345.

22. Ahmad, S. A.; Liu, W.; Jung, Y. D.; Fan, F.; Reinmuth, N.; Bucana, C. D. and Ellis, L. M., Differential expression of angiopoietin-1 and angiopoietin-2 in colon carcinoma. *Cancer*, **2001**. *92*(5): 1138-1143.

23. Audero, E.; Arisio, R.; Bussolino, F.; Sismondi, P. and De Bortoli, M., Angiopoietin-2 expression in breast cancer correlates with lymph node invasion and short survival. *Int. J. Cancer*, **2003**. *103*: 466-474.

24. Niedzwiecki, S.; Stepien, T.; Kopec, K.; Kuzdak, K.; Komorowski, J.; Krupinski, R. and Stepien, H., Angiopoietin 1 (Ang-1), angiopoietin 2 (Ang-2) and Tie-2 (a

receptor tyrosine kinase) concentrations in peripheral blood of patients with thyroid cancers. *Cytokine*, **2006**. *36*(5-6): 291-295.

25. Aebersold, R. and Mann, M., Mass spectrometry-based proteomics. *Nature*, **2003**. *422*: 198-207.

26. Roboz, J., Mass Spectrometry in Diagnostic Oncoproteomics. *Cancer Investigation*, **2005**. *23*(5): 465-478.

27. Calvo, K. R.; Liotta, L. A. and Petricoin, E. F., Clinical Proteomics: From Biomarker Discovery and Cell Signaling Profiles to Individualized Personal Therapy. *Bioscience Reports*, **2005**. *25*(1/2): 107-125.

28. Meyerson, M. and Carbone, D., Genomic and Proteomic Profiling of Lung Cancers: Lung Cancer Classification in the Age of Targeted Therapy. *Journal of Clinical Oncology*, **2005**. *23*(14): 3219-3226.

29. Petricoin, E. F. and Liotta, L. A., Proteomic approaches in cancer risk and response assessment. *Trends Mol Med*, **2004**. *10*(2): 59-64.

30. Kagan, C. R.; Murray, C. B.; Nirmal, M. and Bawendi, M. G., Electronic Energy Transfer in CdSe Quantum Dot Solids. *Physical Review Letters*, **1996**. *76*(9): 1517-1520.

31. Micic, O. I.; Jones, K. M.; Cahill, A. and Nozik, A. J., Optical, electronic, and structural properties of uncoupled and close-packed arrays of InP quantum dots. *J. Phys. Chem. B*, **1998**. *102*: 9791–9796.

CHAPTER III

SENSITIVE AND MULTIPLEXED DETECTION OF PROTEOMIC ANTIGENS VIA QUANTUM DOT AGGREGATION

Summary

A rapid, single step, solution phase method for quantifying multiple proteomic biomarkers is described. Nanoscale quantum dot-antibody conjugates self-assemble into microscale aggregates in the presence of a specific antigen through antibody-antigen molecular recognition. These aggregates are easily discriminated from the individual components by flow cytometry. Quantum dot aggregates can be quantified and correlated to the antigen concentration. Two quantum dot populations with distinct emission spectra are used for detecting two proteomics antigens in a single reaction volume. Multiplexed detection of vascular endothelial growth factor A and angiopoietin-2 is demonstrated at the physiologically relevant, picomolar concentration range. Non-multiplexed detection of the antigens is also demonstrated, with a femtomolar sensitivity limit. This technique may be optimized for low cost early detection and frequent screening of cancers and other diseases as well as detection of the biological response to therapy.

Introduction

Research in functional genomics and proteomics is leading to the discovery and clinical validation of a large number of molecular biomarkers. These markers are thought to be associated with specific diseases, variants and disease progression states. Biomarker-based understanding of a many pathologies is poised to significantly improve patient outcomes for a many major diseases including cancers, Alzheimer's disease, vascular pathologies and others. It is expected that techniques based on molecular biomarkers will be used for screening, early diagnosis, frequent monitoring, and personalized therapy management of diseases in the coming decades.

Conventional protein detection technologies that are currently used in research settings are not optimal for frequent diagnostic applications. These methods, such as mass spectrometry, ELISA assays, 2D-PAGE and others, are used for identifying and validating proteomic biomarkers, but fall short on one or more of the important parameters of speed, sensitivity, multiplexing capability or production of quantitative data. Perhaps most important from the point of view of clinical utility, ease of implementation and cost are not favorable for these techniques due to the requirement for highly trained personnel and difficulties in automation.

A variety of nanoscale and microscale technologies have been proposed and demonstrated over the last few years for efficient and cost effective detection of molecular biomarkers from biological samples. These techniques take advantage of a variety of nanostructures including micro-cantilevers[1], metallic, semiconductor or polymer nanoparticles[2], carbon nanotubes[3] and more[4].

In a recent publication, we have demonstrated a sensitive, rapid, single step, solution phase antigen detection technique based on nanoparticle self assembly and flow cytometry[5]. Quantum dots (QDs) were conjugated with polyclonal antibodies (Ab) using a streptavidin-biotin interaction[6]. In the presence of the appropriate antigen molecules (mouse IgG and angiopoietin-2) these QD-Ab conjugates rapidly self-assembled into colloidal structures with sizes one to two orders of magnitude larger than the constituents (quantum dot-antibody (QD-Ab) conjugates and proteomic antigens). The proportion of these self assembled structures to the total events counted by flow cytometry was shown to be a function of the relative concentrations of the QD-Ab conjugates and the antigen molecules, among other factors. The quantification of these microscale aggregates was easily achieved on a conventional flow cytometer. We also proposed that due to the multiparametric characterization capabilities of flow cytometers, it would be possible to detect multiple antigens from a single sample using QDs with distinct emissions spectra.

In the present paper we extend our previous work to demonstrate multiplexed detection of two proteomic antigens. Angiopoietin-2 and vascular endothelial growth factor A were detected simultaneously in the 1 pM to 100 pM concentration range using two QD-Ab conjugates with distinct emissions spectra. The detection sensitivity limit for non-multiplexed detection is also improved, by an order of magnitude improvement compared to the previous work, to 50 fM. The detection of two distinct aggregate populations was achieved by optimizing flow cytometric data acquisition parameters to minimize the baseline noise that occurs due to non specific antigen-antibody reactions as well as uncertainties in measuring QD aggregate fluorescence with the flow cytometer. It

is expected that multiplexed antigen detection sensitivity can be improved to approach the individual antigen detection sensitivity by improving sample preparation and modifying data acquisition parameters.

Detection of pathogens by molecular recognition-based self-assembly was proposed as far back as 1956 in the form of the latex agglutination test[7], which is still used for detecting bacteria[8-10], and for determining blood types, but is unsuitable for sensitive detection of low concentration small molecules. Nanoparticle-based variants of the agglutination test have been demonstrated for small molecules such as DNA fragments[11] and proteins[12]. In both these demonstrations, the change in plasmon resonance due to self assembly of the metal nanostructures was spectroscopically monitored. Small molecules have also been detected using quantum dots using antibody-mediated coincidence of multiple quantum dots with different emission wavelengths[13, 14]. Flow cytometric microsphere-based immunoassay (FMBA) has been proposed for the simultaneous detection of multiple proteins[15, 16]. FMBA assays are essentially antigen capture sandwich immunoassays on microspheres, and use microsphere size and/or fluorescence intensity as discriminating characteristics for multiplexing. Compared to these techniques, antigen mediated quantum dot agglomeration demonstrated here, combined with flow based detection on a microfluidic device, has the potential to offer better sensitivity, ease of use, speed, and cost of testing.

The multiplexed detection of two candidate cancer biomarkers involved in angiogenesis is demonstrated in this paper. It has been demonstrated that the use of biomarker panels – multiple biomarkers evaluated concurrently - results in a significantly improved diagnostic and prognostic performance compared to the use of a single

proteomic biomarker single discriminating protein [17-19]. One of the biomarkers evaluated in this paper is vascular endothelial growth factor A (VEGF), a 21 kDa protein. VEGF is a strong angiogenetic factor, and elevated serum levels have been detected in melanoma, pituitary, colorectal, breast, and prostate cancers[20]. In the control population, mean plasma VEGF concentration quoted in the literature is 1-9 pM, and in the presence of cancer, the mean value increases to 15-24 pM, based on the type and stage of the cancer studied[20, 21]. The other biomarker evaluated in this paper is angiopoietin-2 (ang-2), a 66kDa protein, is involved in neo-angiogenesis[22, 23]. Due to the importance of neo-angiogenesis in the proliferation of various cancers, ang-2 is a protein of interest as cancer marker and therapy target[24, 25] and has also been shown to correlate with the invasiveness and growth of various cancers[22, 26] The mean normal physiological plasma concentration of ang-2 is 22 pM for females, while elevated concentration for female breast cancer patients is 30 pM. In males, the mean concentration in control population is 20 pM, and mean elevated concentration for prostate cancer patients is about 40 pM[27].

The molecular recognition mediated self assembly utilized in this technique is not directly affected by the choice of nanoparticle in the nanoparticle-antibody conjugate probe used. However, QDs present an ideal combination of properties that make them an excellent choice for this application. The unique fluorescence properties of QDs [28-31] facilitate detection of aggregates as well as discrimination from other microparticulates that may be present in solution. Surface modification for biological applications - including conjugation with proteins and antibodies [6, 32, 33] and

multiplexed biological applications [34-36] have been well explored. Hence, QDs are widely recognized to be suitable for *ex-vivo* diagnostic technology[37, 38].

Experimental

Materials

Streptavidin-coated quantum dots with 705 nm (QD705, #Q10161MP) and 585 nm (QD585, #Q10111MP) fluorescence emissions were purchased from Invitrogen (Carlsbad, CA) and used as received. Biotin conjugated anti-angiopoietin-2 polyclonal antibody (aA2, #BAF623), biotin conjugated anti-VEGF polyclonal antibody (aVEGF, #BAF293), recombinant human angiopoietin-2 (Ang2, #623-AN), and recombinant human vascular endothelial growth factor A (VEGF, #293-VE) were purchased from R&D Systems (Minneapolis, MN), reconstituted in Tris-buffered saline (TBS) containing 0.1% bovine serum albumin (BSA) and stored at -20°C. Appropriate dilutions of all antibodies and antigens were prepared in phosphate buffered saline (PBS) with 0.1% BSA immediately prior to use. All buffers were filtered through 0.2 μm filters. All other reagents were ACS reagent grade. Deionized water with 18 MΩ resistance was used for preparing buffers. Flow cytometric measurements were carried out on Beckton Dickinson (BD) FACSCalibur.

Quantum dot-antibody conjugation

Using the optimized protocol described previously[5], quantum dot-streptavidin conjugates (QD) and biotinylated anti-angiopoietin-2 polyclonal antibody (aA2) or anti-

VEGF polyclonal antibody (aVEGF) were mixed in PBS-BSA at QD:antibody molar ratio of 1:3 and 1nM QD concentration. The conjugate was used as synthesized after incubation for 30 minutes at room temperature.

Antigen Induced Self Assembly

The QD-antibody (QD-Ab) conjugate solution and the antigen or control solution at the appropriate dilutions and volumes were added to PBS-BSA for a 500 μL final volume. BSA, similar to ang-2 in terms of molecular weight, acted as a negative control for Ang2 and VEGF. The reaction mixtures were incubated at room temperature for 60 minutes and then analyzed by flow cytometry. Baseline event distribution of QD-Ab dispersed in PBS-BSA was also analyzed. Non-multiplexed detection was carried out by reacting 5 fM to 500 pM VEGF with 10 pM QD705-aVEGF conjugates, and 5 fM to 500 pM Ang2 with 10 pM aA2, both in 500 μL final volumes. Ten different concentration values of each antigen were examined, and three datasets of each antigen were acquired from three different experiments. For multiplexed detection, the antigen mixture was prepared in PBS-BSA by sequentially adding appropriate volumes and dilutions of the VEGF and Ang2 stock solutions. The mixture of QD705-aVEGF and QD585-aA2 were added to these antigen solutions for a final concentration of 10 pM of each of the QD-Ab populations in 500 μL final volumes. Experiments with 5 fM to 500 pM VEGF concentrations with no Ang2, 1 pM 10 pM or 100 pM Ang2 were carried out. The inherent variability of the QD-Ab dilution caused a large effect on the fraction of agglomerates observed. Hence, only the datasets with base QD-Ab count within 2000+/-200 were utilized for analysis.

Flow cytometric characterization

The size, fluorescence and number of the aggregates in the incubated samples were characterized by flow cytometry. The basic flow cytometric protocol followed was similar to the one used in our previous publication[5]. Briefly, signal amplification for the flow cytometer parameters forward scatter (FSC) and side scatter (SSC) detectors and fluorescence detectors with 585+/- 21nm (FL2) and 650nm long pass filters (FL3) were optimized for characterizing small particles. The forward scatter and side scatter performance was calibrated by using 0.2, 0.5, 1, 2 and 2.8 μm latex calibration particles. In **Figure 1.a**, the regions indicated by R1, R2, R3, R4 and R7 correspond to the 0.2, 0.5, 1, 2 and 2.8 μm latex calibration particles respectively. Aggregates were defined as particles with forward scatter greater than 10 a.u. This corresponds to a nominal size greater than approximately 0.5 μm, as well as the observed differentiation of the individual QD-Ab conjugates from the large aggregates inherent in the agglomeration process and the measurement protocol[5]. The data was acquired at low flow rate (12 +/-3 μL/min) for one minute, and either the FL2 or FL3 channels individually for non-multiplexed detection or both sequentially for multiplexed detection were used as triggers to minimize noise from non-fluorescent micro-particles in the reaction mixture. In our previous publication, the fraction of aggregates was defined as the event fraction appearing in the upper right quadrant (UR) of the FSC vs. SSC plot. Since the aggregates appear in this quadrant regardless of the fluorescence intensity in the FL2 and FL3 channels, detection of multiple QD populations requires an approach influenced by QD fluorescent color. To achieve multiplexed detection, the fraction of aggregates was

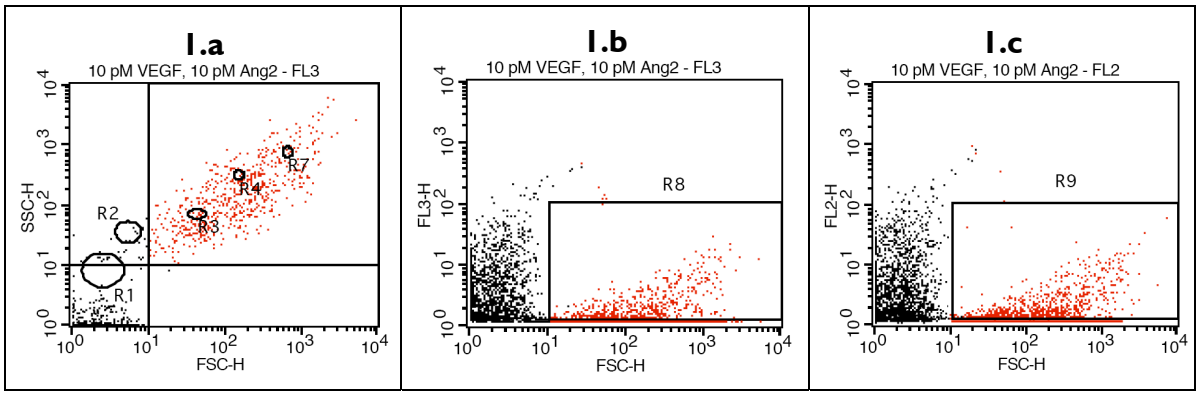

Figure 1: Characterization of multifluorescent reaction mixture by flow cytometry. The QD-Ab:antigen aggregates were characterized by flow cytometry. The panels show the raw data acquired from a multiplexed sample containing 10 pM Ang2 and 10 pM VEGF as well as the appropriate QD-Ab conjugates. Panel **a** shows that optimized flow cytometric detection parameters enable the resolution of individual QD-Ab conjugates and small aggregates (black dots, bottom left quadrant) from the micron scale aggregates (red dots, upper right quadrant). The regions labeled R1, R2, R3, R4 and R7 indicate 0.2, 0.5, 1, 2 and 2.8 μm calibration particles respectively. Panels **b** and **c** show the FL vs. FSC data representation of the events representing aggregates acquired with FL3 and FL2 triggers, respectively. The regions R8 and R9 demarcate areas on these charts corresponding to the aggregates (FSC>10, as in panel **a**). The events in R8 and R9 are counted as single antigen aggregates mediated only by VEGF and Ang2 respectively. The bottom edges of R8 and R9 are specified such that false positives are reduced but not more than 1% of the events in an equivalent non-multiplexed experiment are counted as false-negative.

instead characterized in the FSC vs. FL3 plot in region R8 for the QD705 quantum dot population (**Figure 1.b**) and FSC vs. FL2 plot in region R9 for the QD585 quantum dot population (**Figure 1.c**). The lower boundary of regions R8 and R9 was raised to minimize the QD585 aggregates count in the QD705 population and *vice versa*. The gating was adjusted to limit this loss of aggregate events to 1% of total number of events in the triggering population, as determined by characterizing non-multiplexed samples.

Statistical analysis of the datasets was carried out using the SigmaStat 3.1 software. The t-test was utilized to determine whether experimental parameters, including the concentration of the non-specific antigen in the multiplexing mixture, signal acquisition optimization and gating geometry, had a statistically significant effect on the relationship between antigen concentration and agglomerate percentage. When t-values for two datasets compared are close to zero, the difference between the two datasets and the effect of the experimental parameters is statistically insignificant[39].

Results

Non-multiplexed detection of VEGF and Ang2 was achieved from 50 fM to 100 pM. **Figure 2** shows the correlation between aggregates, as a percent of total number of events counted, and antigen concentration. In these non-multiplexed aggregation experiments, the concentrations of either antigen from 50 fM to 100 pM produced a log linear correlation with the fraction of events detected as aggregates. The two correlations have statistically different slopes: 6.96+/-0.30 for Ang2 and 4.60+/-0.21 for VEGF. The background aggregate concentration caused by non-specific assembly of QD-Ab conjugates in the PBS-BSA buffer has a value of 1.39+/-0.3% for QD705-aVEGF and

1.56+/-0.38% for QD585-aA2. A t-test comparison of the QD585-aA2:Ang2 agglomeration percentage from 500fM to 100pM [Ang2] in the current data and in the previously published data[5] indicates no statistically significant difference based on a t-value of 0.073. Over the range of antigen concentrations measured, the two lower antigen concentration values of 5 fM and 10 fM generate aggregates that are within three standard deviations of the background non-specific aggregate count. The samples with 500 pM antigen concentration also deviate from the log-linear correlation.

Quantitative multiplexed detection of both antigens in the physiologically relevant concentration range was also achieved. Multiplexed detection of the two antigens was demonstrated over the 1 pM to 100 pM concentration range. The relationship between the VEGF concentration and percent aggregates (R8%) is log linear even in the presence of Ang2 (**Figure 3**). The slope +/- standard error values of the correlation for the multiplexed detection of VEGF at 0, 1, 10 and 100 pM Ang2 are 3.9+/- 0.33, 4.0 +/- 0.28, 4.1+/- 0.33 and 4.3 +/- 0.35 respectively. The slope for non-multiplexed detection of VEGF is 4.6 +/- 0.31. The t-test comparisons of the QD705-aVEGF:VEGF aggregate percentages from 1pM to 100 pM [VEGF] in all experiments have a range of t-values from -0.039 to 0.077, indicating no statistically significant effect of Ang2 concentration on VEGF detection (**Table 1**). The VEGF-negative control experiments with Ang2 added at the appropriate concentration to the multiplexed QD-Ab mixture determined the limit of VEGF detection. The highest percentage of non-specific aggregates + three standard deviations (P=99.7%), formed in the negative control experiment with 100 pM Ang2 resulted in a sensitivity limit of 1 pM for VEGF. The background aggregate percentage increased with increasing Ang2 concentration. At 100 pM Ang2 background non-specific

aggregate percentage was 6.4 +/- 0.87%, compared to the background aggregate percentage in the non-multiplexed experiments (1.4 +/- 0.1%).

Quantitative multiplexed detection of Ang2 was also achieved from the same set of samples, as measured by R9 aggregate% (**Figure 4**). The change in VEGF concentration in the samples does not have a statistically significant effect on the detection of Ang2 in the range of concentrations examined. The t-values for these data range from -0.046 to 0.043.The t-tests for the multiplexed sample datasets were carried out for R9% values of the four concentrations of Ang2 – 0, 1, 10 and 100 pM, for each concentration of VEGF and for the non-multiplexed Ang2 detection data set.

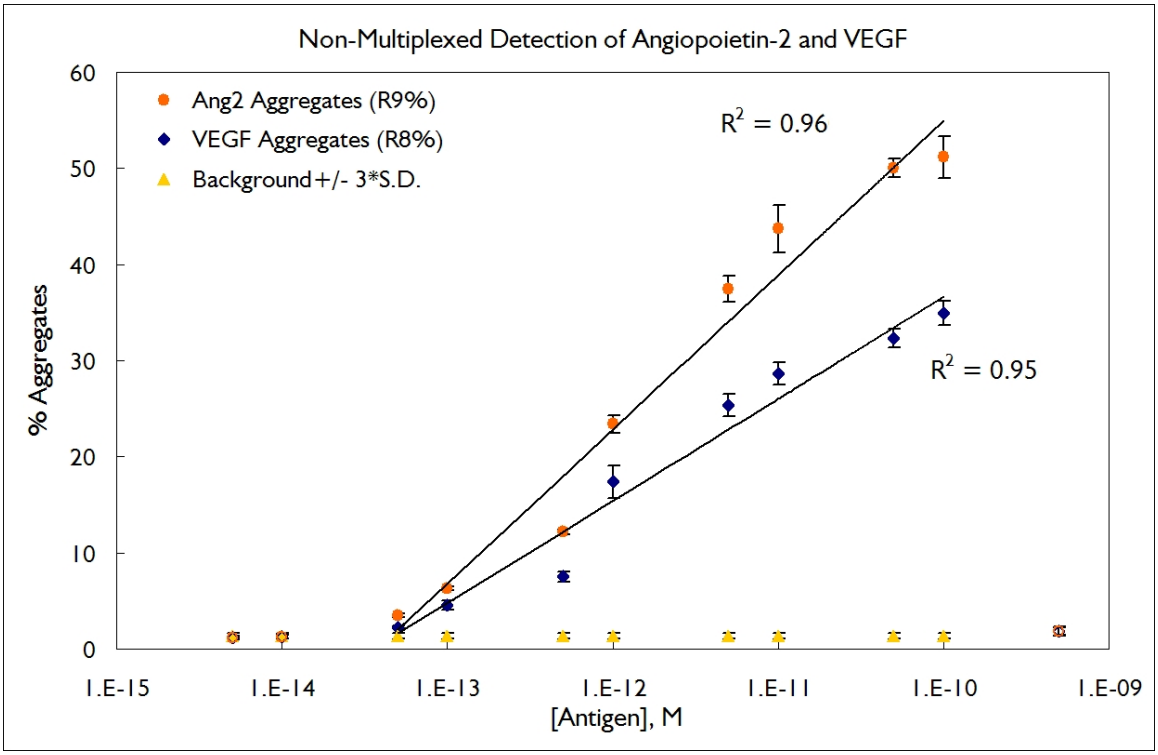

Figure 2: Non-multiplexed detection of VEGF and Angiopoietin-2. A sensitivity limit of 50 fM was achieved when the antigens were reacted with 10 pM QD-Ab. The relationship between antigen concentration and fraction of aggregates detected was log-linear for both antigens, but with statistically different slopes: 6.96+/-0.30 for Ang2 and 4.60+/-0.21 for VEGF. A t-test comparison for the current Ang2 data with previously published data[5] indicates no statistically significant difference. Thus, the change in gating strategy to accommodate multiplexed detection has no effect on the quantification of aggregates. Percent aggregates formed for antigen concentrations less than 50 fM were within three standard deviations of the mean non-specific aggregate count in the absence of the specific antigens, i.e. the background noise. Aggregate formation in the presence of 500pM antigen was close to background level, suggesting a quenching of the agglomeration process due to the excess antigen. Data represents the mean and standard deviation of values observed from n=3 experiments.

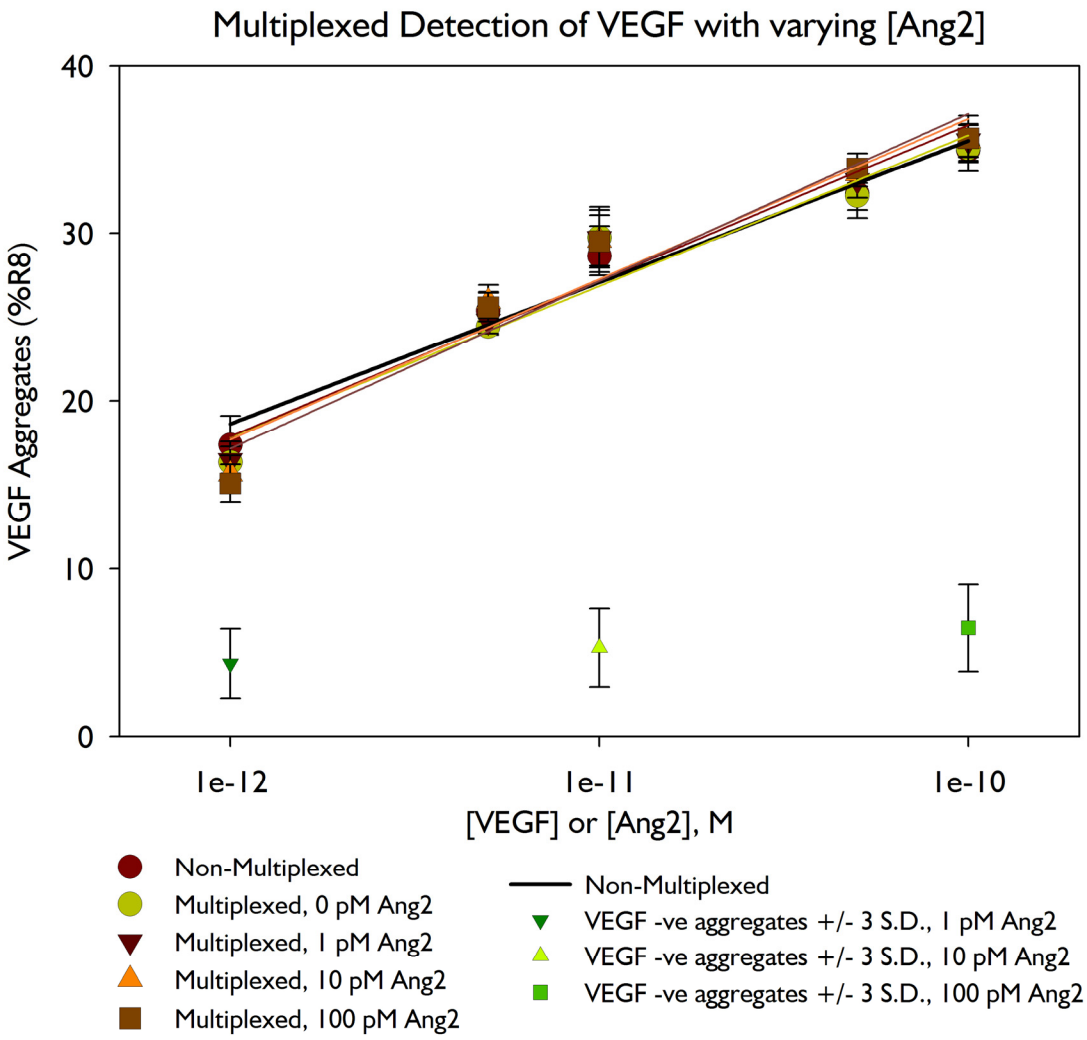

Figure 3: Multiplexed detection of VEGF. 10 pM QD705-aVEGF conjugates were incubated with of 0, 1, 10, and 100 pM Ang2 and 10 pM QD585-aA2 conjugates. The log-linear VEGF detection correlation is statistically equivalent across Ang2 concentrations as determined by t-tests. The correlation between aggregate population and VEGF concentration was also statistically identical to the non-multiplexed antigen detection experiments. The fractions of QD705-aVEGF:VEGF aggregates, as well as the background event count, were determined by flow cytometry from region R8. The detection scheme was effective in the physiologically relevant range of 1-100 pM. The VEGF detection sensitivity limit is 1 pM due to the background noise (green data points at the bottom of the chart) resulting from nonspecific interactions between both the QD-Ab conjugates, as well as non-specific QD-Ab:antigen interactions. Data represents the mean and standard deviation of values observed from n=3 experiments.

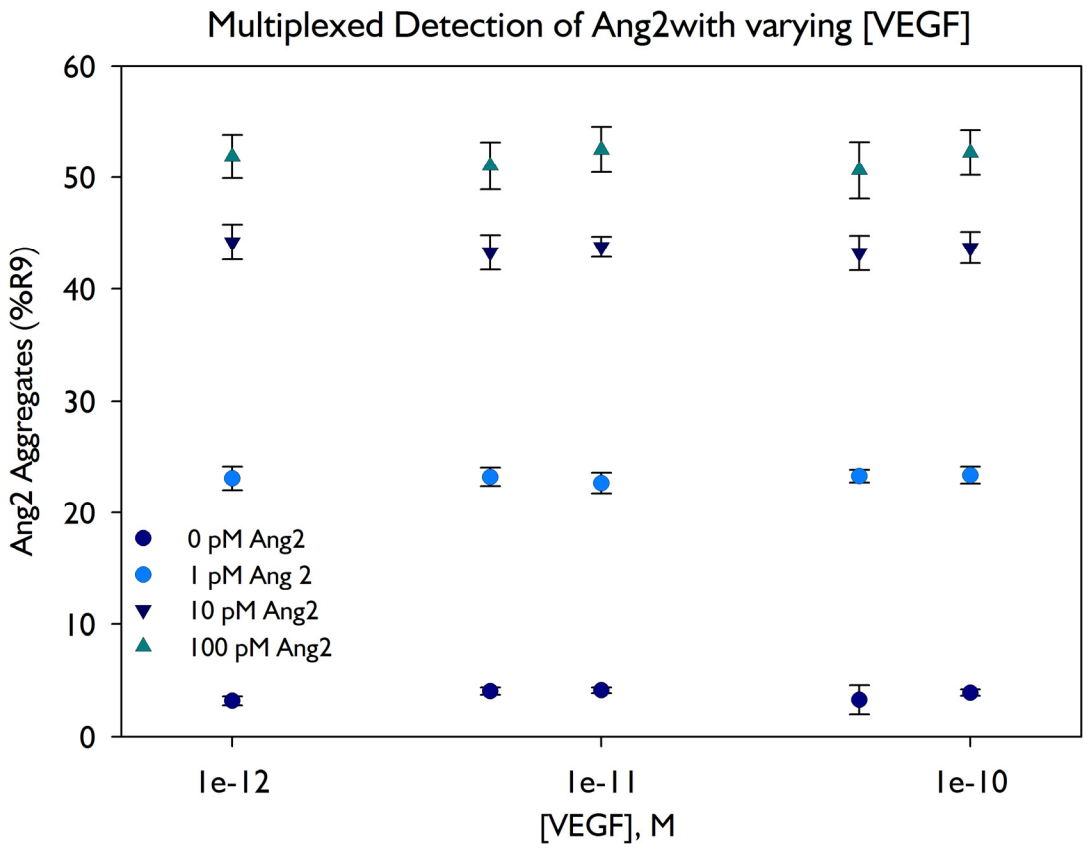

Figure 4: Multiplexed detection of angiopoietin-2. 1, 10 and 100 pM angiopoietin-2 in the presence of 1, 5, 10, 50, and 100 pM VEGF. The varying VEGF concentration does not have a statistically significant effect on the quantitative detection of Ang2, as determined by t-tests. The data is from the same samples as in Figure 3, the fractions of QD585-aA2:Ang2 aggregates were quantified in region R9 of the FL2 vs. FSC data space. The percent Ang2 aggregates in the multiplexed detection experiments are also statistically identical to the percent aggregates in the non-multiplexed experiment, based on t-test comparisons. Data represents the mean and standard deviation of values observed from n=3 experiments.

Table 1: t-test comparison of non-multiplexed VEGF detection and multiplexed VEGF detection at various angiopoietin-2 concentrations.

t-value	**Non-Multiplex**	**0 pM Ang2**	**1 pM Ang2**	**10 pM Ang2**	**100 pM Ang2**
100 pM Ang2	0.043	0.077	0.007	-0.017	0
10 pM Ang2	0.062	0.097	0.025	0	
1 pM Ang2	0.037	0.073	0		
0 pM Ang2	-0.039	0			
Non-Multiplexed	0				

The t-values are close to zero, indicating that there is no statistically significant difference between these datasets. Thus, the presence or absence of QD585-aA2 and Ang2 does not significantly affect the VEGF detection curve. Each cell in the array shows t-test performed between the mean percent agglomerates dataset for 1pM to 100 pM [VEGF], and [Ang2] as indicated in header of the intersecting row and column.

Discussion

Multiplexed detection of proteomic antigens with molecular recognition-mediated nanoparticle self-assembly is feasible in the physiologically relevant concentration range. Since this technique is based on antibody-antigen interaction, it is expected that detection sensitivity similar to that demonstrated here would be achievable for a variety of proteomic biomarkers subject to the dissociation constant (k_d) ranges for the specific polyclonal antibody-biomarker pairs. The reproducibility of the equilibrium aggregate percentage suggests the feasibility of self-assembly based quantification of antigens, even though individual QD-Ab:Ag interactions are presumably random. The fundamental feasibility of quantum dot self-assembly for multiplexed protein quantification has been demonstrated here as a proof of concept. Significant improvements in the materials and methods, including adoption of microfluidic based instrumentation, is appropriate to translate technique as a routine clinical, personal, or research proteomic profiling tool. The results also establish that the adjustments made to the data acquisition process and gating strategies to enable multiplexed detection do not have a statistically significant effect on the quantification of aggregates.

As expected from the mechanism of antibody-antigen interaction, the presence of a large excess of antigen in the solution rapidly associates with antibody binding sites and inhibits the QD aggregation process. This is manifested in the low aggregate count for both antigens in the non-multiplexed experiments at the highest concentration (500 pM, **Figure 2**). This antigen concentration corresponds to a 50:1 antigen to QD-Ab ratio. At the 3x antibody:QD molar ratio used to prepare the QD-Ab conjugates, the actual ratio of antigens to antibody binding sites is approximately 8:1. This is comparable to the 10-

fold molar excess of antigens commonly used for antibody blocking in conventional antibody-antigen based reactions. Due to this effect, for clinical implementation, optimized QD-Ab concentrations may be required for each target antigen based on the expected concentration range. We have previously demonstrated that it is possible to extend the dynamic range of this technique by using multiple QD-Ab concentrations[5]. Such multiple antigen:QD-Ab stoichiometries can be easily implemented at low cost on second generation microfluidic-based instrumentation

Another interesting feature observed from the non-multiplexed data is that the lower limit of detection is far lower than what would be expected based on simple stoichiometric considerations. Using the 10 pM QD-Ab concentration, it is possible to detect 50 fM antigen in the non-multiplexed reaction, an antigen:QD-Ab ratio of 1:200, or antigen:antibody binding site ratio of 1:600. While such ratios are not uncommon in conventional antibody-anigen based reactions, stoichiometric considerations suggest that the large excess of antibody binding sites would limit the formation of large aggregates. However, the presence of a statistically significant number of aggregates at this antigen concentration indicates that the aggregate formation is strongly favored. This may result from the lower free energy of the aggregates compared to the individual components. Theory-based calculations and simulations will be performed to test this hypothesis, but are not a part of this experimental study.

The difference in the fraction of agglomerates observed for the two antigens at identical concentration, and consequently, the different slopes for the two detection curves, indicate that the number of aggregates formed is affected not only by QD-Ab:antigen ratio, but also by other characteristics, potentially including antibody-antigen

affinity and the size of the antigen. We have also reported this effect previously – the slope for the detection curves of Ang2 and mouse IgG is different[5]. Similar effects are also observed in other antibody based protein detection methods. For example, different characteristic detection curves are obtained in commercial ELISA mothods for different antigen-antibody pairs.

We have also confirmed that multiplexed detection of both of the antigens tested is feasible in the physiologically relevant concentration range. The aggregate fraction is not significantly affected by the presence of the multiple antigens in the reaction mixture. T-tests show that the effect of multiplexing on the detection curve within the 1 pM to 100 pM concentration range is statistically insignificant for both the antigens. The effect of multiple antigens in the reaction mixture on the agglomeration of a QD-Ab:antigen pair is of critical significance for a multiplexed antigen profiling technique. Since there are numerous antigens present in a complex biological sample, measurement robustness against these non-specific reactions is an important factor in determining the suitability of a technique for application as a multiplexed diagnostic. The antigen sensitivity limit is reduced in a multiplexed sample relative to the sensitivity in non-multiplexed equivalent due to increased background noise. The adverse characteristic may be through antibody-antigen cross reactivity and/or non-specific nanoparticle interactions. In the technique demonstrated here, the characterization of the aggregates was carried out with flow cytometry, and the aggregates were counted in the FL vs. FSC space. The aggregates with high intensity in one fluorescence channel register a low fluorescence aggregates in the detection channel. The gating strategy enables the exclusion of a large number of

these false positive detections. Once the gating strategy is optimized, it need not be adjusted for the set of antigens.

Conclusion

In summary, we have established that the quantum dot agglomeration-based protein detection technique is capable of multiplexed quantification of proteomic antigens. The protein detection is currently carried out simultaneously for two antigens at physiologically relevant concentrations in a simple physiological buffer. Further optimization of the reagents and biological samples, as well as of the incubation and data acquisition protocols, may provide the ability to quantify proteins from physiological samples. These optimizations may also improve the sensitivity limits and dynamic range of this technique. This simple, quantitative and low cost method may be suitable for clinical application with further optimization.

References

1. Arntz, Y.; Seelig, J. D.; Lang, H. P.; Zhang, J.; Hunziker, P.; Ramseyer, J. P.; Meyer, E.; Hegner, M. and Gerber, C., Label-free protein assay based on a nanomechanical cantilever array. *Nanotechnology*, **2003**. *14*(1): 86-90.

2. Salata, O. V., Applications of nanoparticles in biology and medicine. *Journal of Nanobiotechnology*, **2004**. *2*(1): 3.

3. Wang, J., Carbon-Nanotube Based Electrochemical Biosensors: A Review. *Electroanalysis*, **2005**. *17*(1): 7-14.

4. Ferrari, M., Cancer nanotechnology: opportunities and challenges. *Nature Reviews Cancer*, **2005**. *5*(3): 161-171.

5. Soman, C. P. and Giorgio, T. D., Quantum Dot Self-Assembly for Protein Detection with Sub-Picomolar Sensitivity. *Langmuir*, **2008**. *24*(8): 4399-4404.

6. Goldman, E. R.; Balighian, E. D.; Mattoussi, H.; Kuno, M. K.; Mauro, J. M.; Tran, P. T. and Anderson, G. P., Avidin: a natural bridge for quantum dot-antibody conjugates. *J. Am. Chem. Soc*, **2002**. *124*(22): 6378–6382.

7. Plotz, C. M. and Singer, J. M., The latex fixation test. I. Application to the serologic diagnosis of rheumatoid arthritis. *Am J Med*, **1956**. *21*(6): 888-92.

8. March, S. B. and Ratnam, S., Latex agglutination test for detection of Escherichia coli serotype O157. *Journal of Clinical Microbiology*, **1989**. *27*(7): 1675-1677.

9. van Griethuysen, A.; Pouw, M.; van Leeuwen, N.; Heck, M.; Willemse, P.; Buiting, A. and Kluytmans, J., Rapid Slide Latex Agglutination Test for Detection of Methicillin Resistance in Staphylococcus aureus. *Journal of Clinical Microbiology*, **1999**. *37*(9): 2789-2792.

10. Sulahian, A.; Tabouret, M.; Ribaud, P.; Sarfati, J.; Gluckman, E.; Latgé, J. P. and Derouin, F., Comparison of an enzyme immunoassay and latex agglutination test for detection of galactomannan in the diagnosis of invasive aspergillosis. *European Journal of Clinical Microbiology & Infectious Diseases*, **1996**. *15*(2): 139-145.

11. Storhoff, J. J.; Elghanian, R.; Mucic, R. C.; Mirkin, C. A. and Letsinger, R. L., One-pot colorimetric differentiation of polynucleotides with single base imperfections using gold nanoparticle probes. *J. Am. Chem. Soc*, **1998**. *120*(9): 1959–1964.

12. Hirsch, L. R.; Jackson, J. B.; Lee, A.; Halas, N. J. and West, J. L., A Whole Blood Immunoassay Using Gold Nanoshells. *Analytical Chemistry*, **2003**. *75*: 2377-2381.

13. Ho, Y. P.; Kung, M. C.; Yang, S. and Wang, T. H., Multiplexed Hybridization Detection with Multicolor Colocalization of Quantum Dot Nanoprobes. *Nano Lett*, **2005**. *5*(9): 1693-1697.

14. Agrawal, A.; Tripp, R. A.; Anderson, L. J. and Nie, S., Real-Time Detection of Virus Particles and Viral Protein Expression with Two-Color Nanoparticle Probes. *Journal of Virology*, **2005**.

15. Camilla, C.; Mely, L.; Magnan, A.; Casano, B.; Prato, S.; Debono, S.; Montero, F.; Defoort, J. P.; Martin, M. and Fert, V., Flow Cytometric Microsphere-Based Immunoassay: Analysis of Secreted Cytokines in Whole-Blood Samples from Asthmatics. *Clinical and Vaccine Immunology*, **2001**. *8*(4): 776-784.

16. Kellar, K. L. and Iannone, M. A., Multiplexed microsphere-based flow cytometric assays. *Exp Hematol*, **2002**. *30*(11): 1227-37.

17. Calvo, K. R.; Liotta, L. A. and Petricoin, E. F., Clinical Proteomics: From Biomarker Discovery and Cell Signaling Profiles to Individualized Personal Therapy. *Bioscience Reports*, **2005**. *25*(1/2): 107-125.

18. Petricoin, E. F. and Liotta, L. A., Proteomic approaches in cancer risk and response assessment. *Trends in Molecular Medicine*, **2004**. *10*(2): 59-64.

19. Roboz, J., Mass spectrometry in diagnostic oncoproteomics. *Cancer investigation*, **2005**. *23*(5): 465-78.

20. Polanski, M. and Anderson, N. L., A list of candidate cancer biomarkers for targeted proteomics. *Biomarker Insights*, **2006**. *2*: 1-48.

21. Miyashita, M.; Tajiri, T.; Yanagi, K.; Shimizu, T.; Futami, R.; Sasajima, K. and Tokunaga, A., Serum levels of vascular endothelial growth factor, basic fibroblast growth factor and endostatin in human metastatic liver tumors. *Hepatogastroenterology*, **2003**. *50*(50): 308-9.

22. Lobov, I. B.; Brooks, P. C. and Lang, R. A., Angiopoietin-2 displays VEGF-dependent modulation of capillary structure and endothelial cell survival in vivo. *Proceedings of the National Academy of Sciences*, **2002**. *99*(17): 11205-11210.

23. Maisonpierre, P. C.; Suri, C.; Jones, P. F.; Bartunkova, S.; Wiegand, S. J.; Radziejewski, C.; Compton, D.; McClain, J.; Aldrich, T. H. and Papadopoulos, N., Angiopoietin-2, a natural antagonist for Tie2 that disrupts in vivo angiogenesis. *Science*, **1997**. *277*(5322): 55-60.

24. Carmeliet, P. and Jain, R. K., Angiogenesis in cancer and other diseases. *Nature*, **2000**. *407*(6801): 249-257.

25. Polanski, M. and Anderson, N. L., A List of Candidate Cancer Biomarkers for Targeted Proteomics. *Biomarker Insights*, **2006**. *2*.

26. Audero, E.; Arisio, R.; Bussolino, F.; Sismondi, P. and De Bortoli, M., Angiopoietin-2 expression in breast cancer correlates with lymph node invasion and short survival. *Int. J. Cancer*, **2003**. *103*: 466-474.

27. Caine, G. J.; Blann, A. D.; Stonelake, P. S.; Ryan, P. and Lip, G. Y. H., Plasma angiopoietin-1, angiopoietin-2 and Tie-2 in breast and prostate cancer: a comparison with VEGF and Flt-1. *European Journal of Clinical Investigation*, **2003**. *33*: 883-890.

28. Talapin, D. V.; Rogach, A. L.; Kornowski, A.; Haase, M. and Weller, H., Highly luminescent monodisperse CdSe and CdSe/ZnS nanocrystals synthesized in a hexadecylamine-trioctylphosphine oxide-trioctylphospine mixture. *Nano Lett*, **2001**. *1*(4): 207-211.

29. Hines, M. A. and Guyot-Sionnest, P., Synthesis and characterization of strongly luminescing ZnS-capped CdSe nanocrystals. *J. Phys. Chem*, **1996**. *100*(2): 468-471.

30. Ebenstein, Y.; Mokari, T. and Banin, U., Fluorescence quantum yield of CdSe/ZnS nanocrystals investigated by correlated atomic-force and single-particle fluorescence microscopy. *Applied Physics Letters*, **2002**. *80*(21): 4033.

31. Underwood, D. F.; Kippeny, T. and Rosenthal, S. J., Ultrafast Carrier Dynamics in CdSe Nanocrystals Determined by Femtosecond Fluorescence Upconversion Spectroscopy. *J. Phys. Chem*, **2001**: 436-443.

32. Bruchez Jr, M., Semiconductor Nanocrystals as Fluorescent Biological Labels. *Science*, **1998**. *281*(5385): 2013-2016.

33. Dubertret, B., In Vivo Imaging of Quantum Dots Encapsulated in Phospholipid Micelles. *Science*, **2002**. *298*(5599): 1759-1762.

34. Chan, W. C. W.; Maxwell, D. J.; Gao, X.; Bailey, R. E.; Han, M. and Nie, S., Luminescent quantum dots for multiplexed biological detection and imaging. *Current Opinion in Biotechnology*, **2002**. *13*(1): 40-46.

35. Xu, H., Multiplexed SNP genotyping using the QbeadTM system: a quantum dot-encoded microsphere-based assay. *Nucleic Acids Research*, **2003**. *31*(8): 43-43.

36. Gao, X.; Chan, W. C. W. and Nie, S., Quantum-dot nanocrystals for ultrasensitive biological labeling and multicolor optical encoding. *Journal of Biomedical Optics*, **2002**. *7*(4): 532-537.

37. Goldman, E. R.; Medintz, I. L. and Mattoussi, H., Luminescent quantum dots in immunoassays. *Analytical and Bioanalytical Chemistry*, **2006**. *384*(3): 560-563.

38. Klostranec, J. M. and Chan, W. C. W., Quantum dots in biological and biomedical research: recent progress and present challenges. *Adv. Mater*, **2006**. *18*: 1953–1964.

39. Ott, L., *An introduction to statistical methods and data analysis*. 1993: Duxbury Press North Scituate, Mass.

CHAPTER IV

KINETICS OF MOLECULAR RECOGNITION MEDIATED NANOPARTICLE SELF-ASSEMBLY

Summary

Nanoscale quantum dot-antibody conjugates have been shown to self-assemble to form micron-scale aggregates in the presence of specific proteomic antigen. The self-assembly process exhibits sigmoidal kinetics, suggesting that nucleation limits aggregation. Self-assembly kinetics in this study are characterized by flow cytometric analysis of the aggregation reaction over time. A range of physiologically relevant concentrations of the protein angiopoietin-2, a candidate cancer biomarker, are incubated with quantum dots conjugated with a polyclonal mixture of anti-angiopoietin-2 antibodies. Antigen concentration modulates the slopes and inflection times of the sigmoidal kinetics curves. An understanding of self-assembly kinetics in this system may lead to improvements in sensitivity and specificity of this novel proteomic biomarker detection technique and improve the screening, diagnostics, and therapy response monitoring for cancers and other diseases. This approach to studying the kinetics of nanoparticle self-assembly may also provide a valuable tool for understanding the fundamental characteristics of nanoscale particle aggregation.

Introduction

Directed self-assembly of nanostructures into microstructures through intermolecular interactions is an important phenomenon in many biological systems. Assembly of virus coat proteins into capsids[1], of microtubulin into microtubules[2], and of collagen[3] and fibrinogen into their respective fibrils are just a few examples where self-assembly plays a critical role in biological processes. Programmed self assembly using biomolecular interactions as a route to synthesis of novel nanostructured materials has also been an area of active investigation in the recent past[4, 5]. Techniques aimed at molecular diagnostics have also been demonstrated using nanoparticle self assembly mediated by molecular interactions, including polynucleotide interactions[6] and antibody-antigen interactions[7].

In a recent publication[8], we demonstrated a novel technique for sub-picomolar quantitative detection of proteomic antigens using single step fluid phase incubation. In this technique, quantum dots (QD) conjugated with polyclonal antibodies (Ab) through the streptavidin-biotin interaction[9] are incubated with specific antigens in a physiological buffer. The molecular recognition between the antibodies and antigens causes aggregation of the nanoscale conjugates and proteins, resulting in the formation of microscale structures. These larger structures can be easily distinguished from the individual components based on differences in light scattering properties and by other analytical techniques. By sequentially characterizing very small volumes of the reaction mixture, such as via flow cytometry, the microscale aggregates can be quantified. At equilibrium, the antigen concentration and the fraction of events that are classified as aggregates are correlated through a log-linear relationship. Using multiple quantum dot

populations with distinct fluorescence emissions, multiplexed detection of two antigens is also feasible (unpublished data) and can, presumably, be extended through the use of alternately biofunctionalized QD with additional fluorescence emission characteristics.

In this short communication, we describe the kinetics of QD-Ab aggregation mediated by angiopoietin-2. The kinetics of self assembly of bio-macromolecules has been studied for many systems, including virus capsid assembly[1, 10], microtubule formation[2, 11, 12], fibril assembly[3] and other protein aggregation phenomena[13-16]. Theoretical[17-22] and computational[23-25] studies on these systems illuminate the mechanisms that drive the self-assembly processes. Previous work as also examined factors that influence the kinetics, such as the concentration of various moieties, agitation and presence of agents that promote or inhibit intermolecular interaction. These factors may be utilized for promotion or inhibition of aggregation [1, 14, 26, 27]. Understanding the kinetics of the present system may improve the specificity and sensitivity of the proposed diagnostic method. Similar studies yielded improvements to the conventional surface based enzyme linked immunosorbent assay (ELISA), and informed the development of the kinetic ELISA method[28]. While the current study explores the kinetics of highly specific molecular interaction mediated self-assembly, nanoscale material aggregation is important in a wide variety of applications. Controlled aggregation and/or prevention of non-specific aggregation are important considerations for various technologies that use nanomaterials, regardless of the presence or absence of molecular recognition. The techniques developed in this study may provide a novel method of quantitatively characterizing important aspects of nanoscale phenomena.

Experimental

Materials

Streptavidin-coated quantum dots with 705 nm fluorescence emission (QD705, #Q10161MP) were purchased from Invitrogen (Carlsbad, CA) and used as received. Biotin conjugated anti-angiopoietin-2 polyclonal antibody (aA2, #BAF623), and recombinant human angiopoietin-2 (ang2, #623-AN) were purchased from R&D Systems (Minneapolis, MN), reconstituted in Tris-buffered saline (TBS) containing 0.1% bovine serum albumin (BSA) and stored at -20°C. Appropriate dilutions of all antibodies and antigens were prepared in phosphate buffered saline (PBS) with 0.1% BSA immediately prior to use. Deionized water with 18 $M\Omega.cm^{-1}$ resistance was used for preparing buffers. All buffers were filtered through 0.2 μm filters. All other reagents were ACS reagent grade. Flow cytometric measurements were carried out with an unmodified Beckton Dickinson (BD) FACSCalibur, and the associated software.

Quantum Dot – Antibody Conjugation

Quantum dot-streptavidin conjugates (QD) and biotinylated anti-angiopoietin-2 polyclonal antibody (aA2) were mixed in PBS-BSA at QD:antibody molar ratio of 1:3 and 1nM QD concentration. The conjugate was incubated for 30 minutes at room temperature and then used as synthesized. The stoichiometry in this protocol has been previously optimized to obviate the need to separate un-reacted antibodies from the QD-Ab conjugates[8]. The QD-aA2 conjugate solution and the ang2 or control solution at the appropriate dilutions and volumes were added to PBS-BSA for a final volume of

500 μL. BSA, similar to ang-2 in terms of molecular weight, was used as a negative control for Ang2.

Agglomeration Kinetics Measurement Protocol

The reaction mixtures were incubated at room temperature and analyzed by flow cytometry at five minute intervals from t=5 minutes to t=90 minutes, as well as immediately after sample preparation, nominally t=1 minute. Thus, each experiment consisted of nineteen different samples, one for each time point. The influence of ang2 concentration on aggregation kinetics was characterized by carrying out the aggregation reaction with 1 pM, 10 pM, and 100 pM ang2. Control measurements were made at the same time points on samples identical except for the presence of ang2. To compensate for the effect of the variability in the QD-aA2 dilution on the fraction of agglomerates observed, only the datasets with base QD-aA2 count within 2000+/-200 were utilized for analysis. Three such datasets for each antigen concentration comprised the analyzed data set.

The size, fluorescence and number of the aggregates in the incubated samples were characterized by flow cytometry. The basic flow cytometric protocol followed was similar to the one used in our previous publication[8]. Briefly, signal amplification parameters for the flow cytometer parameters forward light scatter (FSC) and side light scatter (SSC) detectors and fluorescence detector with 650nm long pass filters (FL3) were optimized for characterizing small particles. The FSC and SSC detector performance was calibrated by using 0.2, 0.5, 1, 2 and 2.8 μm latex calibration particles. In **Figure 1**, the regions indicated by R1, R2, R3, R4 and R7 correspond to the 0.2, 0.5, 1,

2 and 2.8 μm latex calibration particles respectively. The data was acquired at low flow rate (12 +/- 3 μL/min) for one minute. The FL3 channel was used as the event trigger consistent with the fluorescence emission characteristics of the 705 nm QDs used in this study. The fraction of aggregates was defined as the event fraction appearing in the upper right quadrant (UR) of the FSC vs. SSC plot. FSC greater than 10 a.u. corresponds to a nominal size greater than approximately 0.5 μm, as well as the observed differentiation of the individual QD-Ab conjugates from the large aggregates inherent in the agglomeration process and the measurement protocol[8]. Analysis of the datasets was carried out using the SigmaPlot 9.01 and SigmaStat 3.1 software.

Results and Discussion

The kinetics of ang2 mediated QD-aA2 aggregation exhibits a sigmoidal behavior, with three distinct phases. The initial rate of aggregate formation is slow, most evident from the kinetics for aggregation triggered by the addition of 1 pM ang2 (**Figure 2**). The second phase characterized by rapid, self-assembled aggregation. The final phase is the reduction of aggregation rate with asymptotic approach to the equilibrium aggregate fraction. Similar sigmoidal kinetics are observed in many intermolecular interaction based self-assembly processes[27, 29] as well for nanoparticle synthesis [30] and polymer synthesis [29, 31]. Sigmoidal kinetics indicate a thermodynamically unfavorable intermediate in the reaction pathway. The key stages in the aggregation reaction are depicted schematically in **Figure 3** where **panel 1** represents the QD-Ab conjugates mixed with antigen molecules. Antibody-antigen recognition creates single

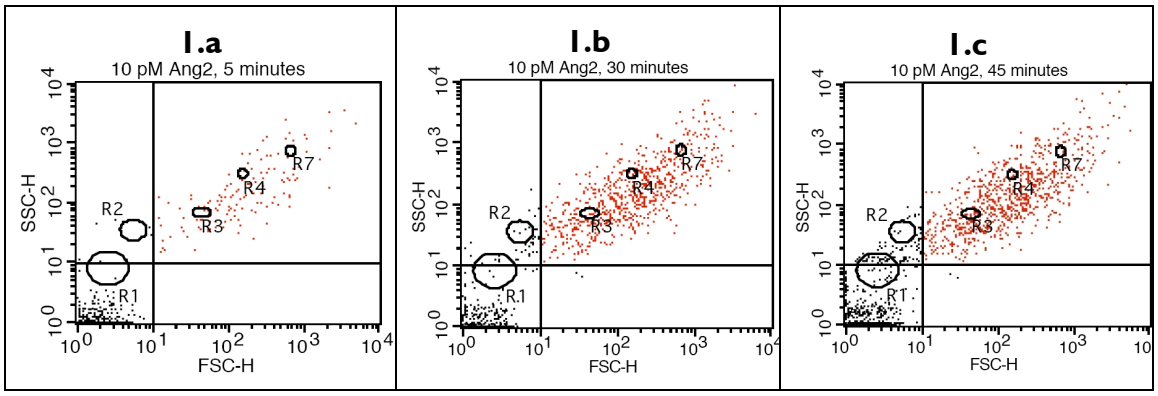

Figure 1: Time dependent change in flow cytometric data. Aggregation kinetics were characterized by flow cytometric analysis of ang2 mediated QD-aA2 aggregation at specific time points. Aggregates are quantified as a fraction of total events. The panels **a**, **b** and **c** show the raw flow cytometric data depicting increasing aggregate formation with time. This data was acquired for the samples with 10 pM QD-aA2 and 10 pM ang2 at 5, 30 and 45 minutes in panels **a**, **b** and **c**, respectively. Each dot represents one particle or 'event' detected. Forward light scatter (FSC-H) and side light scatter (SSC-H) intensities are positively correlated with the size and complexity of the particles. Optimization of the detection parameters enables the resolution of micron scale aggregates (red dots, upper right quadrant) from the individual QD-aA2 conjugates and small aggregates (black dots, bottom left quadrant). The ovals labeled R1, R2, R3, R4 and R7 indicate 0.2, 0.5, 1, 2 and 2.8 μm calibration particles respectively.

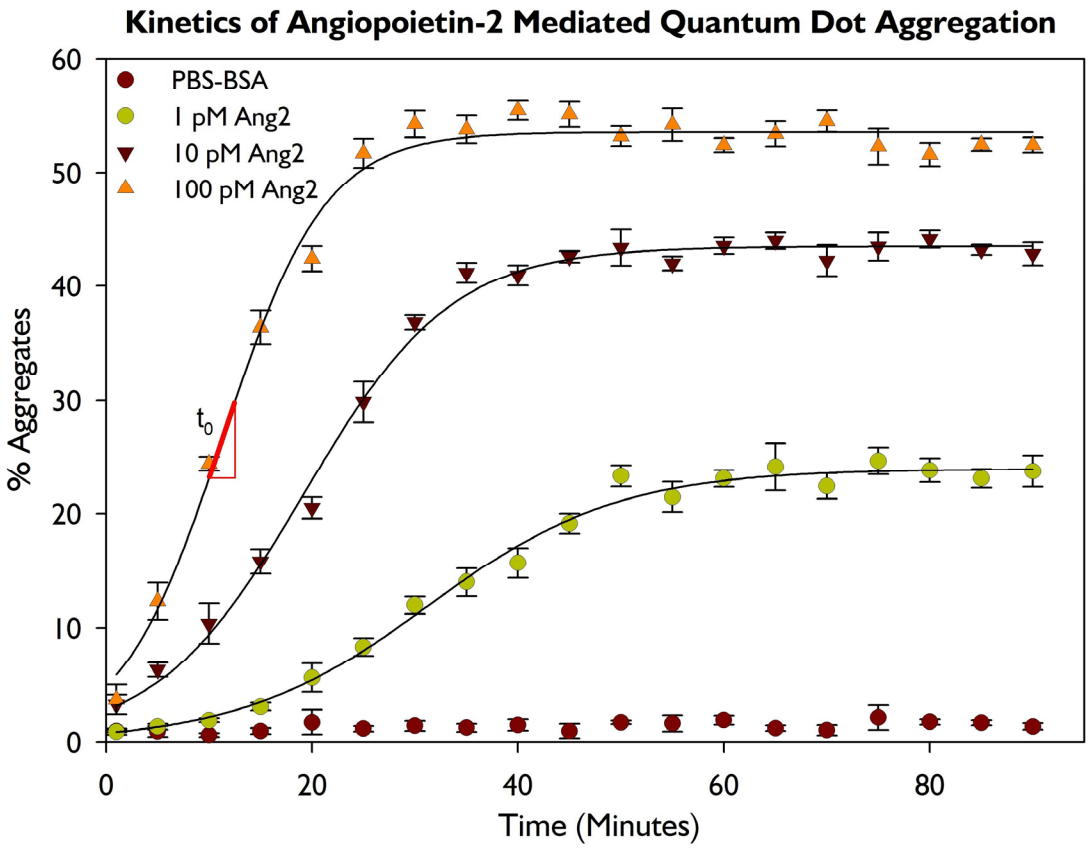

Figure 2: Agglomeration kinetics for a range of angiopoietin-2 concentrations. The QD-aA2:ang2 system exhibits a sigmoidal self-assembly kinetics. The parameters of aggregation kinetics in this system are affected by ang2 concentration, as detailed in **Table 1**. With increasing ang2 concentration, the aggregation rate increases, and time to inflection point (t_0) and time to reach steady state aggregate fraction decreases. The difference between the slopes, including at t_0 and at $t=5$ minutes for the three sigmoid curves suggest the possibility of antigen detection and quantification based on rate of increase in aggregate percent, rather than based on the equilibrium aggregate concentration as described previously[8]. This ability may also be beneficial for detection of molecular biomarkers in complex physiological media, where non-specific intermolecular interactions may have significant effect on the aggregate fraction, especially over long incubation periods. Each data point in the graph represents the mean and standard deviation of data from three different experiments.

QD-Ab:antigen complexes, which interact with each other, free QD-Ab conjugates and additional free antigen molecules. This is phase **i** of interactions which leads to the gradual formation of small complexes that act as nuclei for microscale aggregates. (**Figure 3, panel 2**). During the formation of multi-particle aggregates by molecular recognition, aggregation is favored by the decrease in free energy of the interacting particles, but the entropic cost associated with increased particle organization hinders nucleus formation[32]. Consequently, the probability of formation of micron scale aggregates as well as the aggregation rate are initially low. Once the nuclei have reached the critical size, the presence of multiple binding sites on the nuclei results in rapid growth of the aggregate[33]. This corresponds to phase **ii**, exhibiting rapid growth in the aggregate fraction. The transition from critical nucleus to large aggregates may occur rapidly. Flow cytometric characterization and dynamic light scattering data published previously[8], show only two particle populations – the individual, unaggregated QD-aA2:ang2 conjugates and the micron scale aggregates. While the fraction of micron-scale aggregates changes over time, an intermediate population is not apparent in these data. The lack of detectable concentrations of intermediate is consistent with the data published in the literature for other aggregation systems cited previously. Finally, as the individual components are depleted (**Figure 3, panel 3**), the aggregation rate slows and the system reaches a stable steady state.

Aggregation kinetics observed in the QD-aA2:ang2 system may be described by a three parameter, sigmoidal curve of the form

$$a = \frac{a_{max}}{1 - e^{-(\frac{t-t_0}{\tau})}} \qquad \text{(Equation 1)}$$

In **Equation 1**, a and t are the variables representing aggregate fraction and time, respectively. The constants for the sigmoids are a_{max}, t_0 and τ, where a_{max} is the equilibrium value for a, t_0 is the time point of inflection, and τ is a time constant. These parameters are modulated by the ang2 concentration in contact with the biofunctionalized QDs (**Table 1**). The a_{max} values obtained from the sigmoidal curves fit to the 1 pM, 10 pM, and 100 pM ang2 datasets are statistically equivalent to the steady state aggregate fraction observed previously[8] for the respective ang2 concentrations. t_0, which describes the inflection point for the sigmoidal curve, decreases with increasing ang2 concentration. Nucleation-limited aggregation processes, such as the self-assembly described here, accelerate in response to increased concentration of the bridging agent. This behavior, consistently observed in other systems and predicted in many model representations is confirmed in the present work. Increased ang2 concentration results in more rapid achievement of micron sized aggregates from nanoscale QDs, consistent with an increased rate of interactions between the QD-aA2 conjugates and the free ang2 molecules in solution. Thus, increasing ang2 concentration causes earlier achievement of a significant nucleation subpopulation and more rapid transition to the aggregate growth phase. The effect of increasing ang2 concentration on aggregation rate is also evident in the difference in slopes of the aggregation curves. Antigen concentration modulates the

rate of aggregate formation at the early time points during the low aggregation rate phase as well as at the inflection point (**Table 1**). The different slopes observed for different ang2 concentration indicate that an unknown concentration of the target antigen may be estimated from the rate of increase in aggregate count at incubation times far shorter than those required to achieve steady state. The optimal time point for discriminating among antigen concentrations may be determined through comparative analysis of aggregation profiles. The time constant τ also decreases with increasing antigen concentration and corresponds with the higher rate of aggregation during phase two following nucleation. The ang2 concentration is correlated with the sigmoid coefficients a_{max}, t_0 and t, and the slopes at t=0 minutes and $t=t_0$, with log linear functions with correlation coefficients 0.96, 0.98, 0.99, 0.95 and 0.99 respectively. These correlation coefficient values further support the feasibility of quantitatively detecting the biomarker concentration from one or more of the aggregation kinetics parameters. The control samples in the absence of ang2, do not exhibit time dependent aggregation behavior (**Figure 2**), further suggesting the potential to use kinetic assessments to detect specific antigens in the presence of other proteins.

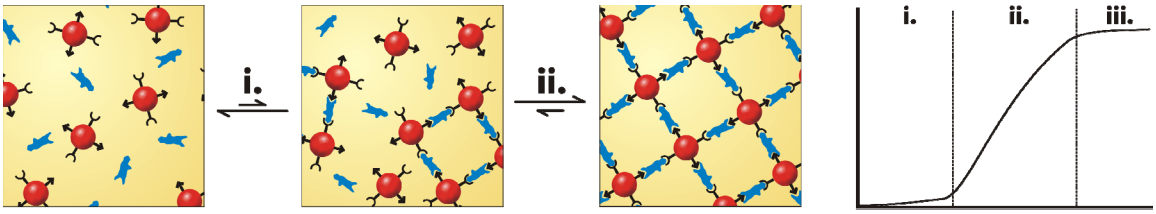

Figure 3: Schematic depiction of nucleation limited agglomeration process. The sigmoidal kinetics observed for QD-aA2:ang2 self assembly suggests a nucleation limited process, which is schematically depicted here. **i -** The entropic cost of particle aggregation may outweigh the reduction in free energy, resulting in slow nucleation. **ii -** The presence of multiple binding sites on nuclei of critical size leads to rapid growth of aggregates. **iii -** The depletion in available free ang2 causes the asymptotic approach to equilibrium aggregate fraction.

Table 1: Modulation of aggregation kinetics parameters by angiopoietin-2 concentration.

Angiopoietin2 concentration (picomolar)	a_{max} (percent)	t_0 (minutes)	τ (minutes)	slope, t=5 min (percent/minute)	slope, $t=t_0$ (percent/minute)
1	23.98	31.41	9.27	0.13	0.65
	+/- 0.35	+/- 0.38	+/- 0.76	+/- 0.02	+/- 0.05
10	43.51	19.18	7.12	0.65	1.52
	+/- 0.35	+/- 0.84	+/- 0.16	+/- 0.05	+/- 0.05
100	53.57	11.35	4.96	1.83	2.68
	+/- 0.30	+/- 0.53	+/- 0.21	+/- 0.09	+/- 0.11

Table 1: Angiopoietin-2 concentration has quantifiable effects on QD-aA2 aggregation kinetics. The sigmoid curves fit to the aggregation data are described by three constants a_{max}, t_0 and τ. The equilibrium aggregate percentage, a_{max}, increases with increasing ang2 concentration, in agreement with previously published data[8]. The inflection time t_0, and time constant τ both decrease with increasing ang2 concentration, indicating faster nucleation and growth of aggregates as a result of higher ang2 concentration. The rates of aggregation, represented by slopes of the sigmoidal curves are also a function of ang2 concentration, including at t=5 minutes, and at $t=t_0$. The concentration dependent aggregation rate may enable rapid detection and quantification of target antigens, as well as resolution of specific and no-specific intermolecular interaction. The values represent mean sigmoid coefficients and slopes obtained by fitting a three parameter sigmoid function to three datasets individually, and the respective standard deviations. The slopes at t=5 minutes and $t=t_0$ were obtained by fitting a linear function to eight sigmoid curve data points centered on the corresponding time points, as generated by Sigmaplot.

Conclusions

The quantifiable and reproducible self-assembly in the QD-aA2:ang2 system exhibits a sigmoidal kinetic behavior, comparable to that observed in other self-assembly processes based intermolecular interaction. The kinetics of aggregation suggest that the rate of aggregation and the equilibrium extent of aggregation are sensitive to the antigen concentration. Further experimental and theoretical research will be used to characterize the kinetics of multiplexed antigen detection and QD-Ab aggregation in complex biological samples, but is not a part of this short communication. Due to its unique characteristics, this multifunctional nano-conjugate based analyte detection technique may provide a novel, simple, and rapid mechanism for detecting molecular biomarker from physiological samples. An understanding of the aggregation kinetics and mechanisms will be particularly important in developing practical implementations of this technology, especially for complex samples containing non specific antigens with weak intermolecular interactions that may support weak QD-Ab aggregation. Nanoscale particle aggregation in solutions is a fundamental phenomenon that affects various technologies that include nanomaterials. The approach demonstrated here for characterizing nanoparticle aggregation kinetics may be applicable for improving the experimental and theoretical understanding of these nanoparticle interaction mechanisms. Such new fundamental knowledge will presumably be important for fields other than directed self-assembly and molecular diagnostics applications of the present work.

References

1. Zlotnick, A. and Stray, S. J., How does your virus grow? Understanding and interfering with virus assembly. *Trends in Biotechnology*, **2003**. *21*(12): 536-542.

2. Flyvbjerg, H.; Jobs, E. and Leibler, S., Kinetics of self-assembling microtubules: an" inverse problem" in biochemistry. *Proceedings of the National Academy of Sciences of the United States of America*, **1996**. *93*(12): 5975-5979.

3. Na, G. C.; Butz, L. J. and Carroll, R. J., Mechanism of in vitro collagen fibril assembly. Kinetic and morphological studies. *Journal of Biological Chemistry*, **1986**. *261*(26): 12290-12299.

4. Whitesides, G. M.; Mathias, J. P. and Seto, C. T., Molecular self-assembly and nanochemistry: a chemical strategy for the synthesis of nanostructures. *Science*, **1991**. *254*(5036): 1312-1319.

5. Yan, H.; Park, S. H.; Finkelstein, G.; Reif, J. H. and LaBean, T. H., *DNA-Templated Self-Assembly of Protein Arrays and Highly Conductive Nanowires*. 2003, American Association for the Advancement of Science. p. 1882-1884.

6. Storhoff, J. J.; Elghanian, R.; Mucic, R. C.; Mirkin, C. A. and Letsinger, R. L., One-pot colorimetric differentiation of polynucleotides with single base imperfections using gold nanoparticle probes. *J. Am. Chem. Soc*, **1998**. *120*(9): 1959–1964.

7. Hirsch, L. R.; Jackson, J. B.; Lee, A.; Halas, N. J. and West, J. L., A Whole Blood Immunoassay Using Gold Nanoshells. *Analytical Chemistry*, **2003**. *75*: 2377-2381.

8. Soman, C. P. and Giorgio, T. D., Quantum Dot Self-Assembly for Protein Detection with Sub-Picomolar Sensitivity. *Langmuir*, **2008**. *24*(8): 4399-4404.

9. Goldman, E. R.; Balighian, E. D.; Mattoussi, H.; Kuno, M. K.; Mauro, J. M.; Tran, P. T. and Anderson, G. P., Avidin: a natural bridge for quantum dot-antibody conjugates. *J. Am. Chem. Soc*, **2002**. *124*(22): 6378–6382.

10. Zlotnick, A.; Aldrich, R.; Johnson, J. M.; Ceres, P. and Young, M. J., Mechanism of Capsid Assembly for an Icosahedral Plant Virus. *Virology*, **2000**. *277*(2): 450-456.

11. Flyvbjerg, H. and Jobs, E., Microtubule dynamics. II. Kinetics of self-assembly. *Physical Review E*, **1997**. *56*(6): 7083-7099.

12. Bonfils, C.; Bec, N.; Lacroix, B.; Harricane, M. C. and Larroque, C., Kinetic Analysis of Tubulin Assembly in the Presence of the Microtubule-associated Protein TOGp. *Journal of Biological Chemistry*, **2007**. *282*(8): 5570.

13. Koo, B. W. and Miranker, A. D., Contribution of the intrinsic disulfide to the assembly mechanism of islet amyloid. *Protein Science*, **2005**. *14*(1): 231.

14. Sluzky, V.; Tamada, J. A.; Klibanov, A. M. and Langer, R., Kinetics of insulin aggregation in aqueous solutions upon agitation in the presence of hydrophobic surfaces. *Proceedings of the National Academy of Sciences of the United States of America*, **1991**. *88*(21): 9377-9381.

15. Speed, M. A.; King, J. and Wang, D. I. C., Polymerization Mechanism of Polypeptide Chain Aggregation. *BIOTECHNOLOGY AND BIOENGINEERING*, **1997**. *54*(4).

16. Spirito, M. D.; Chiappini, R.; Bassi, F. A.; Stasio, E. D.; Giardina, B. and Arcovito, G., Aggregation kinetics and structure of cryoimmunoglobulins clusters. *Physica A: Statistical Mechanics and its Applications*, **2002**. *304*(1-2): 211-219.

17. Endres, D.; Miyahara, M.; Moisant, P. and Zlotnick, A., A reaction landscape identifies the intermediates critical for self-assembly of virus capsids and other polyhedral structures. *Protein Science*, **2005**. *14*(6): 1518.

18. Endres, D. and Zlotnick, A., Model-Based Analysis of Assembly Kinetics for Virus Capsids or Other Spherical Polymers. *Biophysical Journal*, **2002**. *83*(2): 1217-1230.

19. Hagan, M. F. and Chandler, D., Dynamic Pathways for Viral Capsid Assembly. *Biophysical Journal*, **2006**. *91*(1): 42.

20. McPherson, A., Micelle formation and crystallization as paradigms for virus assembly. *BioEssays*, **2005**. *27*(4): 447-458.

21. Zlotnick, A., Theoretical aspects of virus capsid assembly. *J. Mol. Recognit*, **2005**. *18*: 479–490.

22. Zlotnick, A.; Johnson, J. M.; Wingfield, P. W.; Stahl, S. J. and Endres, D., A theoretical model successfully identifies features of hepatitis B virus capsid assembly. *Biochemistry*, **1999**. *38*(44): 14644-14652.

23. Bray, D. and Lay, S., Rapid numerical integration algorithm for finding the equilibrium state of a system of coupled binding reactions. *Bioinformatics*, **1994**. *10*(5): 471-476.

24. Bray, D. and Lay, S., Computer-based analysis of the binding steps in protein complex formation. *Proceedings of the National Academy of Sciences*, **1997**. *94*(25): 13493.

25. Lay, S. and Bray, D., A computer program for the analysis of protein complex formation. *Bioinformatics*, **1997**. *13*(4): 439-444.

26. Chong, C. R. and Sullivan, D. J., Inhibition of heme crystal growth by antimalarials and other compounds: implications for drug discovery. *Biochemical Pharmacology*, **2003**. *66*(11): 2201-2212.

27. Kodaka, M., Interpretation of concentration-dependence in aggregation kinetics. *Biophysical Chemistry*, **2004**. *109*(2): 325-332.

28. Hancock, K. and Tsang, V. C., Development and optimization of the FAST-ELISA for detecting antibodies to Schistosoma mansoni. *J Immunol Methods*, **1986**. *92*(2): 167-76.

29. Kodaka, M., Requirements for generating sigmoidal time–course aggregation in nucleation-dependent polymerization model. *Biophysical Chemistry*, **2004**. *107*(3): 243-253.

30. Towey, T. F.; Khan-Lodhi, A. and Robinson, B. H., Kinetics and mechanism of formation of quantum-sized cadmium sulphide particles in water–aerosol-OT–oil microemulsions. *Journal of the Chemical Society, Faraday Transactions*, **1990**. *86*(22): 3757-3762.

31. Matsumoto, A.; Kodama, K.; Aota, H. and Capek, I., Kinetics of emulsion crosslinking polymerization and copolymerization of allyl methacrylate. *European Polymer Journal*, **1999**. *35*(8): 1509-1517.

32. Sabaté, R. and Gallardo, M., An Autocatalytic Reaction as a Model for the Kinetics of the Aggregation of-Amyloid. *Biopolymers (Peptide Science)*, **2003**. *71*: 190-195.

33. Jarrett, J. T. and Lansbury Jr, P. T., Seeding" one-dimensional crystallization" of amyloid: a pathogenic mechanism in Alzheimer's disease and scrapie? *Cell*, **1993**. *73*(6): 1055-8.

CHAPTER V

CONCLUSIONS

Summary of Research

The dissertation explores a novel molecular diagnostic system based on molecular recognition mediated self-assembly of biofunctionalized nanoparticles. The three Specific Aims detailed in Chapter 1 were explored as described in Chapters II, III, and IV. Chapter II has been published in Langmuir[1], Chapter III is being revised for Nanomedicine: Nanotechnology, Biology, and Medicine (Elsevier)[2] and Chapter IV is under review in Nano Research (Springer)[3]. These chapters describe a new system of materials and methods that are aimed towards clinical development of a new technology for enhancing early diagnosis and therapy monitoring of cancers by monitoring soluble proteomic biomarkers. Furthermore, the novel nanoparticle self-assembly characterization protocol developed here may find broad applications in materials science.

In Chapter II we demonstrated the basic functionality of an *in vitro* system for detecting soluble proteomic biomarkers by characterizing self-assembled agglomerates of biofunctionalized nanoparticles. Quantum dots functionalized with polyclonal antibodies were shown to self-assemble into micron scale agglomerates in the presence of the specific antigens – angiopoietin-2 and mouse IgG, but not the non-specific control antigen – human IgG and bovine serum albumin. These agglomerates were characterized by multiple analytical methods, including dynamic light scattering, electrical sensing zone

method, and flow cytometry. While dynamic light scattering and electrical sensing zone methods were successfully used for demonstrating antigen mediated nanoparticle self assembly, the data was semi-quantitative, especially for the physiologically relevant picomolar and sub-picomolar concentrations.

The protocol developed for flow cytometric analysis of the reaction mixture allowed quantitative measurement of the number of agglomerates per unit volume and correlation of the agglomerate fraction to the antigen concentration. Since molecular recognition mediated self assembly is a two component process similar to agglutination, detection of low antigen concentrations was achieved by using low concentrations of the biofunctionalized nanoparticles. Using 10 pM QD-Ab conjugates, quantitative detection with a sensitivity limit of 500 pM was achieved by flow cytometry. The correlation between the antigen concentration and agglomerate fraction was log linear, with a correlation coefficient above 0.9 for both the antigens. The quantitative and reproducible measurement of antigen concentrations indicates the suitability of this technique for biomarker based clinical diagnostics. Furthermore, using two different concentrations (10 pM and 100 pM) of the QD-Ab conjugates, a large dynamic range of detection was achieved for both the antigens – from 500 pM to 50 nM.

The fluorescence of the nanoparticle agglomerates was found to be comparable to the individual nanoparticles. The observed size of the agglomerates indicated that the agglomerates contained on the order of a thousand individual quantum dots. Based on this estimate, it was originally hypothesized that the fluorescence emission of the agglomerates will be an order of magnitude or more intense compared to the individual nanoparticles. The discrepancy suggested that either most of the quantum dots in the

agglomerates were not being completely excited by the excitation laser, or that the fluorescence emissions of most of the quantum dots were not reaching the fluorescence detector. To investigate the discrepancy between the observed and expected fluorescence of the agglomerates, the bulk fluorescence of the reaction mixture was characterized. These measurements demonstrated a marked decrease in the bulk fluorescence with time, especially for high concentrations of the antigen, but not for the non-specific control, in agreement with the two hypotheses. This observation also prompted an alternate configuration for the microfluidic device design.

Current literature evidence strongly suggests that the clinical power of the biomarker based cancer diagnostics approach is enhanced significantly when biomarker panels – consisting of multiple biomarkers – are quantitatively detected. The availability of multiple fluorescence detection channels on the flow cytometer enabled the detection of multiple proteomic antigens by this method. Multiplexed, quantitative detection of angiopoietin-2 and vascular endothelial growth factor A was achieved by optimizing the flow cytometric characterization protocol to minimize the effect of cross channel fluorescence detection and non-specific antibody-antigen reactions. This is described in Chapter III. The nanoparticle agglomerates were quantified in two different data-spaces – 580 nm fluorescence vs. forward scatter intensity and 650 nm long pass fluorescence vs. forward scatter intensity. Each of the fluorescence intensity channels was used to trigger particle acquisition and characterization in two separate measurements of each sample. Agglomerates that exhibited cross fluorescent emissions exhibited high fluorescence in the data space with the trigger wavelength, but minimal fluorescence in the data space with non-trigger wavelength. Hence, the data spaces were gated to discard the events in

the low fluorescent intensity bins. This resulted in reproducible quantitative detection of the antigens, in the physiologically relevant concentration range of 1-100 pM. To test the reproducibility of the data, t-tests were carried out to compare the data sets in the multiplexed detection experiments with varying concentration of the two antigens, as well as the earlier dataset from non-multiplexed detection. The t-values obtained from these tests revealed that the correlation between antigen concentration and agglomerate fraction was statistically equivalent. The optimized detection protocol also enabled non-multiplexed detection of antigens with increased sensitivity, reducing the sensitivity limit for both angiopoietin-2 and VEGF to 50 fM.

One of the key hurdles in detecting low concentration biomarkers in physiological samples is the presence of large quantities of carrier proteins and antibodies in the serum or plasma, which may react non-specifically with the antibodies on the biofunctionalized nanoparticles, as well as cause nanoparticle agglomeration through other non-specific intermolecular interactions. Preliminary investigation revealed this to be the case for the system under investigation, necessitating significant improvements in materials and methods for sensitive and quantitative detection of biomarkers from complex physiological samples. While a complete solution to this problem was deemed outside the immediate practical scope of this research, one of the key improvements in the method of characterizing the agglomerates was developed. Chapter IV describes the kinetics of nanoparticle agglomeration in the present system. Antibody-antigen reaction kinetics, similar to those utilized in kinetic ELISA, were characterized via flow cytometry. The kinetics of nanoparticle agglomeration in the presence of a range of angiopoietin-2 concentrations was characterized from multiple time points up to ninety minutes. The

agglomerate fraction and time exhibited a sigmoidal correlation curve, which could be described by a three parameter sigmoidal equation. The parameters of the individual curves, as well as slopes at distinct time points were modulated by the antigen concentration, indicating the feasibility of quantitative detection of antigens from parameters other than the steady state agglomeration fraction.

Future Work

The next steps in this research can be broadly demarcated into two interdependent goals. The first is development of this research into a viable diagnostic platform for biomarker panel based cancer diagnosis and monitoring. Ideally, such a technology will be able to detect multiple biomarkers simultaneously from whole or minimally processed blood, in a compact automated instrument. Such an implementation, which may reduce the cost and increase ease of use and robustness of the diagnostic, would significantly enhance the value of molecular diagnostics for the end user.

The second goal is a more detailed understanding of the effect of the multiple materials and methods on characteristics of the self-assembled agglomerates. The sensitivity, specificity, quantitativness, kinetics, and dynamic range of biomarker detection is modulated by various parameters, including antibody-antigen interaction affinity, QD-antibody stoichiometry, size and surface chemistry of QD-Ab conjugates, fluid mixing parameters and presence of competitive and non-specific antigens.

It is anticipated that the specific capabilities of the microfluidic device will inform the design of experiments to elucidate the effect of the materials and methods on the diagnostic capability. Equally, the effect of materials and methods on optimizing the

protein detection capabilities will likely inform the configuration of the diagnostic platform. Some of the possible experimental and computational approaches for achieving these goals are described below.

Effect of antibody-antigen interaction affinity on agglomerate characteristics

The interaction affinity between the polyclonal antibodies and the antigens is expected to be a major factor affecting the kinetics and steady state characteristics of agglomeration. While the work presented in this thesis exhibits the differences in correlation between antigen concentration and steady state agglomeration for several antibody antigen pairs, controlled experiments elucidating the effect of binding affinity on agglomeration characteristics may prove valuable for optimizing the QD-Ab conjugates for sensitivity, dynamic range and quantitativeness.

Such an experiment may be carried out by examining the agglomeration behavior of two antibody-antigen pairs where the antigens have similar molecular weight, and the interaction affinity is known. Alternatively, agglomeration mediated by a single antigen may be characterized with two different polyclonal antibody mixtures with known binding affinity values. In these experiments, the binding affinity values may be characterized by conventional immunochemistry methods if they are not available from the vendors. From the point of view of experimental simplicity, it would be preferable to characterize the agglomeration behavior in this and other experiments on a microfluidic platform, but the established flow-cytometry based protocol is an acceptable alternative. Development of a computational model of the agglomeration process will provide an additional way to rapidly examine the effect of interaction affinity on agglomeration.

Effect of QD-Ab stoichiometry and size on agglomerate characteristics

The number of antibodies per QD-Ab conjugate, as well as the size of the QD would significantly affect the agglomeration geometry, and hence, protein detection parameters. Experiments with alternative QD-Ab stoichometries would inform the optimization of QD-Ab conjugates for protein detection. The careful control of QD-Ab stoichiometry will also involve purification of the conjugate for removal of unbound antibodies. If impact free antibody removal will inform the necessity for this extra step in clinical implementation. The effect of QD core size on the agglomeration behavior can be examined by characterizing the agglomeration behavior of an antibody-antigen pair, where the antibodies are conjugated with different QDs. These factors too can be investigated in a computational model of the agglomeration process along with physical experiments.

Optimization of materials and methods for complex samples

For proteomic profiling applications, whole blood is commonly processed to remove the most prevalent proteins, which include hemoglobin, albumin, complement proteins, immunoglobulins, transferrin, and fibrinogen. These proteins are present in concentrations many orders of magnitude larger than the target biomarkers and cause non-specific aggregation. The removal of these components by conventional proteomics methods, such as separation columns may significantly improve the performance of the biomarker detection method.

Another approach that may significantly reduce non-specific agglomeration is modification of the nanoparticles. It is well known that poly-(ethylene glycol) surface modified nanoparticles have significantly reduced non-specific adhesion to biological surfaces. A similar approach my also help reduce non-specific self-assembly of nanoparticles for diagnostics. Surface modification of quantum dots may also necessitate the development of a protocol for chemically conjugating antibodies to the nanoparticles, rather than streptavidin-biotin based conjugation currently used.

Development of microfluidic device

While the characterization of nanoparticle agglomerates is easily possible with, conventional flow cytometers, these instruments are generally not optimized for accurate characterization of small particles. Furthermore, the optical set up in flow cytometers may not be optimal for characterization of these assemblies, as discussed before. A microfluidic device may overcome both of these challenges, and is currently in development.

Examination of other intermolecular recognition interactions:

It is likely that nanoparticle agglomeration may be achieved from other intermolecular interactions such as for polynucleotides, DNA-Aptamer, and receptor-ligands, interaction. Modifying the present system to examine these interactions would determine the feasibility of detecting non-protein biomarkers with this diagnostic platform.

Risks and benefits of further investment

The work presented here demonstrates that nanoparticle agglomeration based protein detection method works for protein detection with sensitivity comparable to ELISA and possibility of reduced cost and increased ease of use. However, significant improvements are required before it may be considered a viable technology for clinical diagnostics applications. These improvements may or may not be possible. Furthermore, a large number of molecular diagnostics technologies are currently under development, and the competitiveness of this technology, even with significant improvements, is not assured.

If the technology is implemented with competitive performance, the simple, low cost, portable implementation would likely ensure widespread clinical adoption for molecular diagnostics of a large variety of diseases. Furthermore, the technology also has the potential for use for outside the clinical setting investigation of nanomaterials agglomeration.

References

1. Soman, C. P. and Giorgio, T. D., Quantum Dot Self-Assembly for Protein Detection with Sub-Picomolar Sensitivity*. Langmuir*, **2008**. *24*(8): 4399-4404.

2. Soman, C. P. and Giorgio, T. D., Sensitive and Multiplexed Detection of Proteomic Antigens via Quantum Dot Aggregation*. Nanomedicine: Nanotechnology, Biology, and Medicine* **2008**. *(under review)*.

3. Soman, C. P. and Giorgio, T. D., Kinetics of Molecular Recognition Mediated Nanoparticle Self-Assembly*. Nano Research*, **2008**. *(under review)*.

APPENDIX A

PRELIMINARY CHARACTERIZATION OF MOLECULAR RECOGNITION MEDIATED NANOPARTICLE SELF ASSEMBLY

The initial experiments to ascertain the feasibility of this technique were carried out by non-invasive dynamic laser back scatter (DLS) in the Malvern Zetasizer Nano ZS (Malvern Instruments, Malvern, UK). QDot-525 Streptavidin conjugates (QD) (1μM, Invitrogen Corporation, Q10141MP), biotin conjugated goat anti-mouse immunoglobulin specific polyclonal antibody (GaM) (0.5 mg/mL, BD Pharmingen, 553999), Mouse IgG (Mus) (Polysciences, 23873) and Human IgG (Hum) (Polysciences, 23872) were used without further purification. Borate buffer (ACS boric acid/sodium tetraborate, 10 mmol/L, pH 7.4, 0.2 μm filtered) was used for these experiments.

Quantum dot - antibody conjugation was verified by DLS particle size measurement. Particle size measurement of the individual particles shows (**Figure 1.a**) QD at 22 nm, Mus at 28 nm, and GaM at 9 nm and 28 nm. QD-GaM conjugates were prepared by adding GaM with QD:GaM molar ratio of 1:3, and incubating at room temperature for five minutes. The conjugation takes place due to biotin-streptavidin interaction. The particle size distribution after conjugation (**Figure 1.b**) indicates successful conjugation that QD reacts completely to produce a QD-GaM conjugate, with a diameter of 40 nm. It is also seen that some unreacted GaM persists, indicating that there are between two and three GaM per QD in the conjugate nanostructure.

Immunorecognition mediated agglomeration was also verified by DLS measurements. 4μmol/L Mus - the positive antigen, was added to the QD-GaM solution. This mediated the appearance of a new peak beyond 1000 nm (**Figure 1.c**), indicating the formation of microscale agglomerates. Furthermore, the shift of the QD-GaM peak from 40 nm to 70 nm indicates formation of QD-GaM:Mus complexes that do not participate in microscale agglomerates. The addition of Hum – the nonspecific control antigen, does not mediate such agglomeration (**Figure 1.d**) which confirms the immunospecificity of the assay. The formation of large agglomerates in the presence of target antigen is a critical feature for successful application of the proposed approach, and is demonstrated here.

Correlation of QD-GaM-Mus agglomeration with Mus concentration was characterized by measuring particle size and count by electroresisitive meansurements (Beckman-Coulter Multisizer 3, 30 μm aperture). Particle size distribution above 800 nm diameter was assessed. Self-assembly of 2 pmol QD-GaM and 10 μL of antigen or negative control was carried out in 1 mL total volume of borate buffer for one hour at room temperature with continuous gentle mixing followed by dispersion in 9 mL Isoton II (Beckman Coulter, 8546719, 0.2 μm filtered). Particle diameter distribution was measured from 0.8 to 8.0 μm in a 100 μL volume. 100 μg/mL Mus mediates a 115-fold increase in the number of particles between 0.8 to 8.0 μm in diameter relative to the addition of 100 μg/mL Hum, confirming the specificity of self-assembly (**Figure 2**). The limit of detection for Mus in this non-optimized system appears to be approximately 1 μg/mL, a concentration which produces the same number and volume of aggregates as 100 μg/mL Hum or the QD-GaM background in the absence of antigen. The mean,

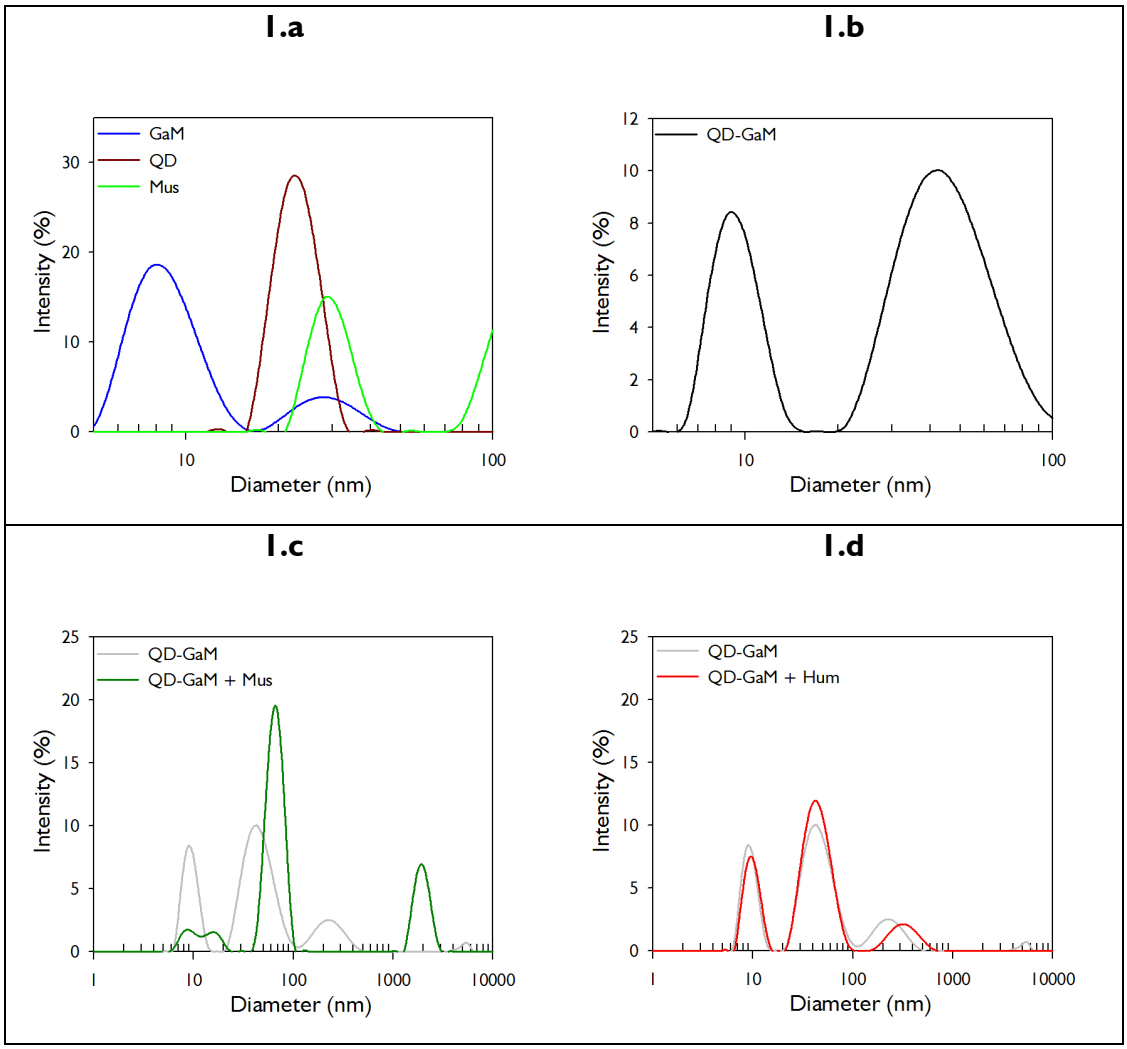

Figure 1. Dynamic light scattering characterization. QD and GaM (**1.a**) conjugate via biotin-streptavidin interaction. Conjugate QD-GaM (**1.b**) has a mean size of around 45 nm. Excess GaM from the conjugation can also be seen. Specific antigen added to the QD-GaM conjugate causes agglomeration (**1.c**) producing a new particle population, while non-specific antigen does not cause this effect (**1.d**).

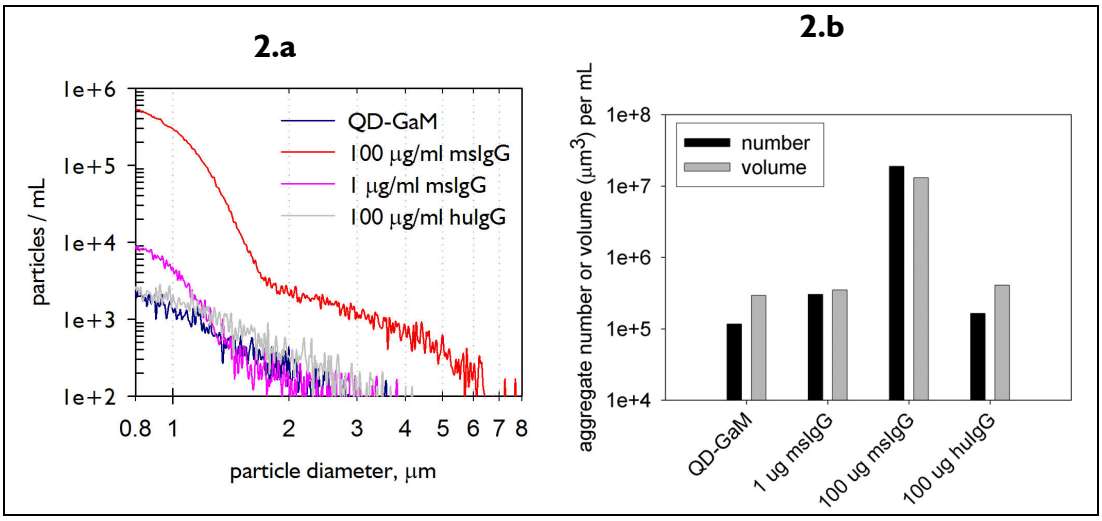

Figure 2 Electrical sensing zone characterization. Mus triggers the formation of microscale aggregates from nanoscale QD-GaM. The particle count and size distribution above 800 nm is a function of Mus concentration.

volume-weighted particle diameter measured by Coulter Counter was 2,780 nm or 1,880 nm for QD-GaM treated with 1 μg/mL or 100 μg/mL Mus, respectively. The equivalent number-weighted particle diameters were 1,050 nm or 990 nm, respectively.

Flow cytometric detection of QD-GaM-Mus agglomerates was also achieved. Flow cytometric detection was optimized in several ways, differing from conventional cellular flow experiments. Instead of forward scatter (FSC) or side scatter (SSC), fluorescence (FL) channels were found to be better event triggers, leading to higher particle count as well as reduced noise. The extinction coefficients of QDs increases with increasing emission wavelength. Accordingly, QDs with longer wavelength generate a higher particle count than QDs with shorter emission wavelength, at equal concentration. Hence for flow cytometric experiments, QD-705 streptavidin conjugate (QD) (1μM, Invitrogen Corporation, Q10161MP) was used. Events were collected using fluorescence intensity in the FL3 channel (appropriate for QD705) as the primary event trigger (Becton-Dickinson FACSCalibur). FL3 gain, SSC gain and FSC amplification were optimized in pilot studies to provide suitable dynamic range for capture of the relevant events.

QD-GaM interaction with antigen (1, 10 or 100 μg/mL Mus - **Figure 3 b, c** and **d**, respectively) or control (PBS buffer or 100 μg/mL Hum - **Figure 3 a** and **e**, respectively) was carried out in a standard flow cytometry tube (1 mL total volume) with incubation for one hour at room temperature. Based on flow cytometry of QD-GaM in the absence of any antigen, it was determined that most QD-GaM events had FSC values of less than 10 arbitrary units (a.u.) at the amplification used. Hence, quad regions were established in the SSC vs. FSC representation to isolate, and identify through color gating (red for

Mus, blue for Hum), events with light scatter characteristics consistent with large particle diameter, based on forward scatter higher as a discriminating parameter.

This flow cytometric detection of self-assembled microscale aggregates formed from nanoscale conjugates and antigens confirms the particle size measurements by DLS (**Figure 1**) and electrical resistance (**Figure 2**), reinforcing the fundamental proof-of-principle for the proposed approach. The flow cytometric data is also correlated with antigen concentration. FSC intensity histogram (**Figure 4.a-d**), as well as aggregates as a fraction of total events and mean diameter (**Figure 4.e**), are some of the parameters that reflect this correlation. FSC intensity histograms reflect the self-assembly of QD-GaM-Mus aggregates modulated by [Mus]. Calibration particles (mean diameters 200, 1000, 2000 and 2866 nm; corresponding to regions R1, R2, R3, and R4 respectively in **Figure 3**) were used to estimate the relationship between FSC intensity and event diameter[1]. The fraction of all events with forward scatter parameter greater than 10 is correlated with Mus concentration between 5 and 100 μg/ml, enabling antigen concentration estimation from measurable aggregate characteristics, at least in the model system tested. The diameter of QD-GaM-msIgG aggregate self-assembly decreases with increasing [Mus] from very large events (2,940 nm, FSC = 1187 a.u.) near the current [Mus] detection threshold (**Figure 4.b**, 1μg/ml Mus) to events centered near 1790 nm diameter (FSC = 345 a.u., **Figure 4.c**) and events centered near 760 nm diameter (FSC = 41 a.u., 100μg/ml, **Figure 4.d**) for the highest [Mus]. The QD-GaM-IgG FSC histogram mediated by the addition of nonspecific control antigen (100 μg/mL Hum, **Figure 4.e**) is visually different from that for the same concentration of Mus.

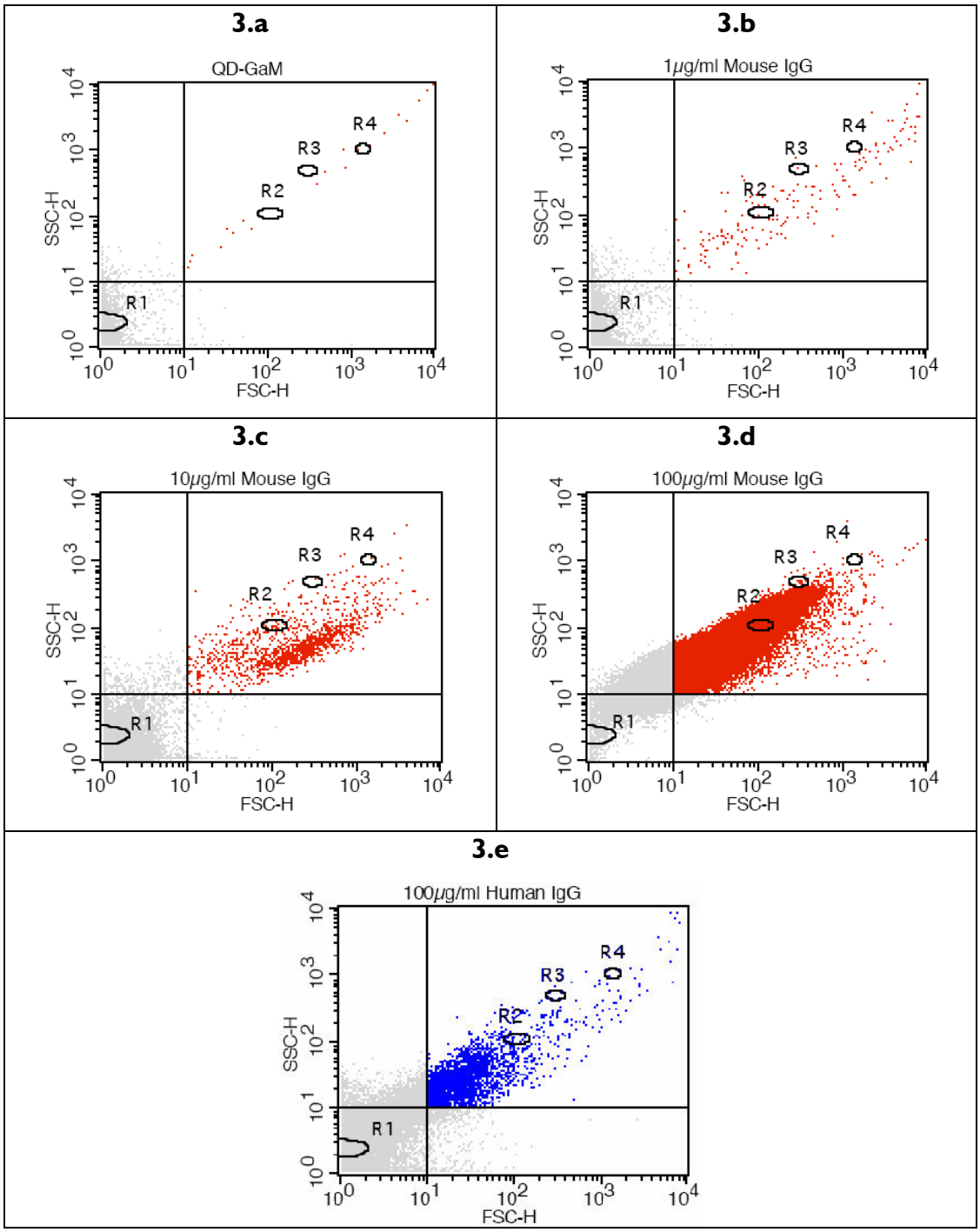

Figure 3 Flow cytometry: FSC-SSC dot plots. Flow cytometry reveals self-assembly of QD-GaM-IgG aggregates modulated by antigen concentration (**a**, **b**, **c**, **d** : [Mus] of 0, 1, 10, 100 μg/mL, respectively). 100 μg/mL of nonspecific control antigen (Hum) (**e**) mediates the self-assembly of smaller and fewer aggregates than the same concentration of Mus.

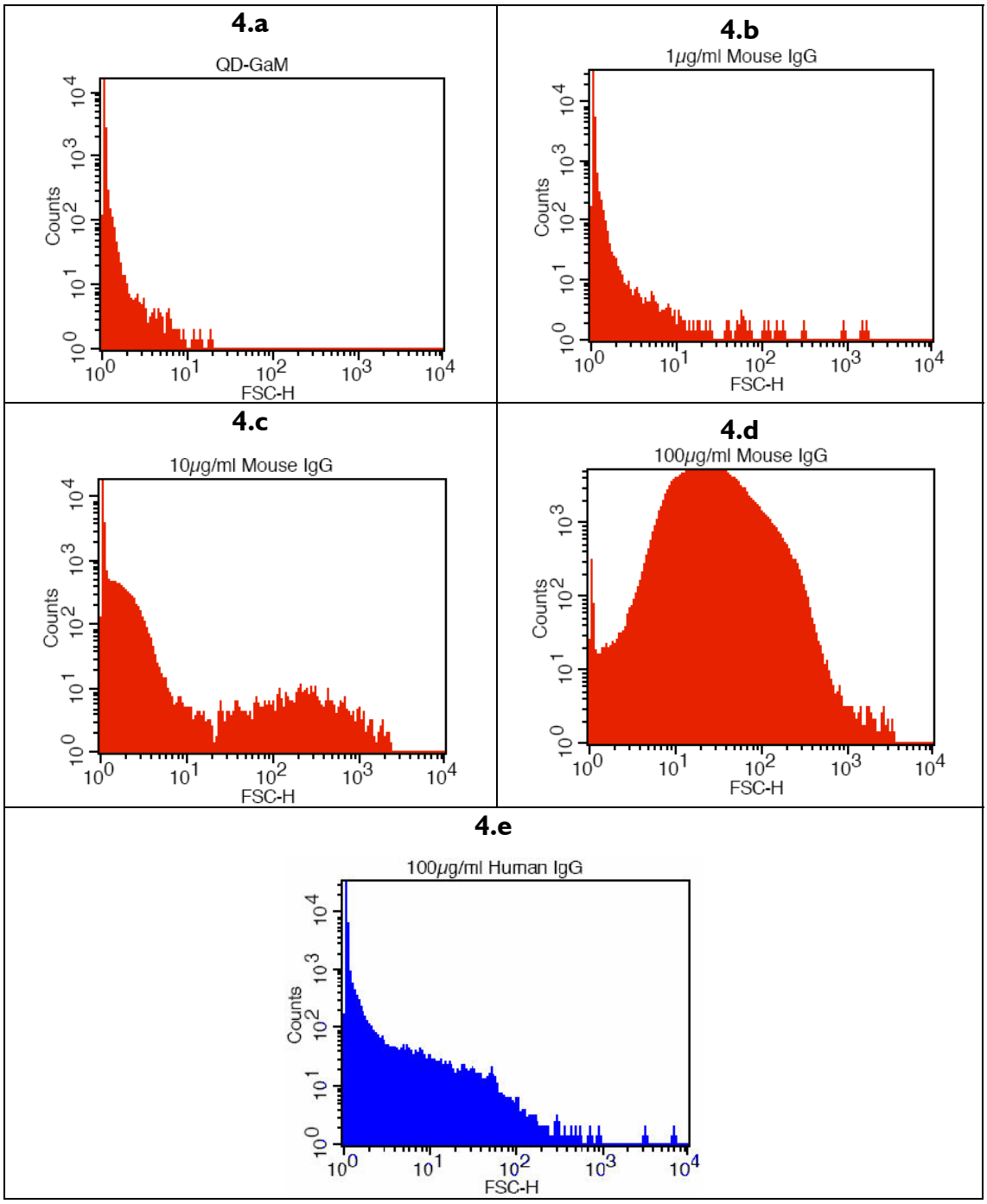

Figure 4 Flow cytometry: FSC histograms. Comparative size distribution of QD-GaM-IgG aggregates modulated by antigen concentration (panels A through D reflect [Mus] of 0, 1, 10, 100 μg/mL, respectively). 100 μg/mL of nonspecific control antigen (Hum, **e**) mediates the self-assembly of smaller and fewer aggregates than Mus (**d**).

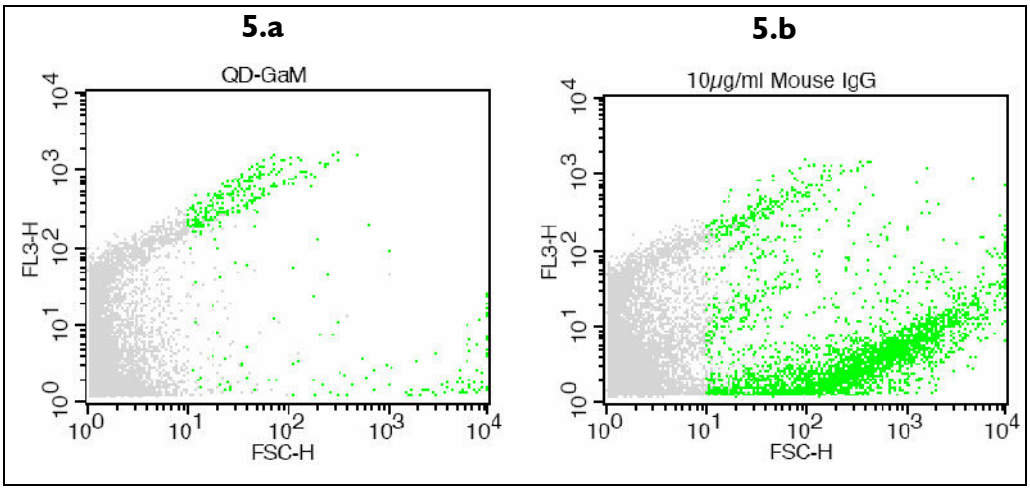

Figure 5 Flow cytometry: fluorescence-FSC dot plots. QD-GaM fluorescence intensity is quenched by self-assembly into QD-GaM-IgG aggregates mediated by antigen. Events greater than approximately 490 nm in diameter are colored green. The bottom subpopulation in panel B represents QD-GaM-Mus aggregates formed in response to 10 μg/mL Mus. FL3 intensity does not increase in proportion with estimated event volume, evidence consistent with QD fluorescence quenching upon binding.

Also, exposure to 100 μg/mL Hum resulted in significantly fewer FL3-positive events (2.71×10^3) than 100 μg/mL Mus (1.02×10^6), both in approximately 60 μL of detection volume. This confirms that gating strategies and statistics can be used to distinguish specific from nonspecific self-assembly. The reduced number of detectable events in flow cytometry for the Hum sample is consistent with the relative lack of aggregates greater than 700 nm diameter obtained by light scattering (**Figure 1**) and electric sizing (**Figure 2**).

Mus, but not Hum, mediates the formation of many self-assembled QD-GaM-IgG aggregates sufficiently large to trigger flow cytometric detection. The use of absolute event counts may provide another sensitive index to distinguish antigen-mediated self-assembly from nonspecific effects. Mean QD-GaM-Mus diameter may be used to characterize antigen mediated self-assembly, especially for low [Mus] where the population of aggregates is low and relatively insensitive to [Mus]. QD-GaM-Mus aggregate characteristics modulated by [Mus] suggest that antigen mediated self-assembly is a complex interaction in which the estimated event diameter decreases as the event fraction and [Mus] increases. This behavior may be related to Mus:QD-GaM stoichiometry and mixing conditions, parameters that will be assessed by experimentally in this work. The use of absolute event counts may provide another sensitive index to distinguish antigen-mediated self-assembly from nonspecific effects. Absolute counts and absolute volumes may be resolved in flow cytometry through the addition of microscale calibration particles of known concentration as the correlation measure. The threshold for Mus detection using FSC gated QD-GaM-Mus event counts in this non-optimized system appears to be 1 μg/ml or 6.6nM. The improvement of immunodetection by

optimizing reaction conditions, stoichiometry, and instrument parameters is one of the goals of specific aim 1 of the proposed research.

The fluorescence intensity of the aggregates is also significantly lower than expected from a linear increase in fluorescence of an agglomerate of multiple quantum dots. This can be seen (**Figure 5.b**) in the FL3 vs. FSC representation of the flow cytometric data as well as in the data bulk fluorescence intensity data (Chapter 2, **Figure 4**). As an example, the QD-GaM-Mus aggregates at FSC intensity of 100 a.u. (1,085 nm diameter) have an FL3 intensity of approximately 1 a.u. and aggregates at FSC intensity of 10,000 a.u. (6,940 nm diameter) have an FL3 intensity of approximately 10 a.u. Thus, large events have more than 250-fold greater volume than small events, but only 10-fold the fluorescence intensity. This behavior is consistent with other observations of QD fluorescence quenching upon surface modification [2, 3]; this response has been used as a biosensor [4, 5]. Other mechanisms, including optical screening, may contribute to this effect and will be assessed by spectrofluorometric assay during antigen-mediated self-assembly as part of Specific Aim 1 of the proposed work.

A reduction in bulk fluorescence emission intensity at 585 nm mediated by the addition of 100 μg/mL Mus (but not 100 μg/mL Hum) suggests that QD quantum yield is quenched by antigen bridging (Chapter 2, **Figure 4**). The observed reduction in overall solution fluorescence intensity is consistent with the reduction in QD-GaM-Mus fluorescence intensity measured by flow cytometry (**Figure 5**). Other measures of nanoparticle self-assembly described here (aggregate size, aggregate fluorescence intensity) have a greater sensitivity to antigen than the 10-100 μg/mL threshold apparent in this non-optimized system. Fluorescence intensity measured in this method is the sum

of QD-GaM and QD-GaM-IgG aggregates. For conditions in which the volume fraction of aggregates is small (approximately 0.001% in these studies (**Figure 2**)), fluorescence quenching due to aggregation must be detected on a relatively large background fluorescence intensity of unaggregated QD-GaM. This disadvantage may be overcome by optimization of the [QD-GaM] and has been successfully demonstrated in other systems [5, 6].

Polychromatic agglomerates have also be detected and characterized. A mixture of two unique QD populations (QD_{585} and QD_{705}) can self assemble though antigen binding to form polychromatic aggregates (**Figure 6**). This evidence supports the spectral unmixing of QD aggregates to simultaneously characterize the presence of multiple antigens in a mixture by flow cytometry. QD_{705}-GaM (**Figure 7.a**) are strongly fluorescent in FL3, but not FL2. QD_{585}-GaM (**Figure 7.b**) are strongly fluorescent in FL2, but not FL3. Equal proportions of QD_{705}-GaM and QD_{585}-GaM mixed with 100 μg/mL Mus, resulted in the self-assembly of aggregates with sizes indistinguishable from those composed of QD_{705} alone (compare **Figure 6.c** and **Figure 3.d**). The polychromatic aggregates, simultaneously emitting significant fluorescence intensity in both FL2 and FL3 (**Figure 6.d**), were composed of both QD cohorts.

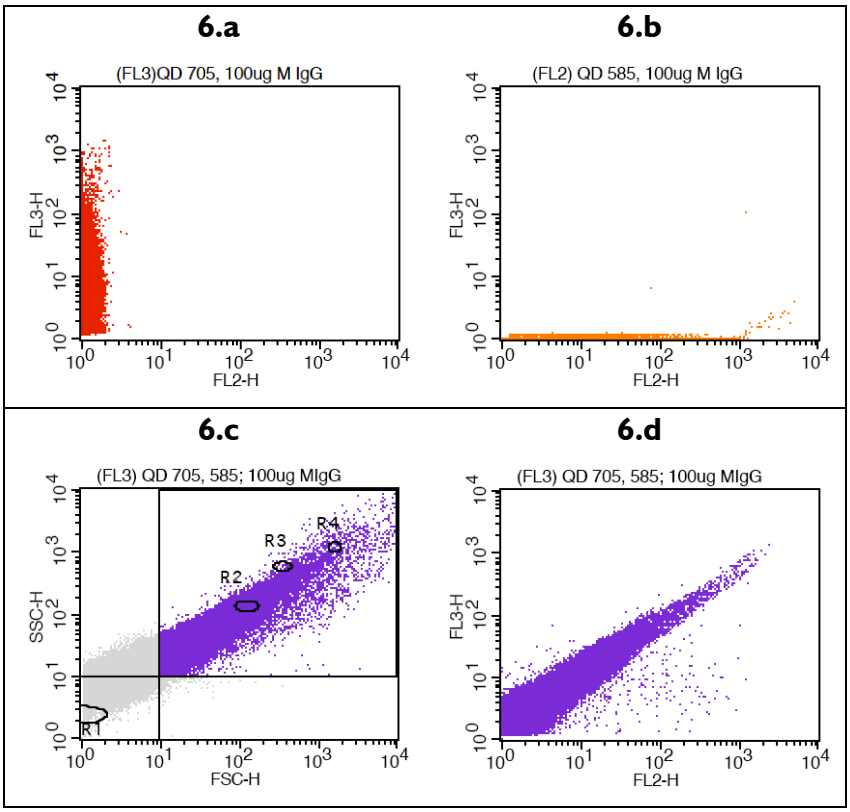

Figure 6 Preliminary multicolor flow cytometry. QD_{705}-GaM (**a**) and QD_{585}-GaM (**b**) are mixed together in equal proportion and exposed to 100 μg/mL msIgG antigen. The self-assembled aggregates are formed (**c**) from both QD cohorts, creating polychromatic events (**d**).

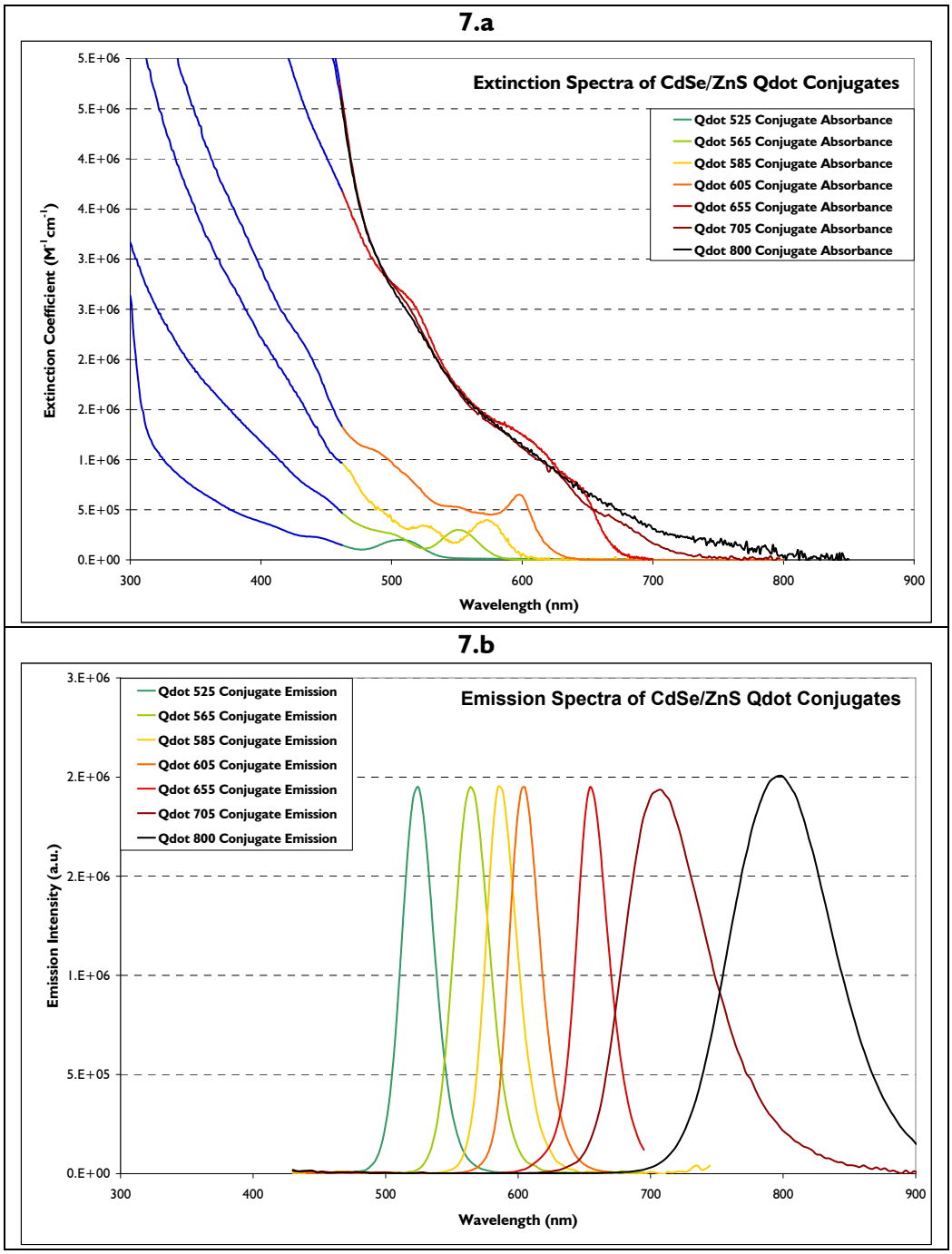

Figure 7 QDot absorption and excitation spectra. Excitation(**a**) and emission (**b**) spectra of CdSe/ZnS quantum dots. Data provided by Quantum Dot Corp.

References

1. Giorgio, T. D. and Purvis, N. B., *Method and apparatus for determining size, surface area and volume normalized fluorescence using forward angle light scatter in flow cytometry*. 1996, U.S.P. Office: United States.

2. Bentzen, E. L.; Tomlinson, I. D.; Mason, J.; Gresch, P.; Warnement, M. R.; Wright, D.; Sanders-Bush, E.; Blakely, R. and Rosenthal, S. J., Surface Modification To Reduce Nonspecific Binding of Quantum Dots in Live Cell Assays*. Bioconjugate chemistry*, **2005**. *16*(6): 1488-1494.

3. Tomlinson, I. D.; Wright, D. W.; Giorgio, T. D.; Blakely, R. D.; Pennycook, S. J.; Hercules, D.; Bentzen, L.; Smith, R. A.; McBride, J. and Vergne, M. J., The quantum dot nanoconjugate tool box*. Proceedings of the SPIE*, **2005**. *5705*: 199-209.

4. Dyadyusha, L.; Yin, H.; Jaiswal, S.; Brown, T.; Baumberg, J. J.; Booy, F. P. and Melvin, T., Quenching of CdSe quantum dot emission, a new approach for biosensing*. Chemical Communications*, **2005**. *25*: 3201-3203.

5. Robinson, A.; Fang, J. M.; Chou, P. T.; Liao, K. W.; Chu, R. M. and Lee, S. J., Probing Lectin and Sperm with Carbohydrate-Modified Quantum Dots*. CHEMBIOCHEM-WEINHEIM-*, **2005**. *6*(10): 1899.

6. Goldman, E. R.; Medintz, I. L.; Whitley, J. L.; Hayhurst, A.; Clapp, A. R.; Uyeda, H. T.; Deschamps, J. R.; Lassman, M. E. and Mattoussi, H., A Hybrid Quantum Dot-Antibody Fragment Fluorescence Resonance Energy Transfer-Based TNT Sensor*. Nanotechnology*, **2003**. *14*(R15): R27.